Radiation from acceleration Particles in relativistic jets with shocks, shear-flow and reconnection

Ken Nishikawa *UAH/Physics*

Collaborators:

P. Hardee (*Univ. of Alabama, Tuscaloosa*)
Y. Mizuno (*National Tsing Hua University, Taiwan*)
J. Niemiec (*Institute of Nuclear Physics PAN*)
I. Duţan (*Institute of Space Science, Rumania*)
M. Medvedev (*Univ. of Kansas*)
B. Zhang (*Univ. Nevada, Las Vegas*)
E. J. Choi (*KAIST*)
K. W. Min (*KAIST*)
Å. Nordlund (*Niels Bohr Institute*)
J. Frederiksen (*Niels Bohr Institute*)
H. Sol (*Meudon Observatory*)
M. Pohl (*U-Potsdam/DESY*)
D. H. Hartmann (*Clemson Univ.*)
A. Marscher (*Boston Univ.*)
J. Gómez (*IAA, CSIC*)
A. Meli (*Unv. of Gent*)

Gamma-Ray Bursts in the Multi-messenger Era,
June 16 - 19, 2014, Paris

Outline of talk

1. **Introduction and Weibel instability**
2. **Recent 3-D particle simulations of relativistic jets**
   * **$e^{\pm}$pair jet into $e^{\pm}$pair, γ= 15 and electron-ion (m_i/m_e = 20) into electron-ion γ= 15 shock structures**
3. **Magnetic field generation and particle acceleration in kinetic Kelvin-Helmholtz instability** (Nishikawa et al. 2014, arXiv:1405.5247)
4. **Global jet simulations with shock and KKHI**
5. **Synthetic spectra in shocks generated by the Weibel instability**
6. **Acceleration in recollimation shock**
7. **Summary**
8. **Future plans**

Key Scientific questions

- How do shocks in relativistic jets evolve?
- How do magnetic fields affect shocks and reconnection?
- How are particles accelerated?
- What are the dominant radiation processes?
- How do 3-D relativistic PIC simulations reveal the dynamics of shock fronts and transition regions (CD and RS)?
- How do shocks in relativistic jets evolve in various ambient plasma- and magnetic field configurations?
- How do magnetic fields generated by the Weibel instability contribute to the emerging radiation?
- How do velocity shears generate magnetic fields and accelerate particles?

-- for some answers see Nishikawa et al. 2006, ApJ, 642, 1267
Ramirez-Ruiz, Nishikawa & Hededal, 2007, ApJ, 671, 1877
Nishikawa et al. 2009, ApJ, 698, L10 --

Plasmas in the Universe

* The major constituents of the universe are made of plasmas.
* When the temperature of gas is more than 10^4K, the gas becomes fully ionized plasmas (4^{th} phase of matter).
* Plasmas are applied to many astrophysical phenomena.
* Plasmas are investigated in several ways
  * particle-in-cell (PIC) (microscopic)
  * magnetohydrodynamics, MHD (macroscopic) (not covered)
  * hybrid (fluid electron and kinetic ions) (not covered)
  * MHD with test particles (fluid mixed with particles) (not covered)
  * particles with photons (not covered)

3D Relativistic particle-in-cell code

Kinetic processes are included in this code

- Particle acceleration can be investigated
- Synthetic spectrra of radiation can be calculated
- Simulation system size is limited due to necessity of resolving Debye length (Skin depth)
- Global dynamics of plasma such as large jets cannot be simulated

This simulation method is complimentary to MHD method which will be described briefly later

Terminal Hotspots

Kino & Takahara 04

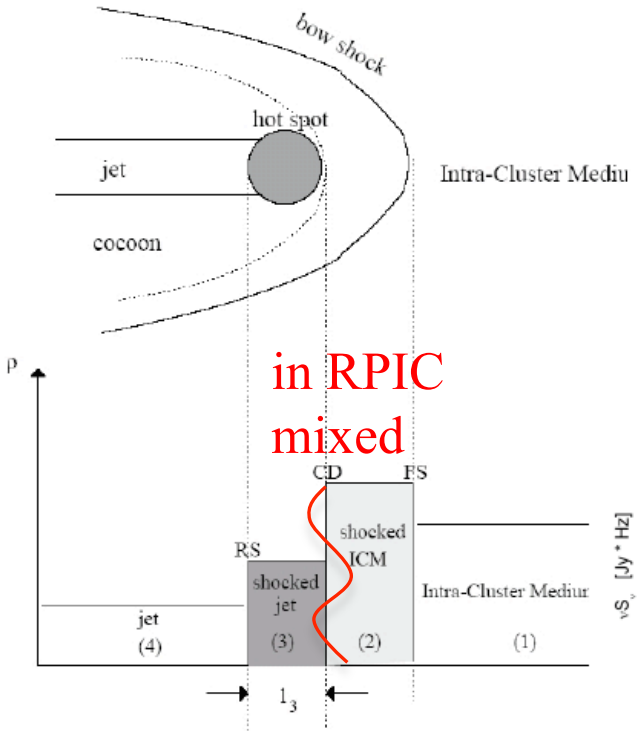

Hotspots in powerful radio sources are understood as the terminal regions of relativistic jets, where bulk kinetic power transported by the outflows from the active centers is converted at a strong shock (formed due to the interaction of the jet with the ambient gaseous medium) to the internal energy of the jet plasma.

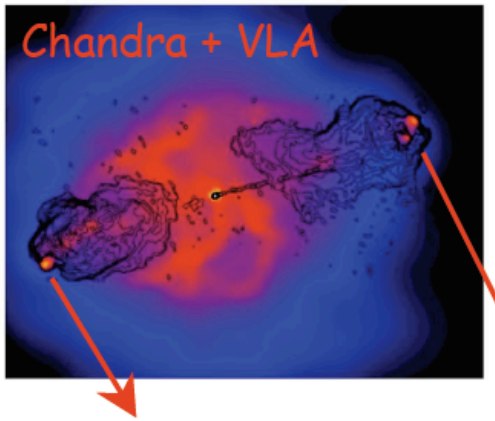

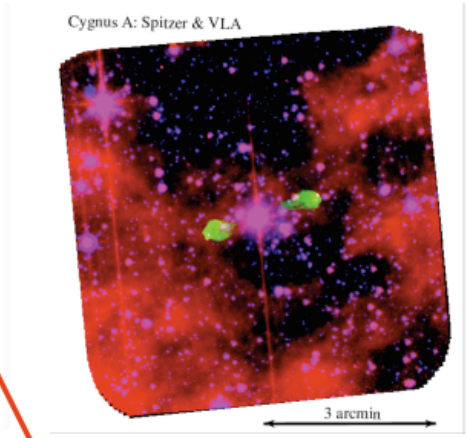

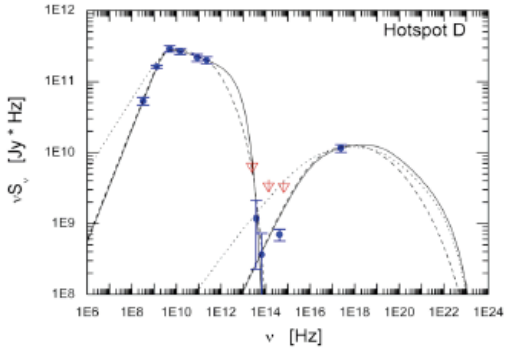

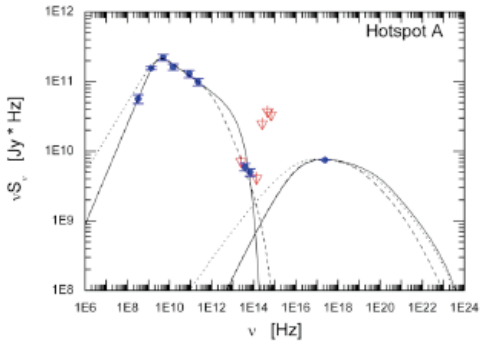

Hotspots of exceptionally bright radio galaxy Cygnus A (d_L = 250 Mpc) can be resolved at different frequencies (VLA, Spitzer, Chandra), enabling us to understand how (mildly) relativistic shocks work (**LS+ 07**).

from the talk by L. Stawarz

Gamma-ray bursts

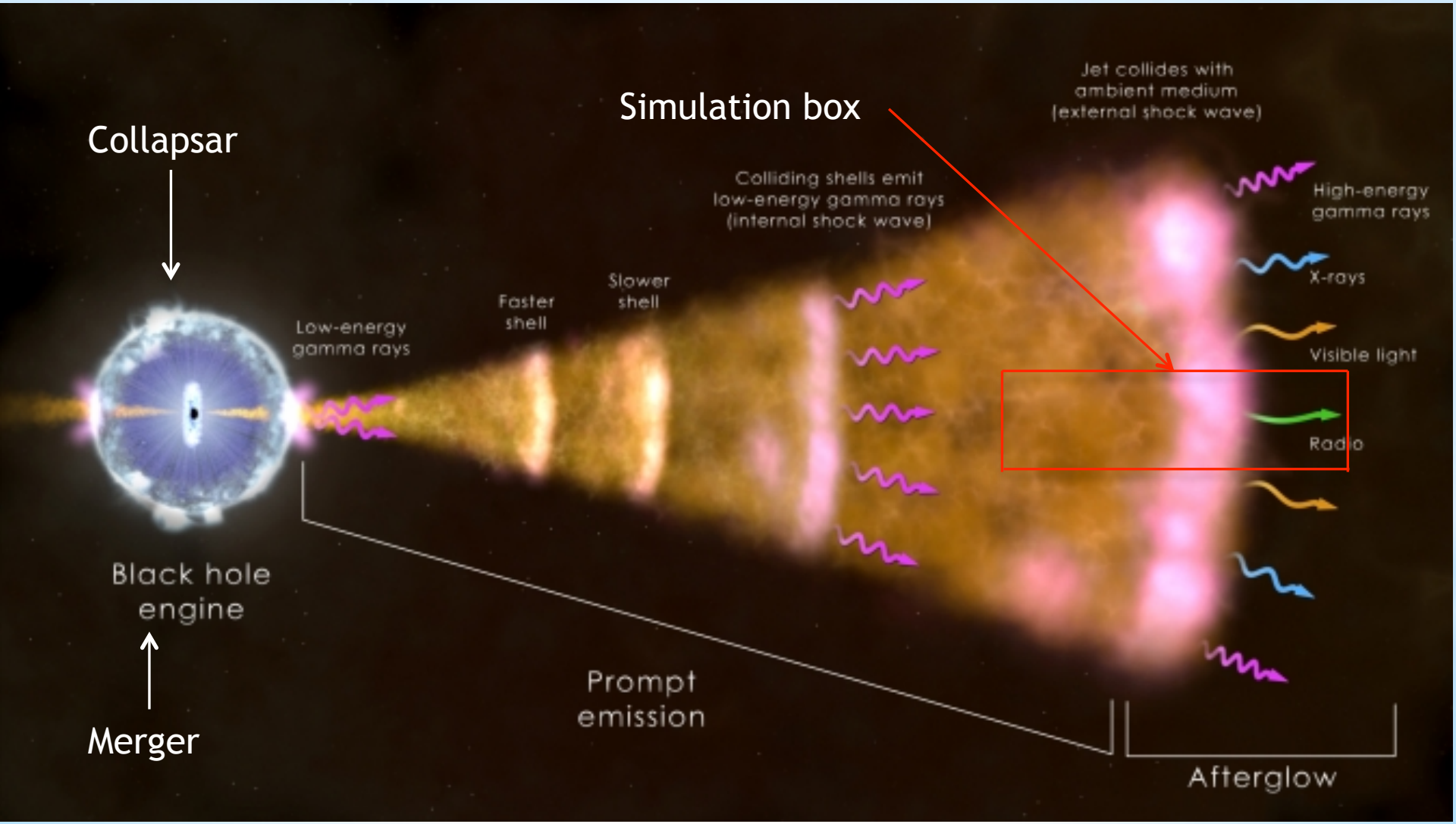

Schematic GRB from a massive stellar progenitor

(Meszaros, Science 2001)

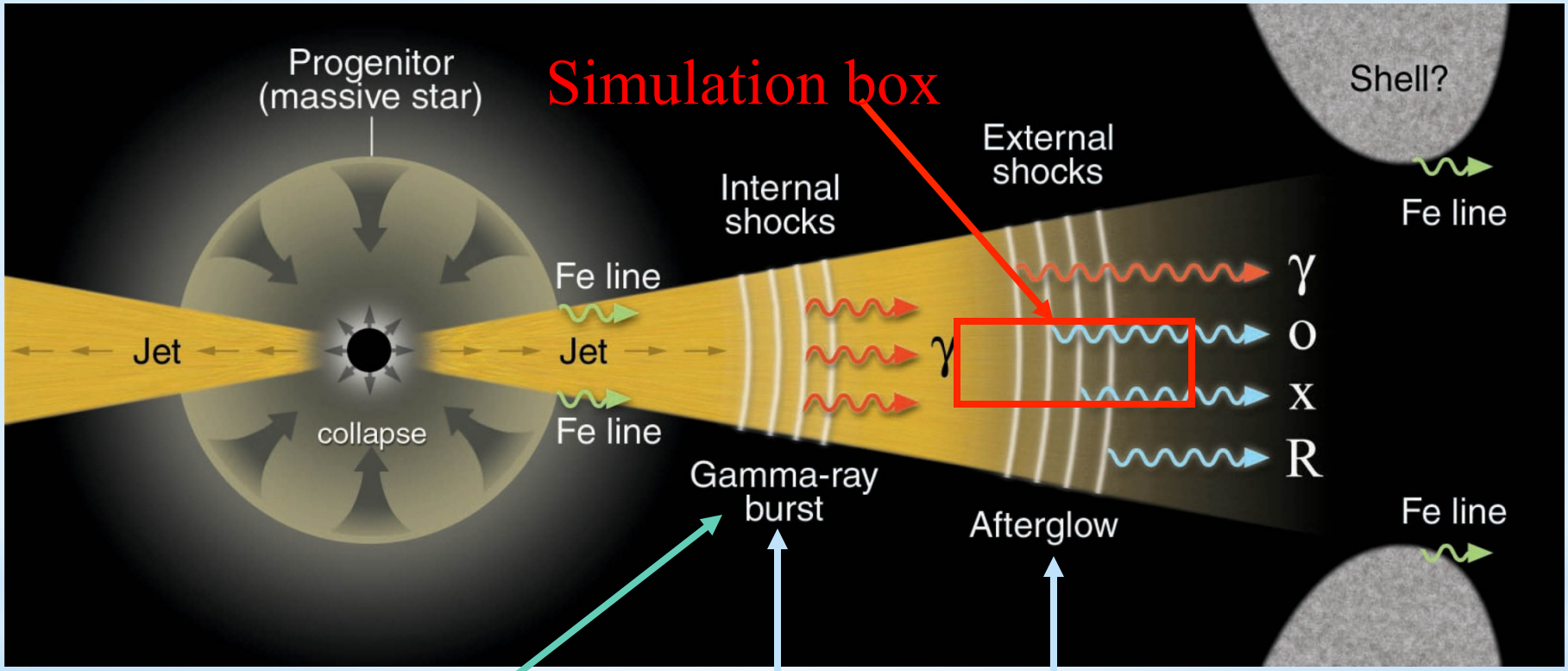

Prompt emission

Polarization ?

Accelerated particles emit waves at shocks

3-D simulation

with MPI code

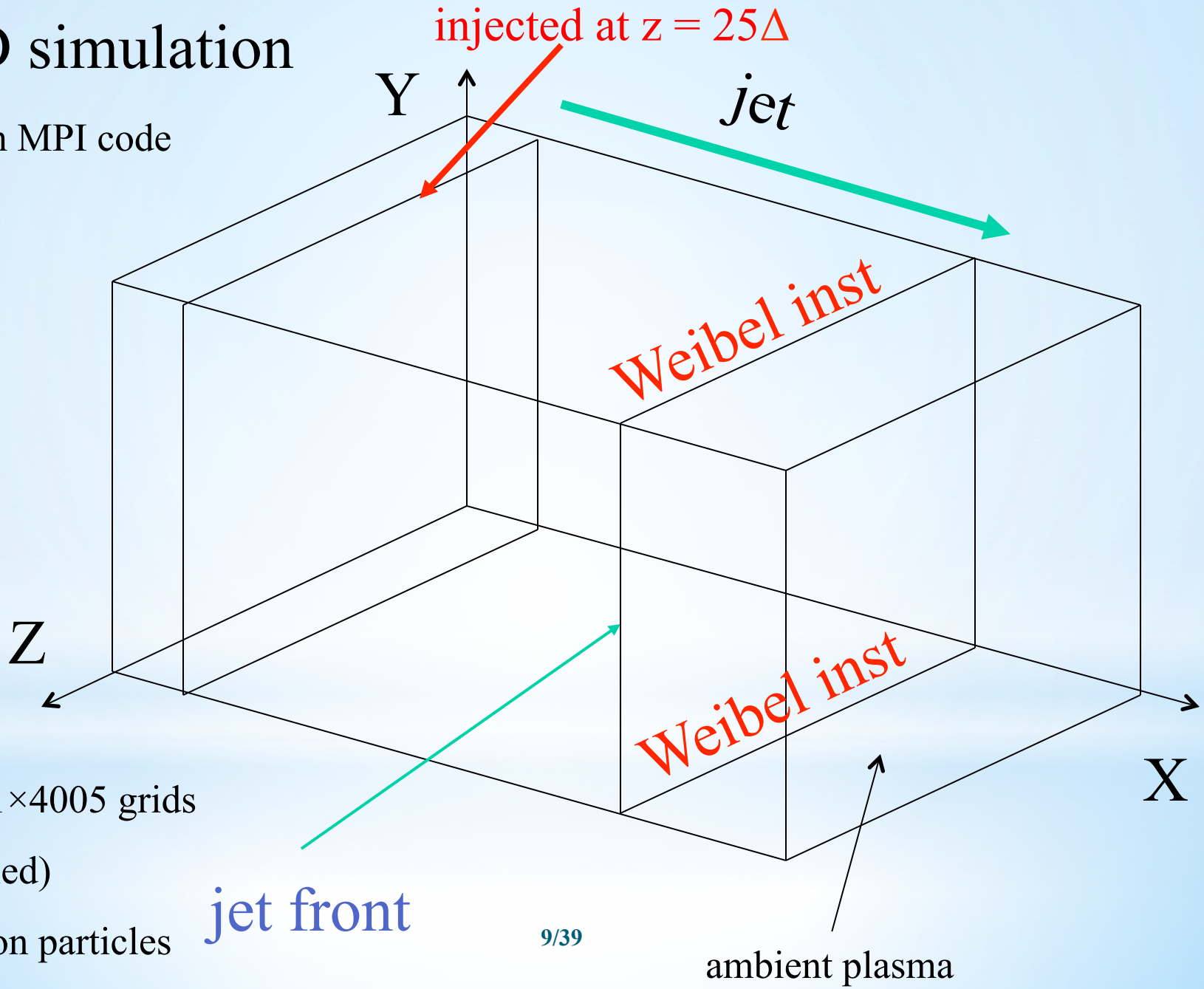

131×131×4005 grids

(not scaled)

1.2 billion particles

Collisionless shock

Electric and magnetic fields created self-consistently by particle dynamics randomize particles

(Buneman 1993)

$$\partial B / \partial t = -\nabla \times E$$
$$\partial E / \partial t = \nabla \times B - J$$
$$dm_0 \gamma v / dt = q(E + v \times B)$$
$$\partial \rho / \partial t + \nabla \bullet J = 0$$

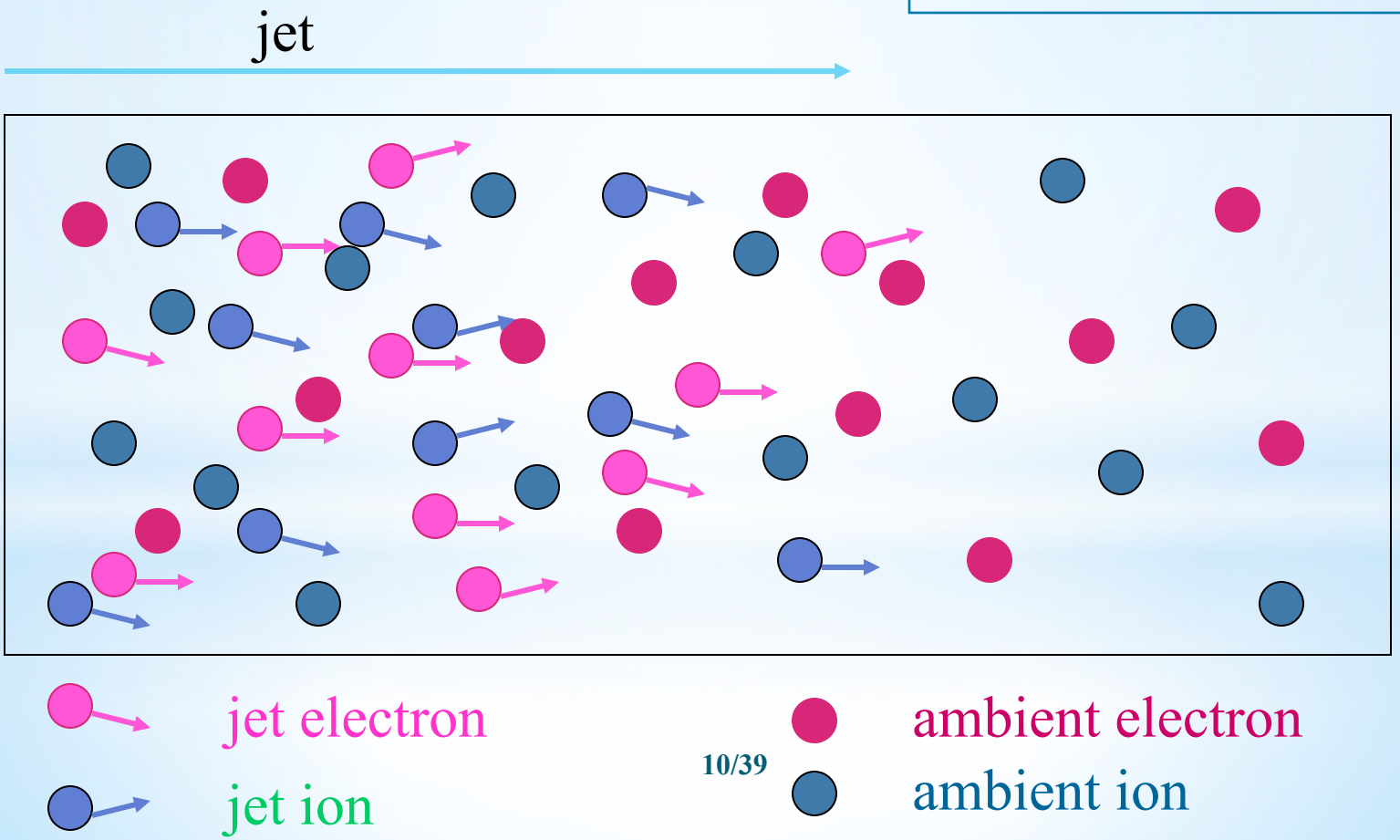

Weibel instability

current filamentation

Time:

$\tau = \gamma_{sh}^{1/2}/\omega_{pe} \approx 21.5$

Length:

$\lambda = \gamma_{th}^{1/2} c/\omega_{pe} \approx 9.6\Delta$

jet

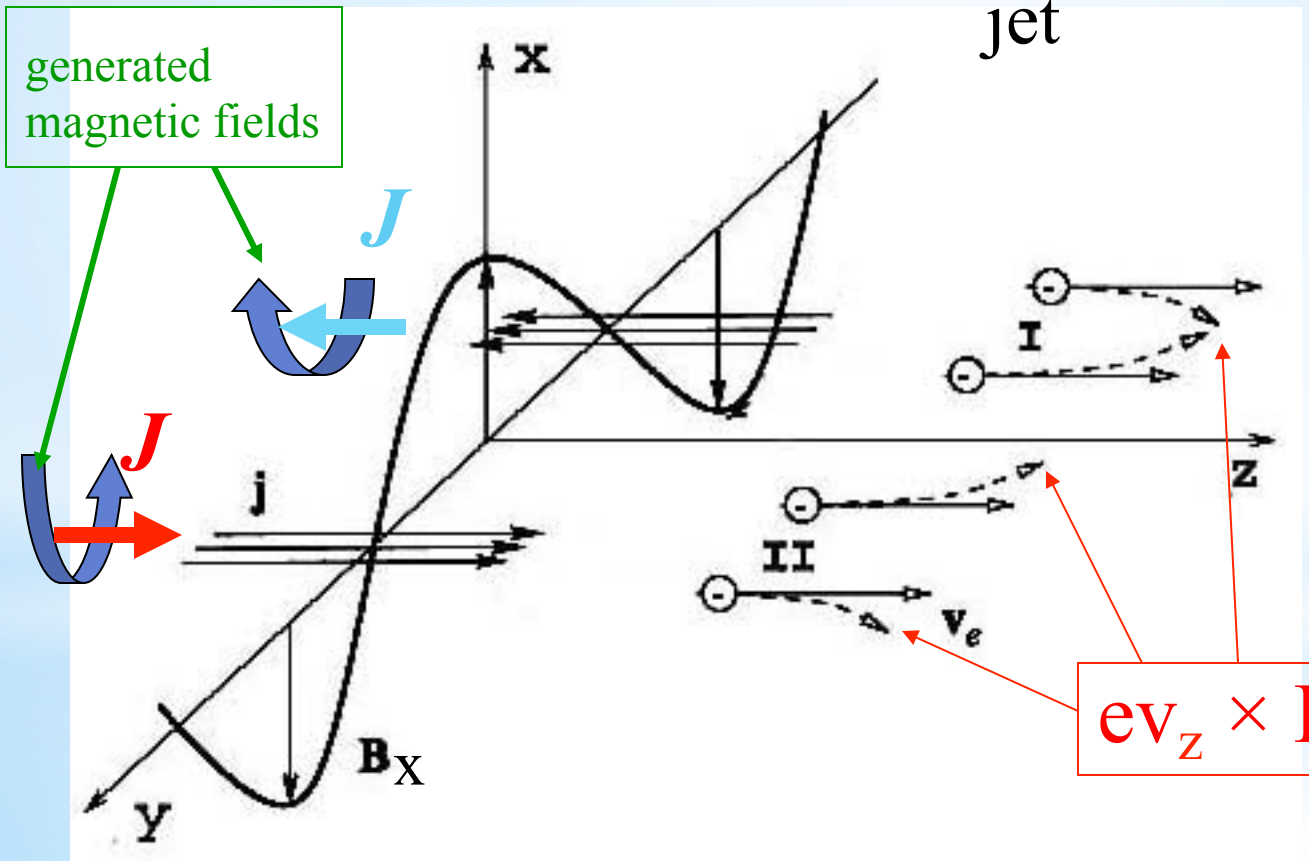

(Medvedev & Loeb, 1999, ApJ)

Evolution of B_x due to the Weibel instability

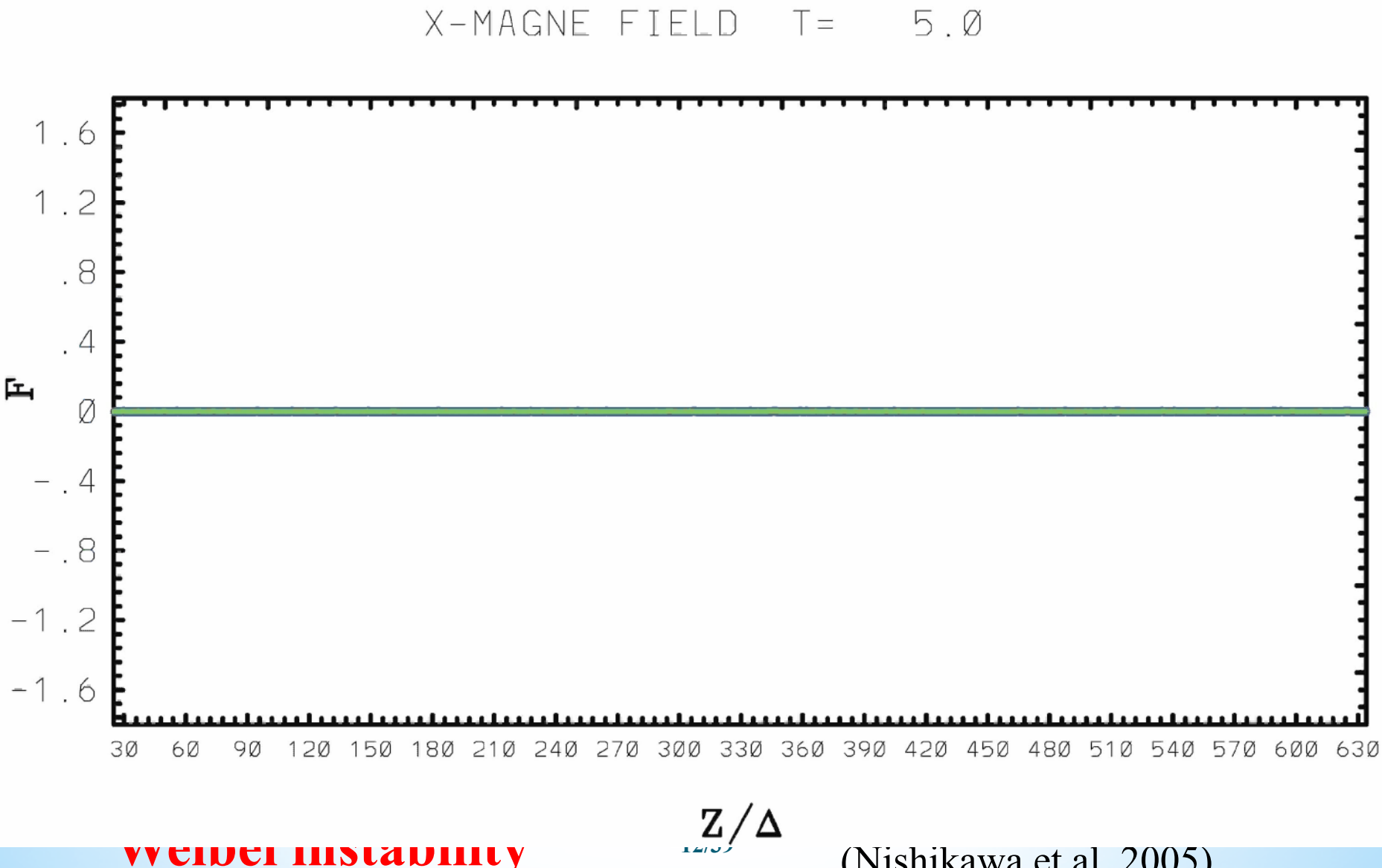

Weibel instability

(Nishikawa et al. 2005)

Ion Weibel instability

ion current

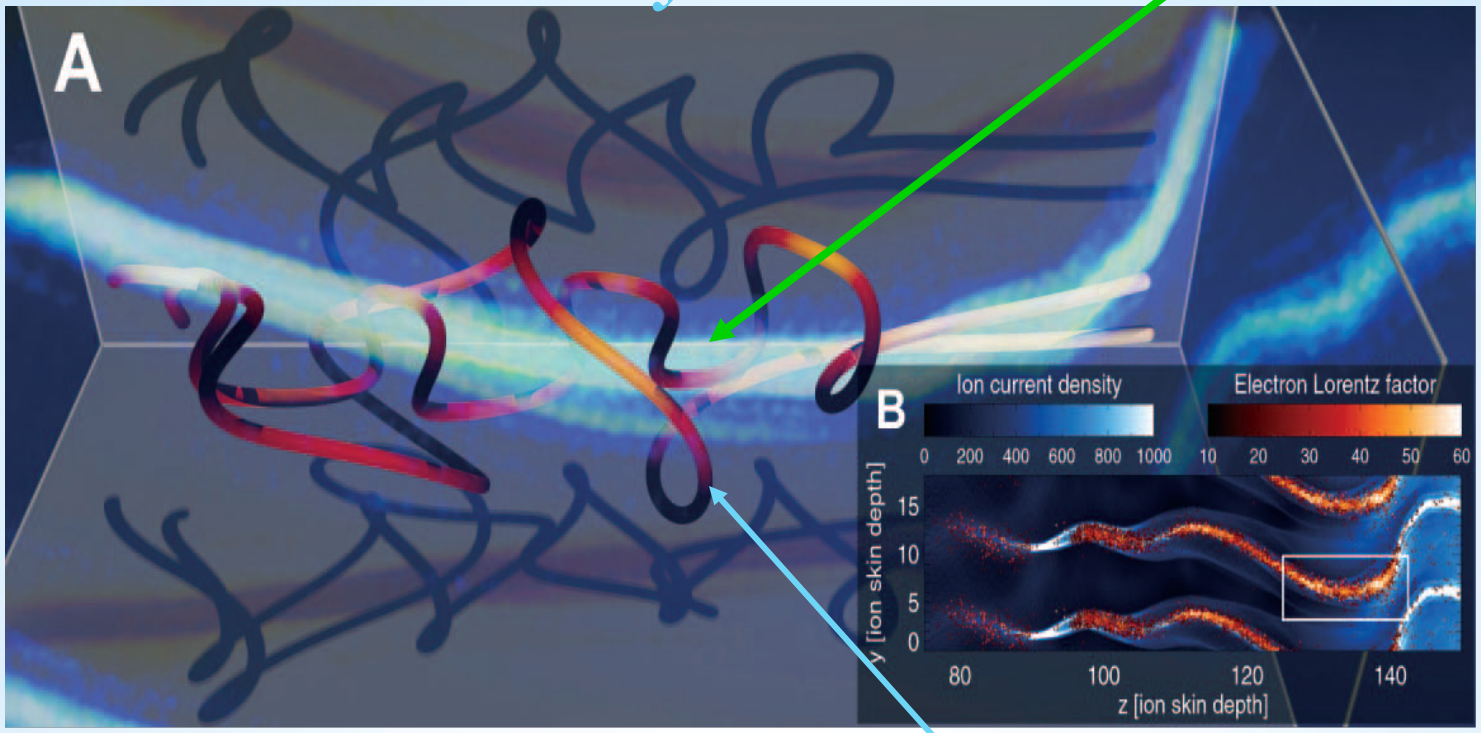

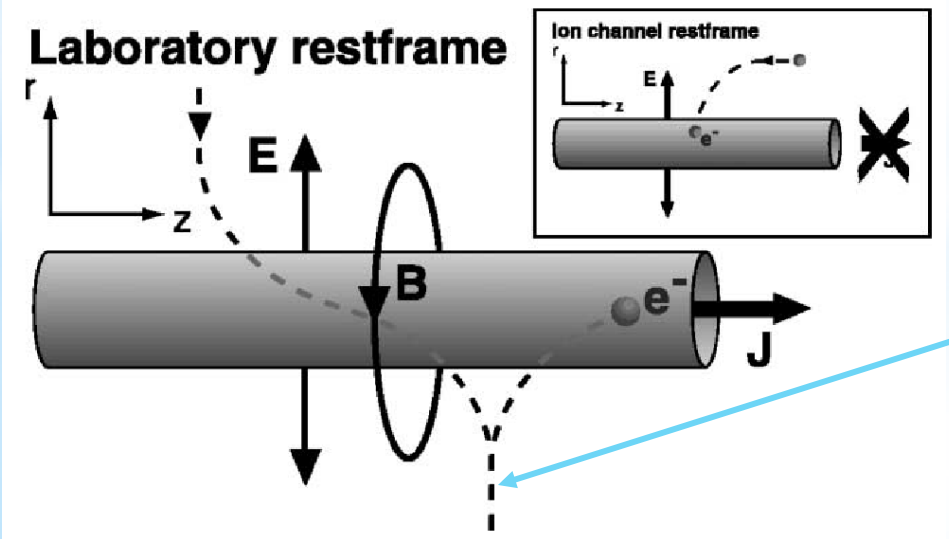

E × B acceleration

electron trajectory

(Hededal et al 2004)

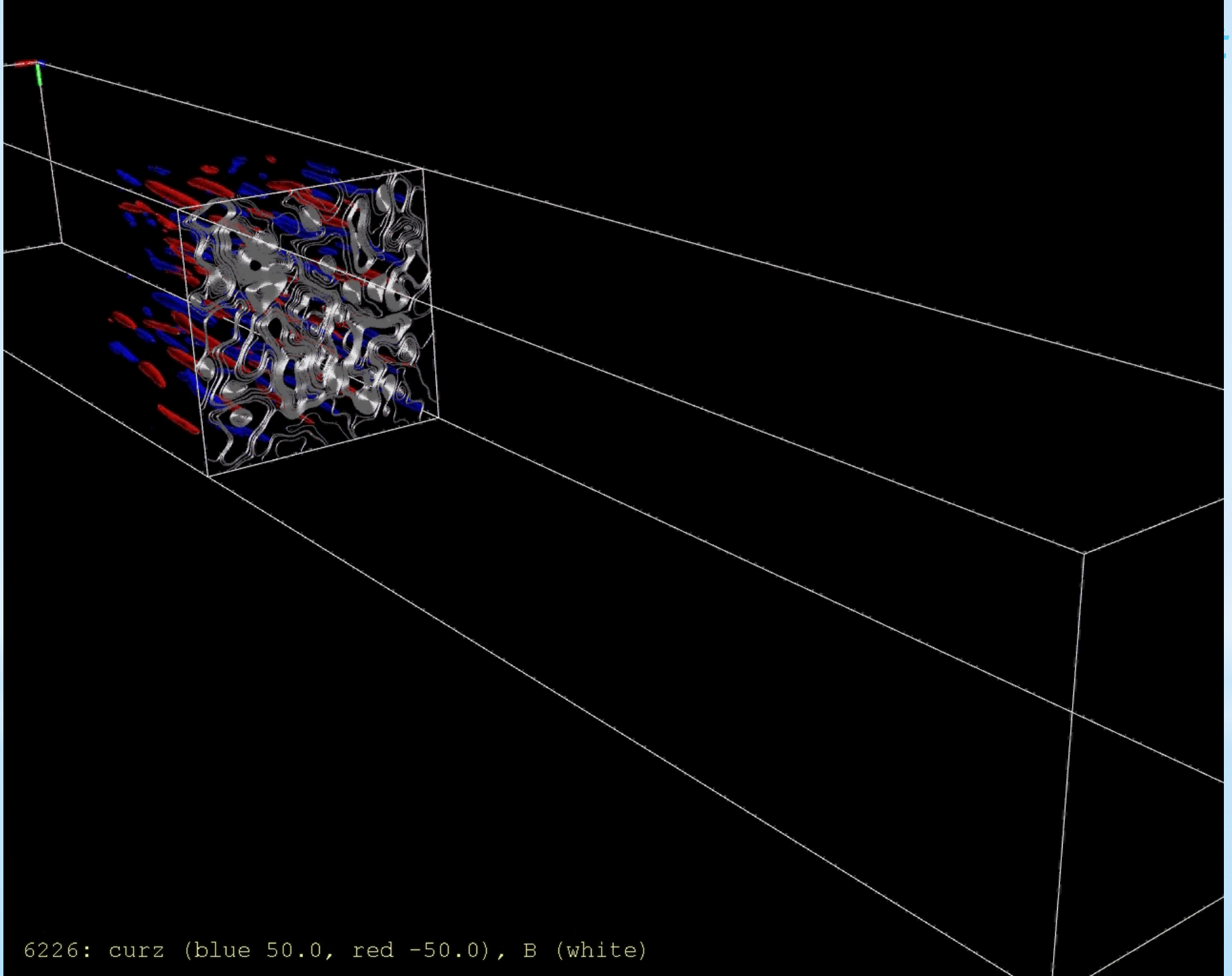
6226: curz (blue 50.0, red -50.0), B (white)

Fermi acceleration (self-consistent with turbulent magnetic field)

$\omega_{pe}t = 8400$

density

ε_B

Av.density

Av. ε_B

electron x-v_x

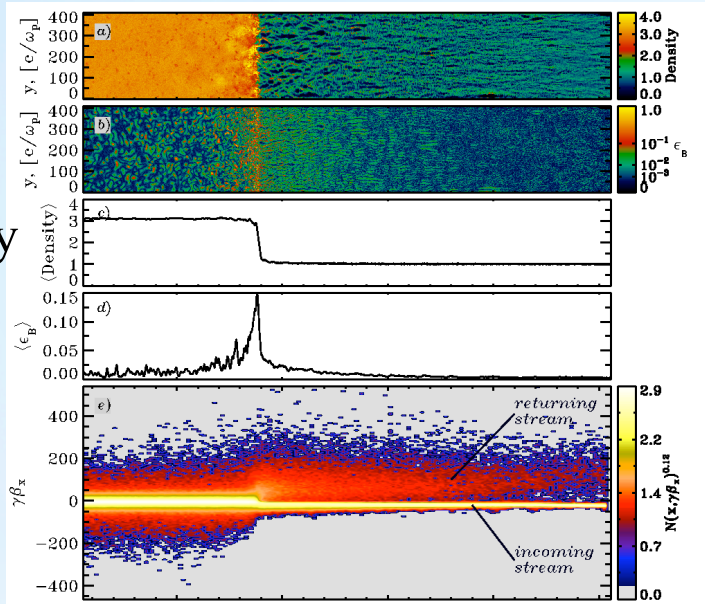

Fermi acceleration has been done with self-consistent magnetic fields (Spitkovsky, ApJ, 2008)

particle spectrum at $\omega_{pe}t = 10^4$

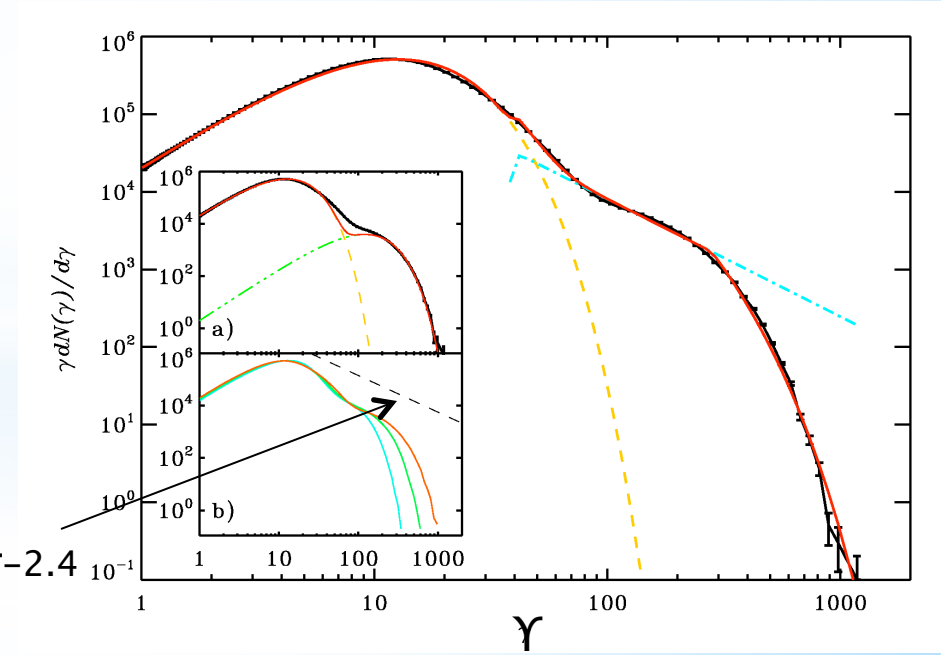

particle trajectories

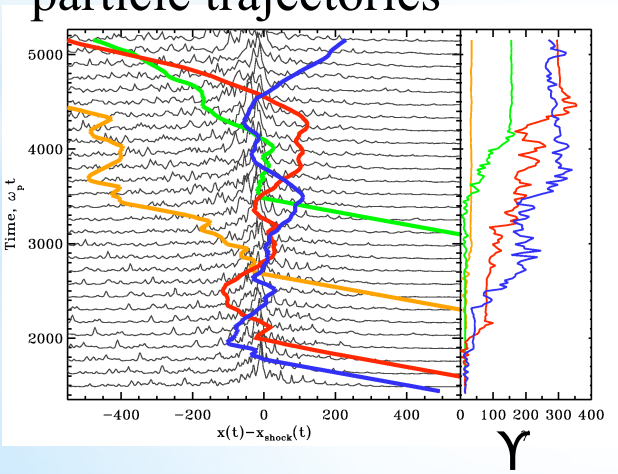

Shock velocity and bulk velocity

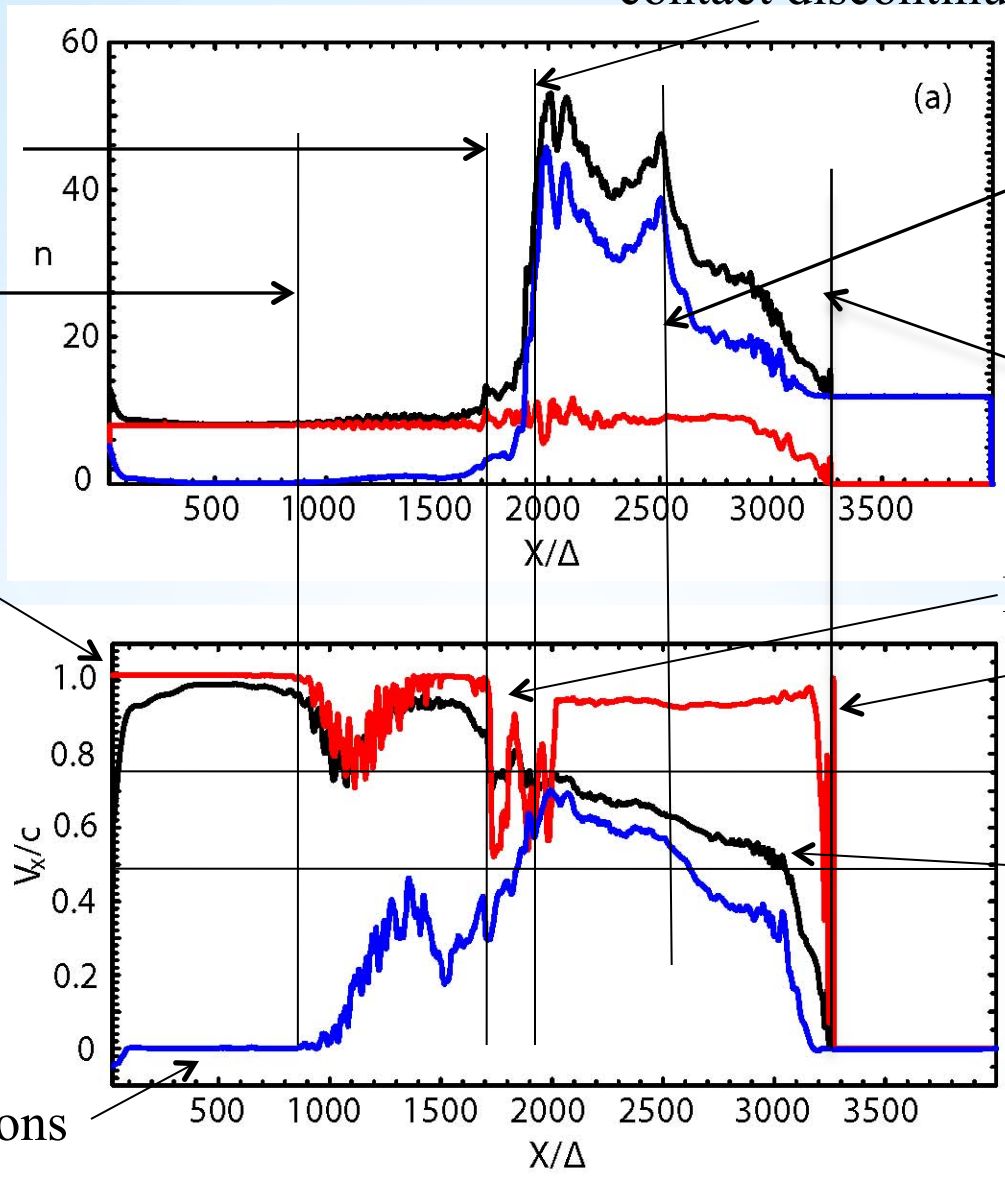

(Nishikawa et al. 2009)

Comparison with different mass ratio (electron-positron and electron-ion)

electron-positron

electron-ion ($m_i/m_e = 20$)

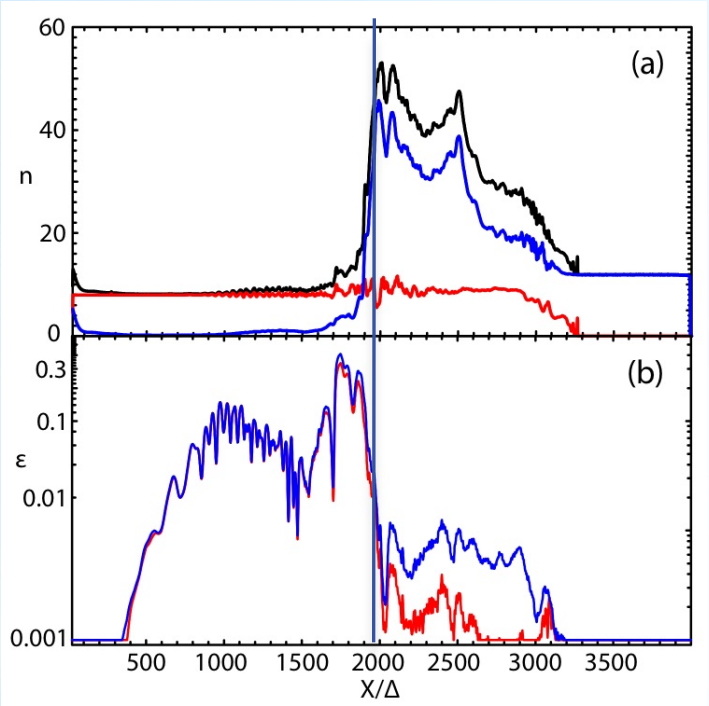

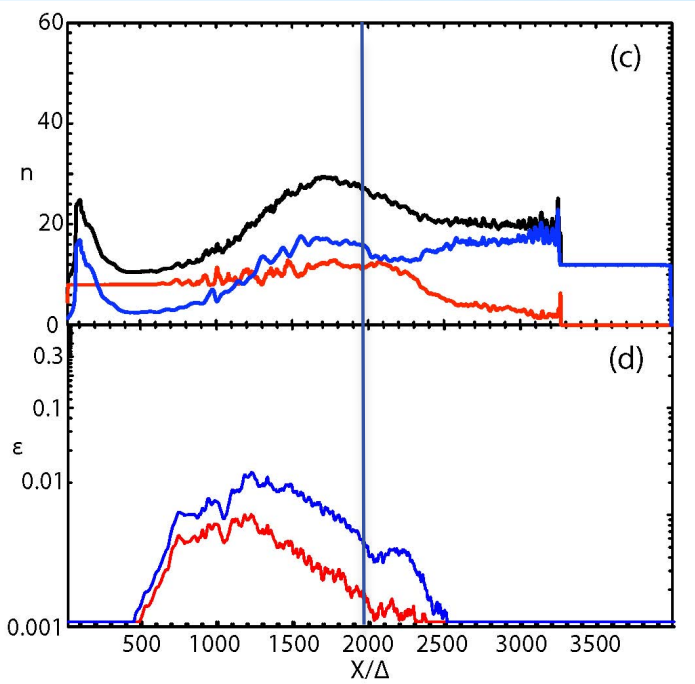

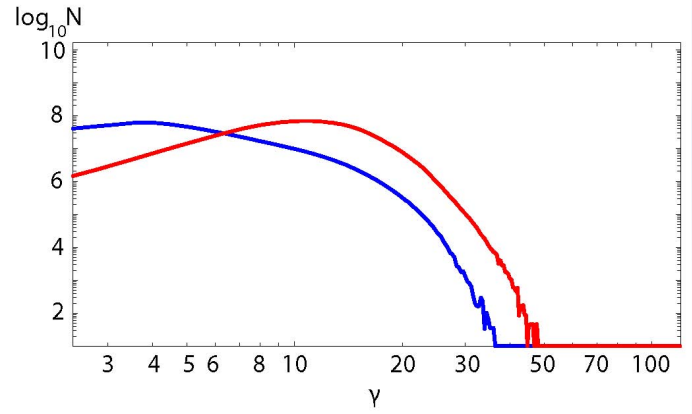

X/Δ>2000

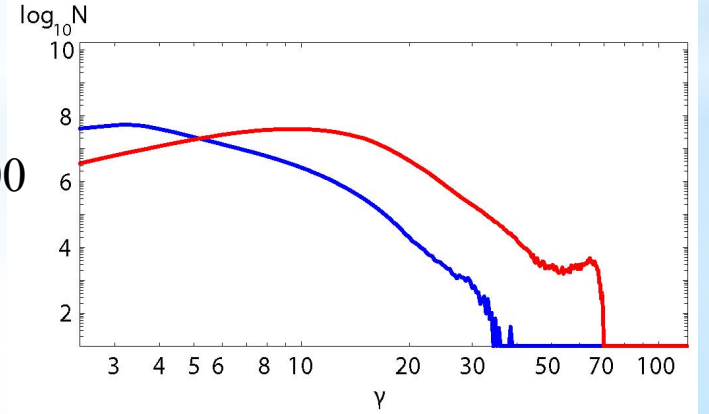

Recent electron-ion simulation (Electrostatic shock and double layer)

$m_i/m_e = 20$

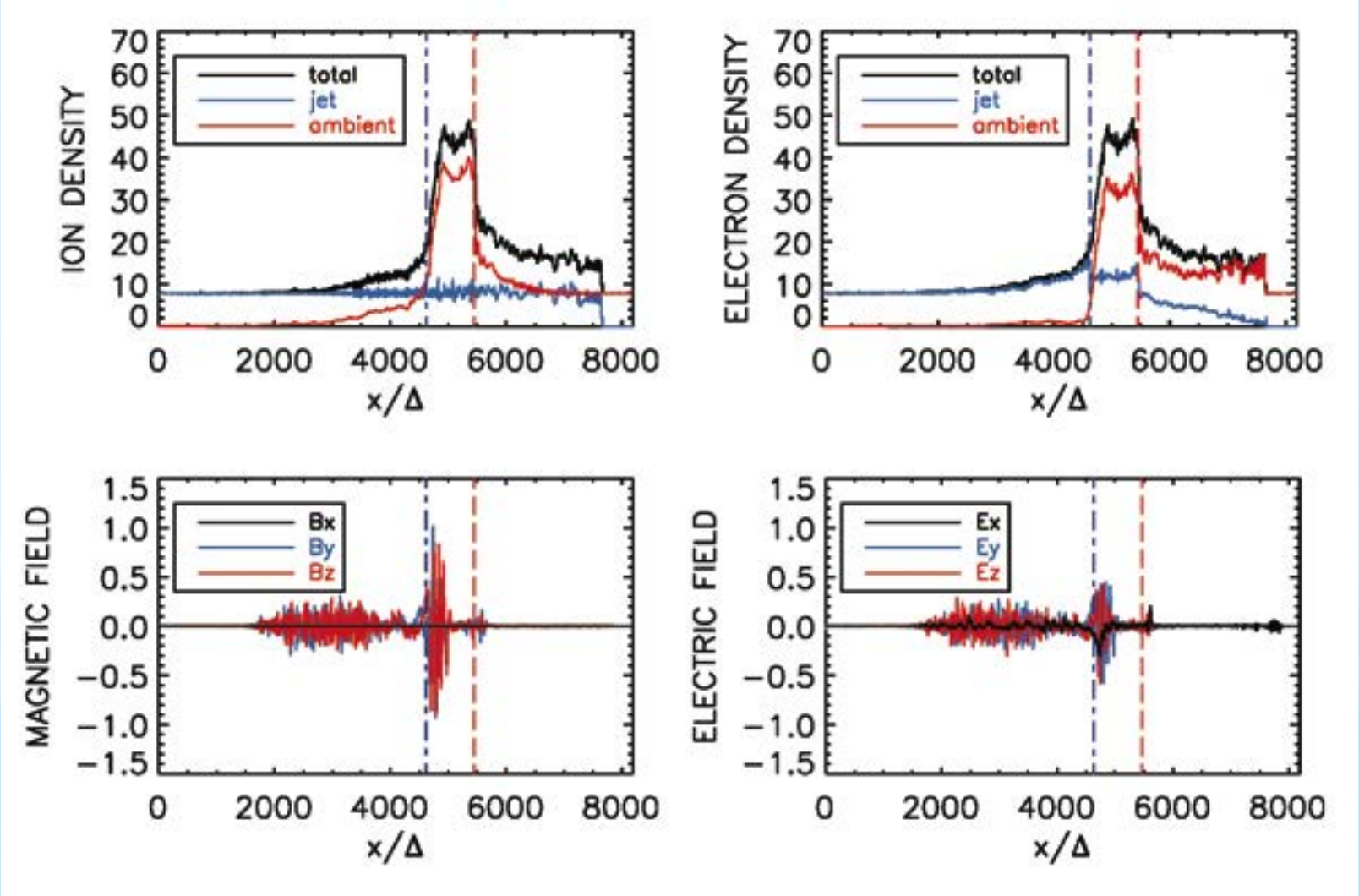

(Choi et al. PoP, 2014)

Shock formation, forward shock, reverse shock

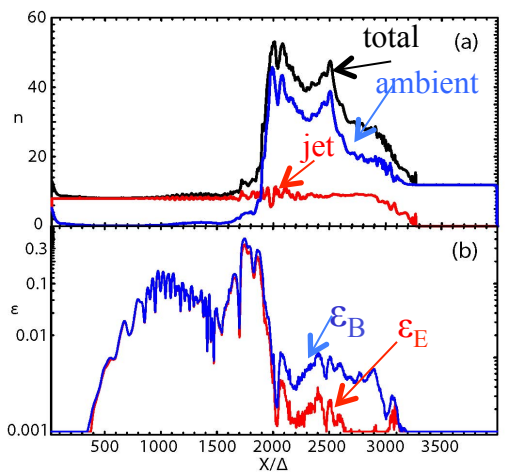

(a) electron density and
(b) electromagnetic field energy (ε_B, ε_E) divided by the total kinetic energy at $t = 3250\omega_{pe}^{-1}$

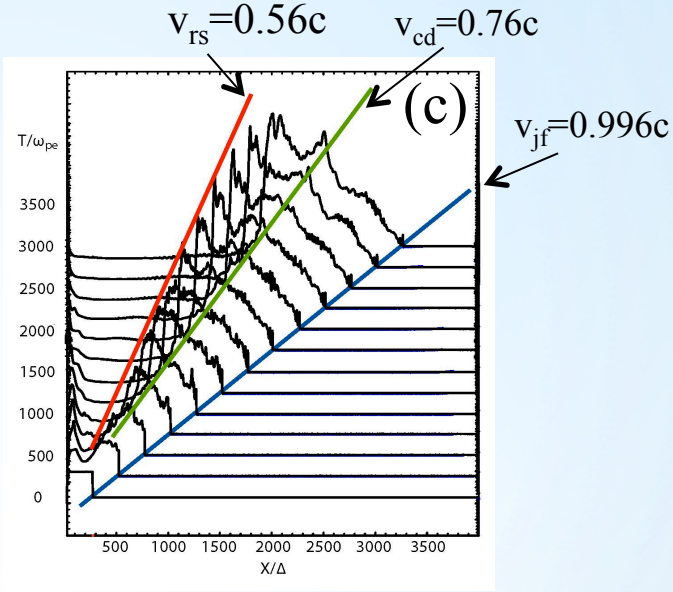

Time evolution of the total electron density. The velocity of the jet front is ~c, the predicted contact discontinuity speed is 0.76c, and the velocity of the reverse shock is 0.56c.

reverse shock region has strong magnetic fields and contributes to radiation

(Nishikawa et al. ApJ, 698, L10, 2009)

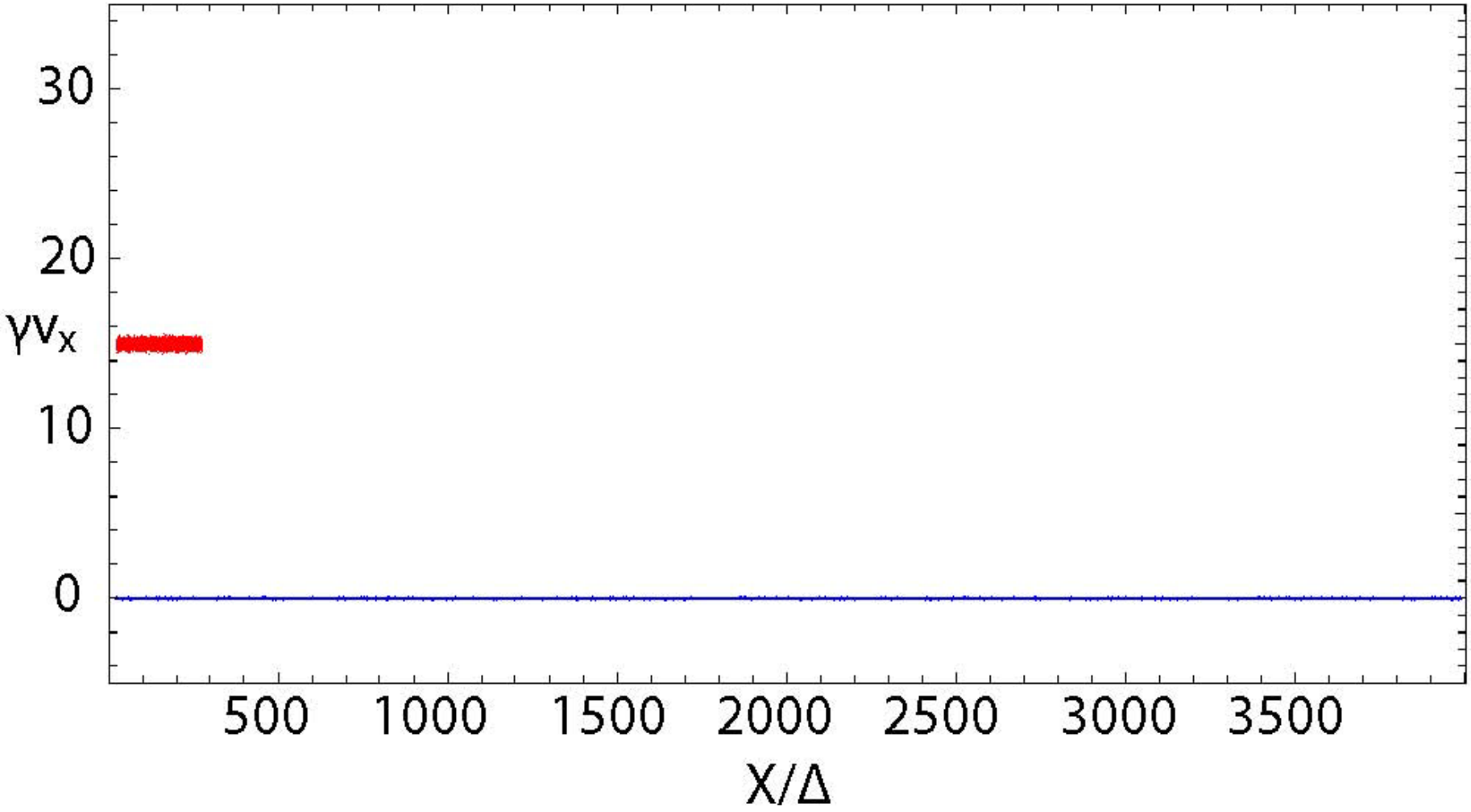

(Nishikawa et al. ApJ, 698, L10, 2009)

Shock … e shock

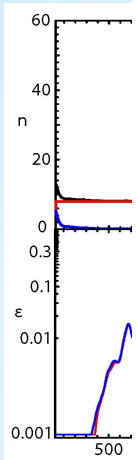

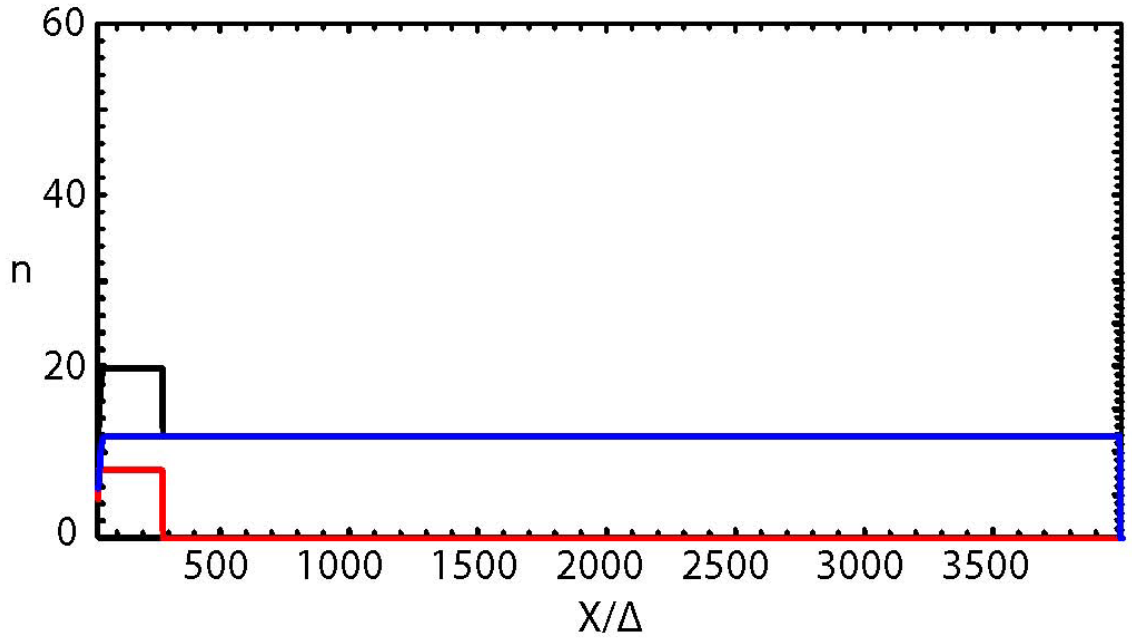

.996c

(a) (

(b)

fiel

divi

kine

t =

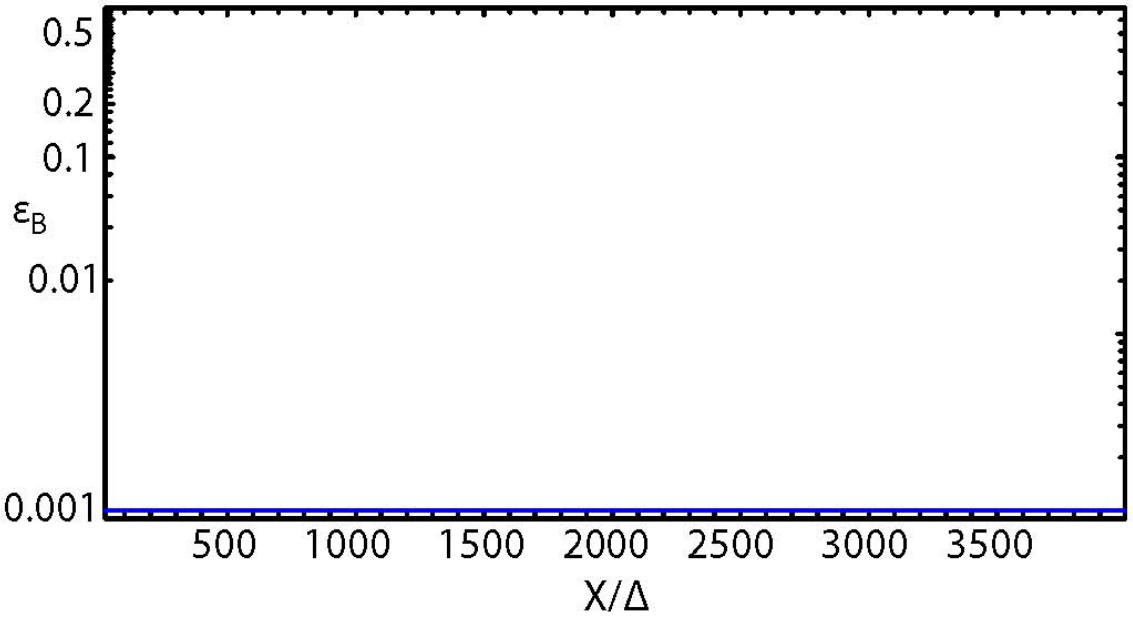

electron

jet front is ~c,

ntinuity speed

the reverse

Shock velocity and structure based on 1-D HD analysis

moving contact discontinuity (CD)

trailing shock
(reverse shock)

leading shock
(forward shock)

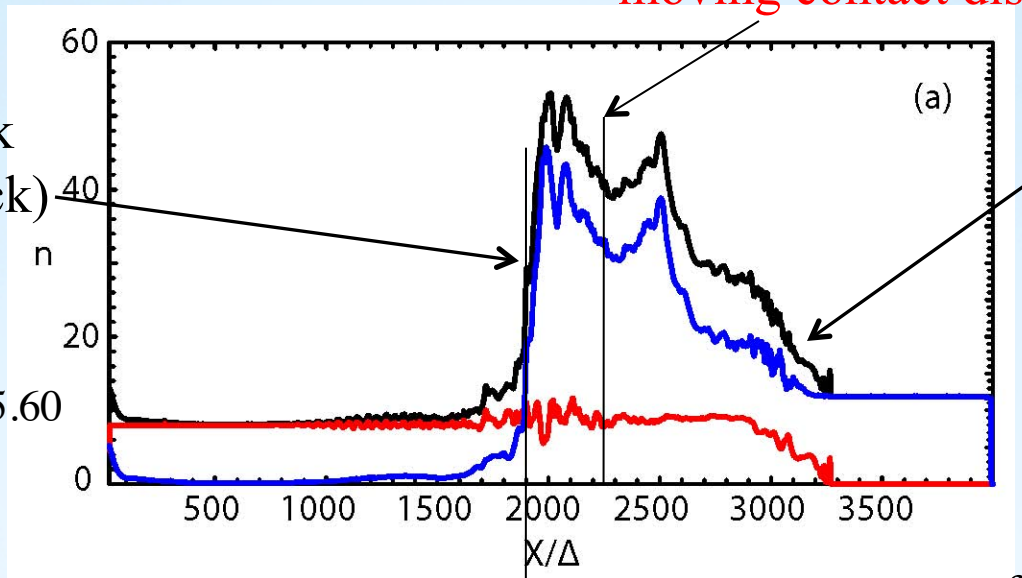

(Nishikawa et al. 2009)

in CD frame

$n_{sj}/\gamma'_{cd} n_j = 3.36$

$\beta_s = 0.417 \quad \gamma'_{cd} = 5.60$

$4/3 < \Gamma = 3/2 < 5/3$

fixed CD

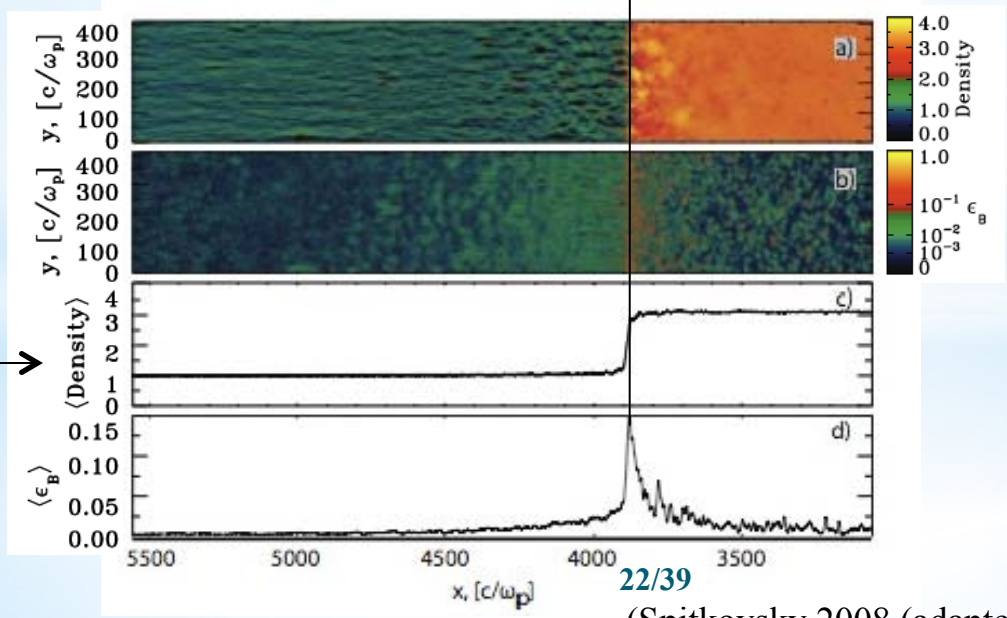

Density

$n_2/\gamma_0 n_1 = 3.13$

$\beta_c = 0.47$

$\gamma_0 = 15$

0

(Spitkovsky 2008 (adapted))

Simulations of Kinetic Kelvin-Helmholtz instability with counter-streaming flows (γ_0 = 3, m_i/m_e=1836)

magnetic field lines

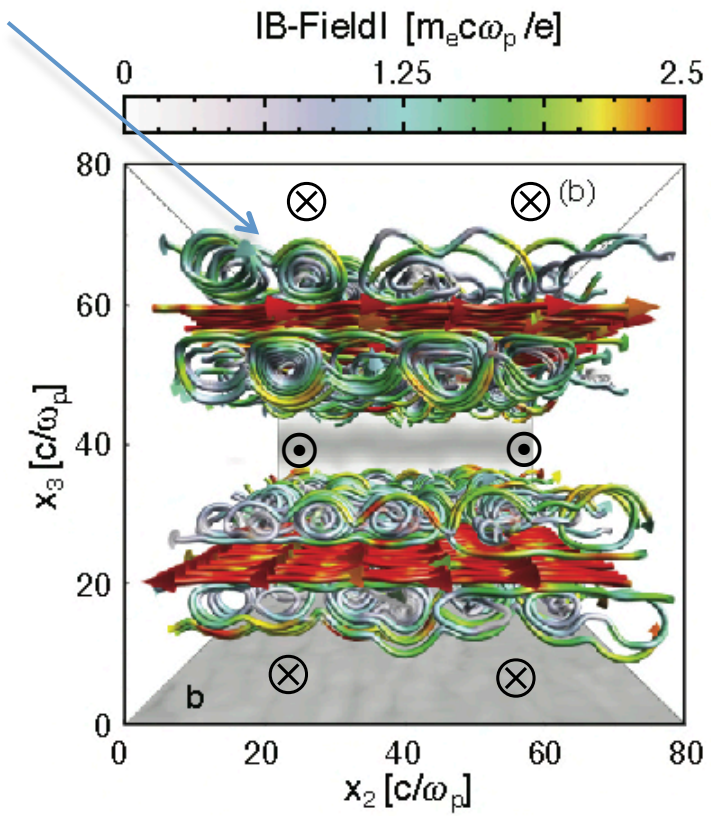

electron density

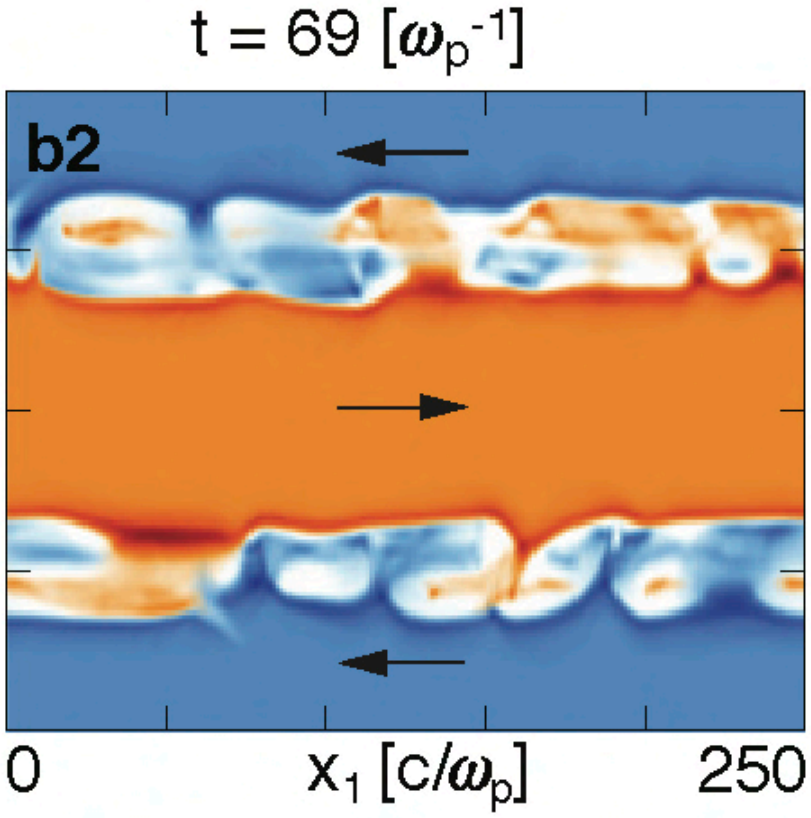

Alves et al. (2012)

Magnetic field lines

(Alves et al. ApJL, 2012)

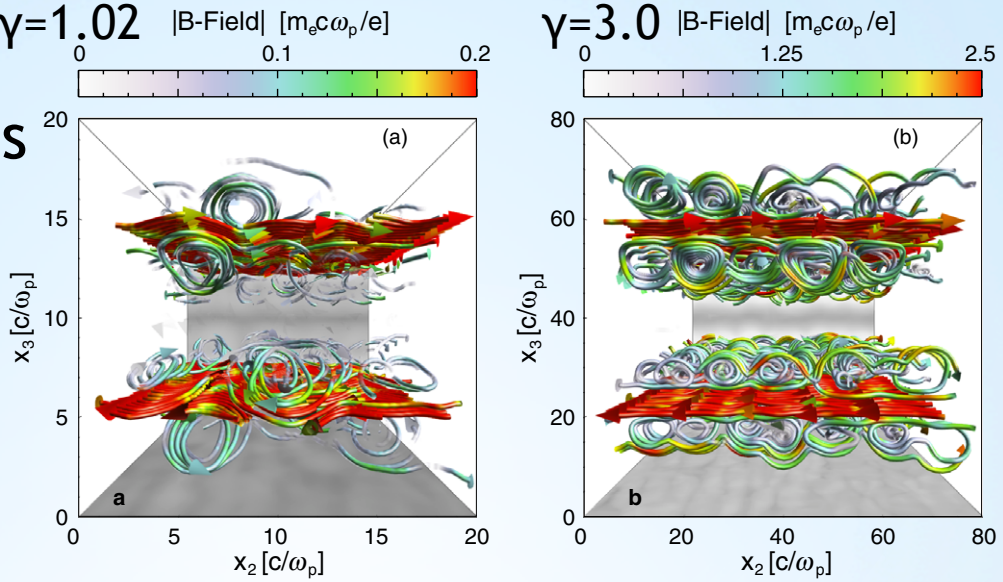

Figure 3. Magnetic field lines generated in (a) the subrelativisitc scenario, and (b) the relativistic scenario, at time $t = 100/\omega_p$.
(A color version of this figure is available in the online journal.)

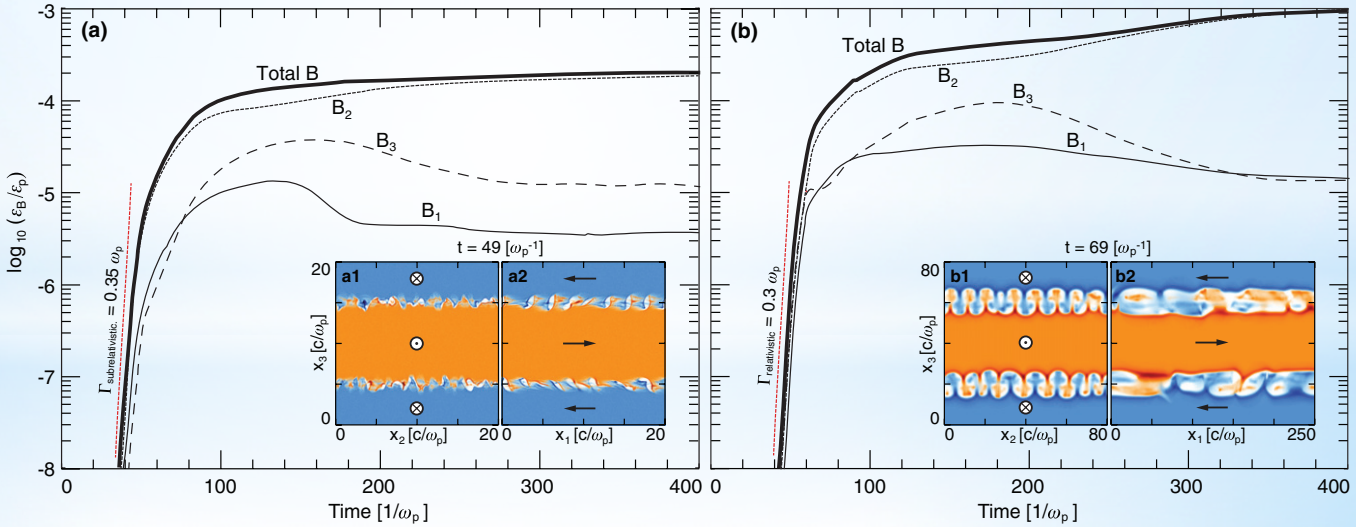

Figure 4. Evolution of the equipartition energy ϵ_B/ϵ_p for a (a) subrelativistic and (b) relativistic shear scenarios. The contribution of each magnetic field component is also depicted. The insets in each frame represent two-dimensional slices of the electron density at $t = 49/\omega_p$ and $t = 69/\omega_p$ for the respective case. The red (blue) color represents the electron density of the plasma that flows in the positive (negative) x_1 direction. Darker regions in the color map indicate high electron density, whereas lighter regions indicate low electron density. Slices for insets (a1), (a2), (b1), and (b2) were taken at the center of the simulation box; (a1) and (b1) are transverse to the flow direction, and slices (a2) and (b2) are longitudinal to the flow direction.

(A color version of this figure is available in the online journal.)

Simulations of KHI with core and sheath jets

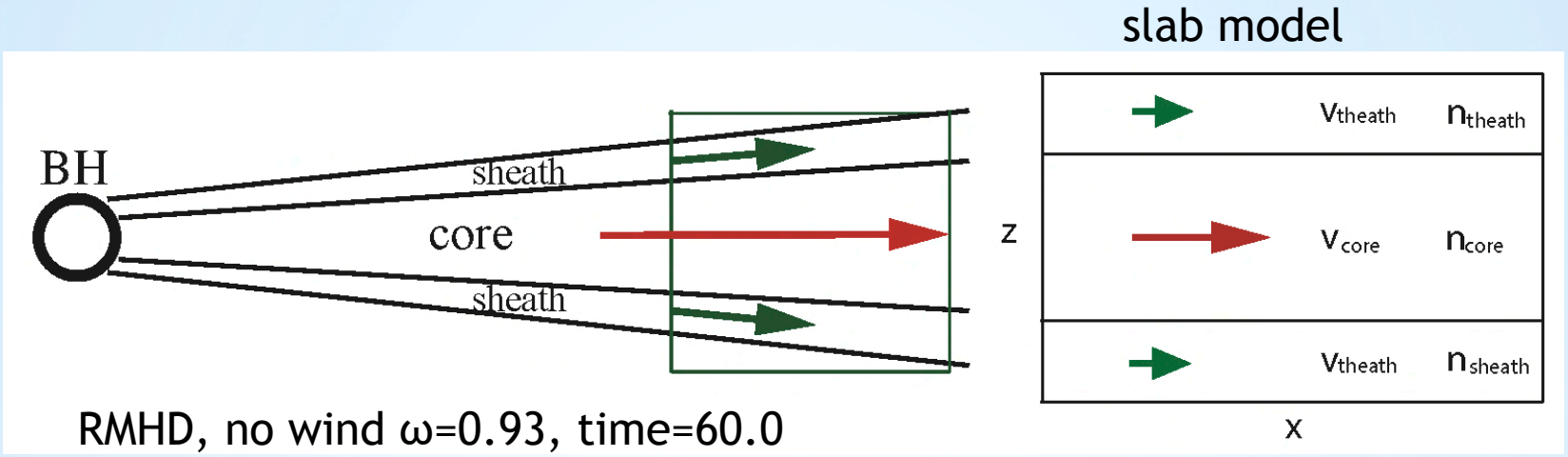

RMHD, no wind ω=0.93, time=60.0

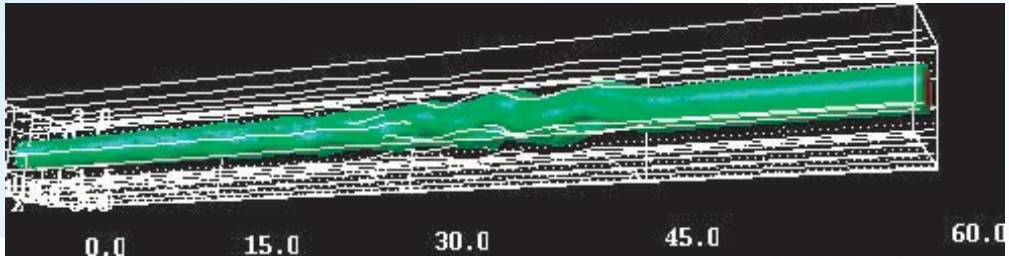

case of $V_{theath} = 0$

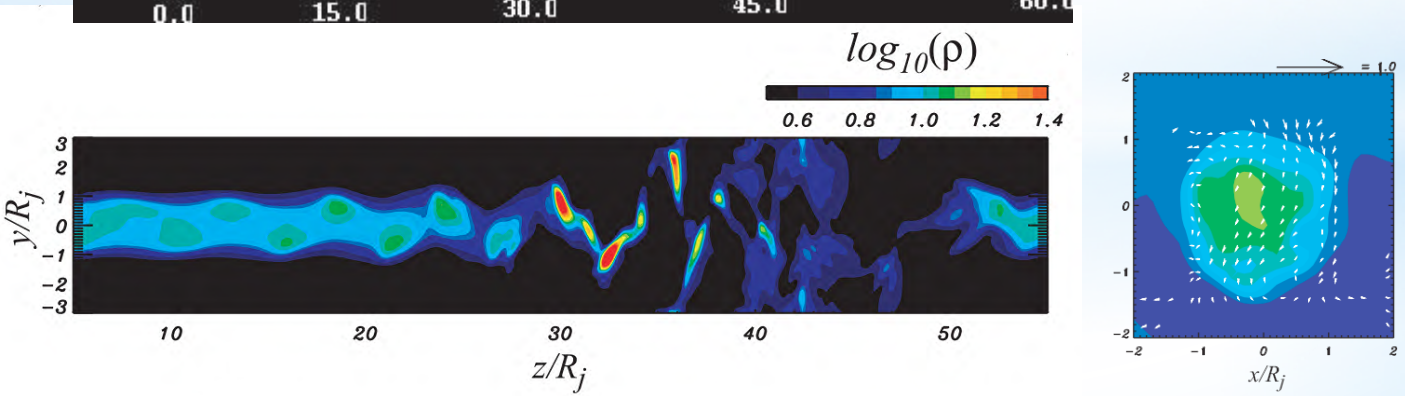

Mizuno, Hardee & Nishikawa, ApJ, 662, 835, 2007

KKHI with Core-sheath plasma scheme

γ_{jt} = 15 $\quad t = 300\omega_{pe}^{-1}$

B_y

e - p $\qquad\qquad$ $e^{\pm}$

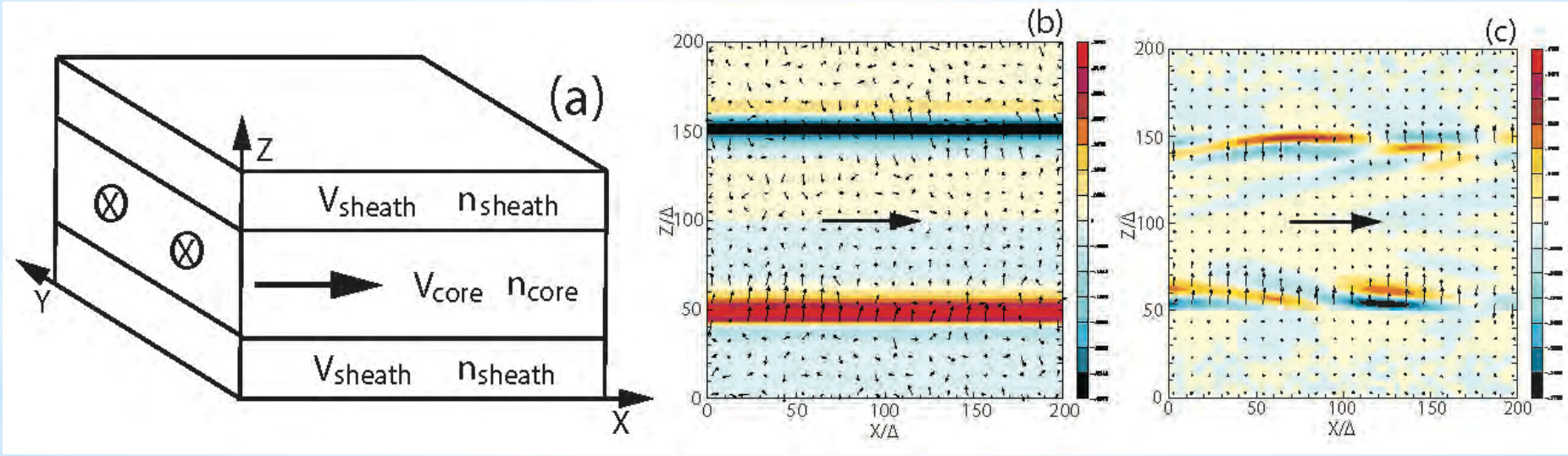

(Nishikawa et al. 2014, arXiv:1405.5247)

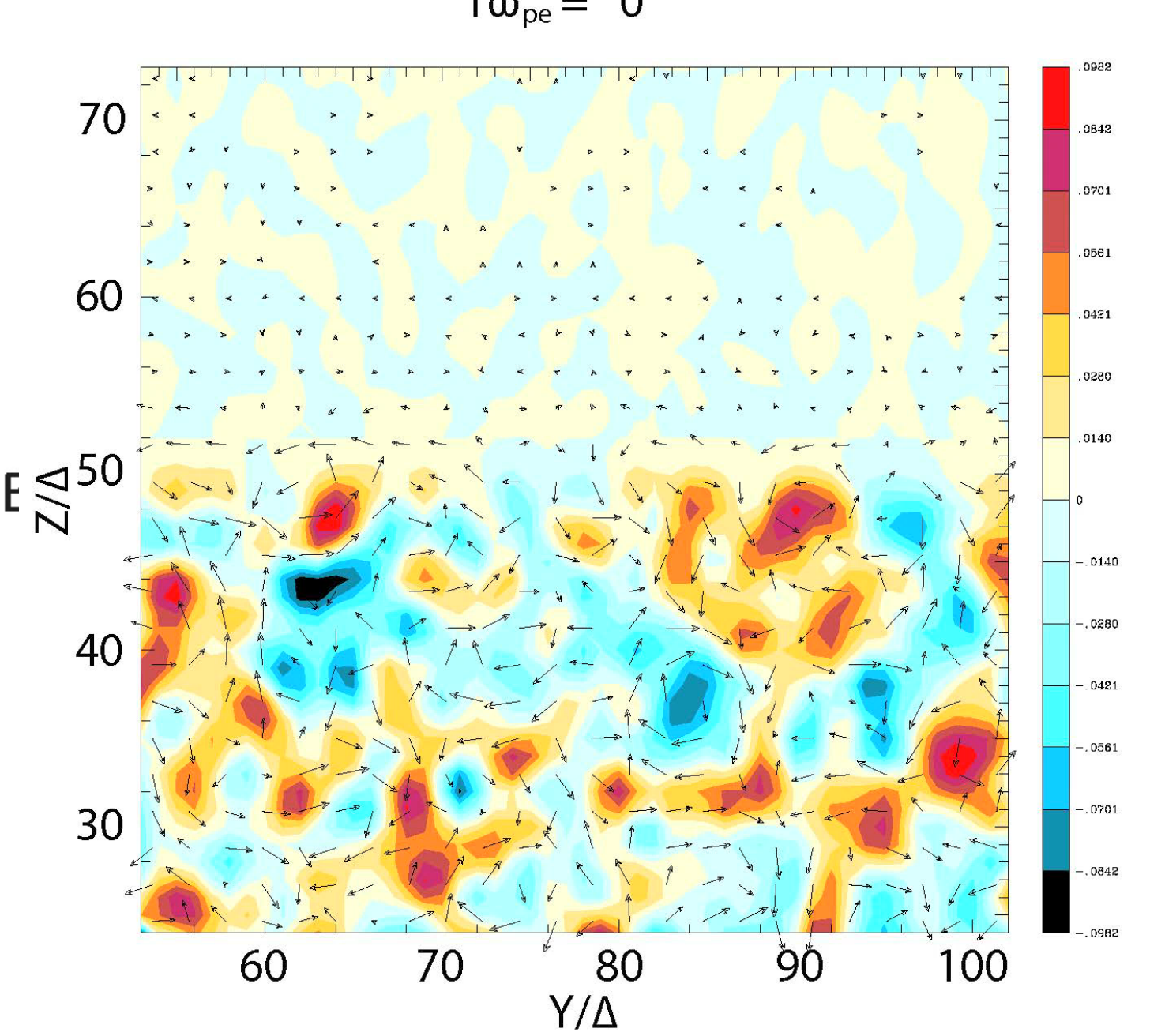
Tω_pe = 0
70
60
50
40
30
Z/Δ
60
70
80
90
100
Y/Δ
.0982
.0842
.0701
.0561
.0421
.0280
.0140
0
-.0140
-.0280
-.0421
-.0561
-.0701
-.0842
-.0982

Evolution of electric and magnetic field energy

$\gamma_j = 15, \quad m_i/m_e = 1836$

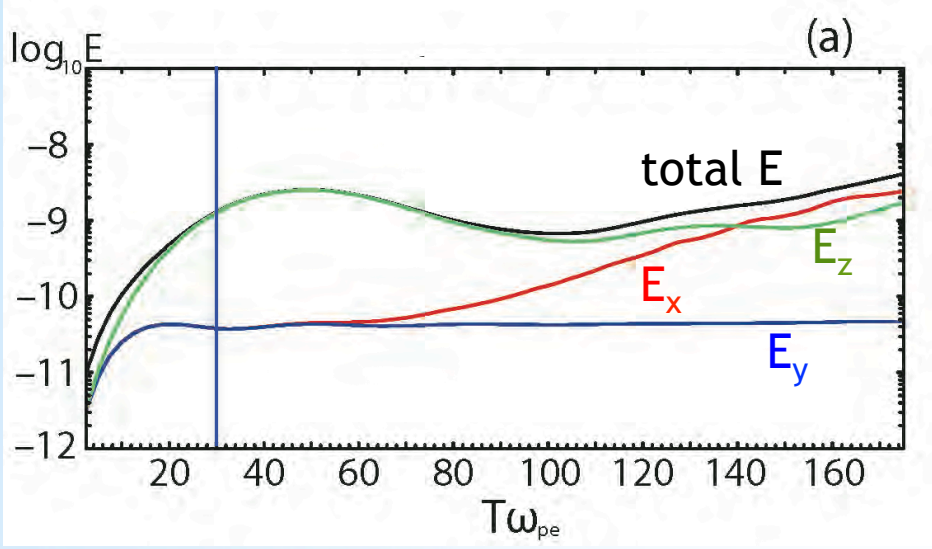

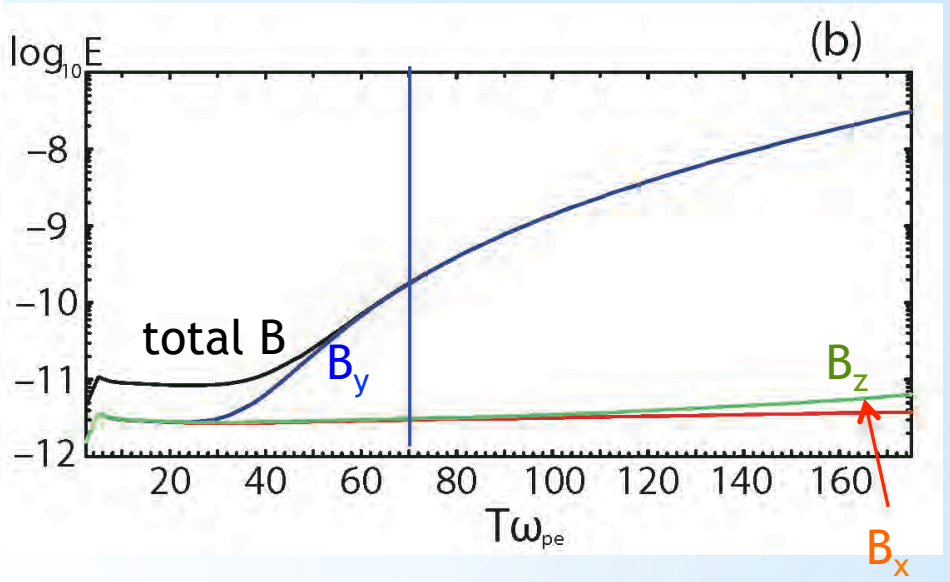

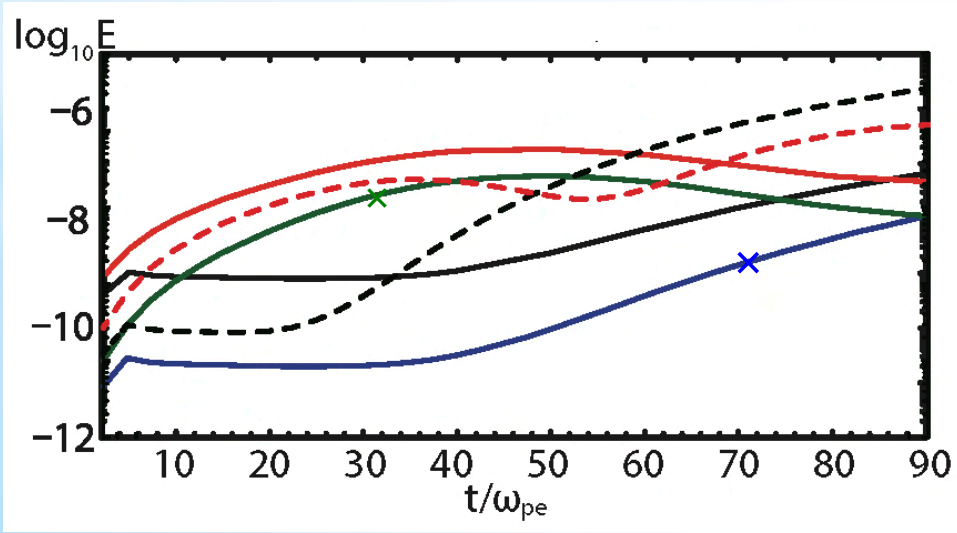

- total E, $\gamma_j = 15$, $m_i/m_e = 20$
- total B, $\gamma_j = 15$, $m_i/m_e = 20$
- total E, $\gamma_j = 15$, $m_i/m_e = 1836$
- total B, $\gamma_j = 15$, $m_i/m_e = 1836$
- total E, $\gamma_j = 1.5$, $m_i/m_e = 20$
- total B, $\gamma_j = 1.5$, $m_i/m_e = 20$

Electric field generation by KKHI with real mass ratio

$\gamma_j = 15$, $m_i/m_e = 1836$, $t = 30/\omega_{pe}$

$t = 70/\omega_{pe}$

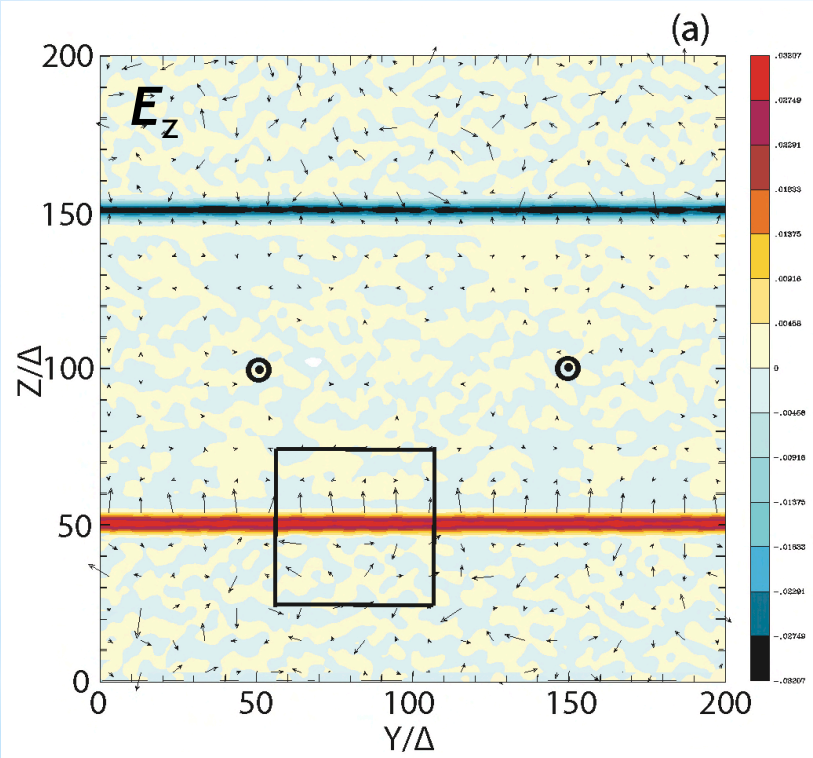

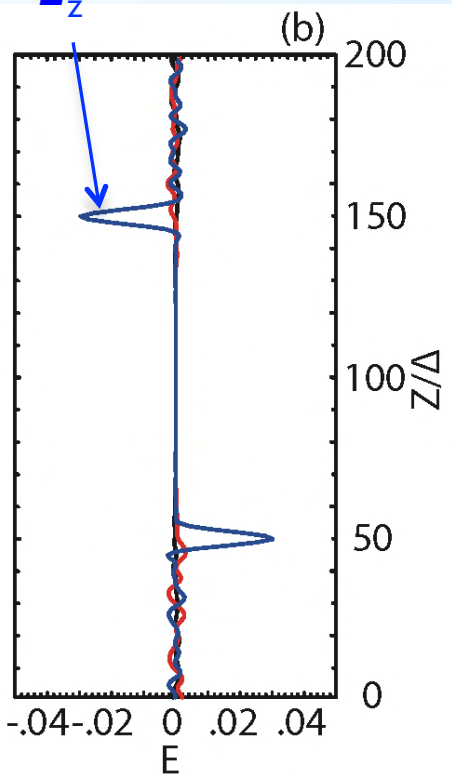

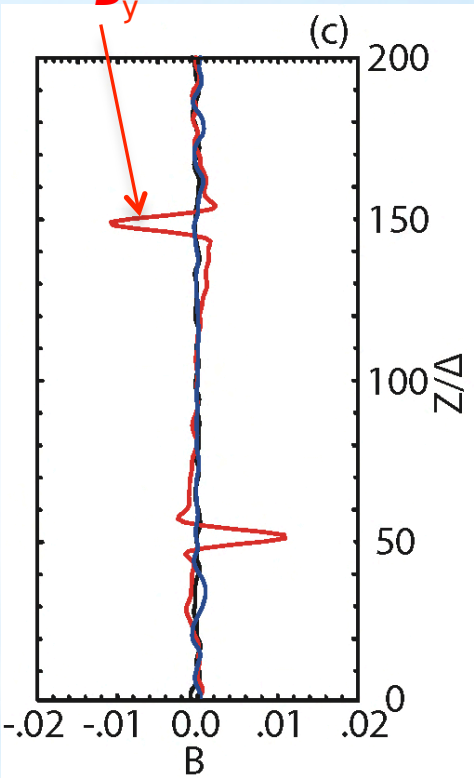

(Nishikawa et al. 2013)

Study of the relativistic velocity shear interface KKHI instability

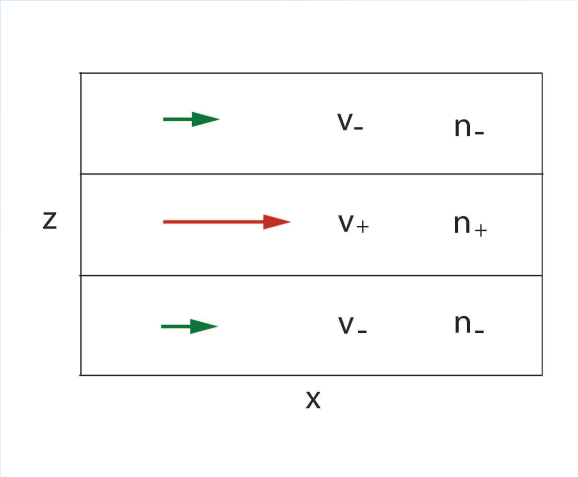

$$\omega_p \equiv 4\pi n e^2/\gamma^3 m,$$

$$e^{i(kx-\omega t)}$$

$$(k^2c^2+\gamma_-^2\omega_{p-}^2-\omega^2)^{1/2}(kV_- -\omega)^2[(kV_+-\omega)^2-\omega_{p+}^2]$$
$$+(k^2c^2+\gamma_+^2\omega_{p+}^2-\omega^2)^{1/2}(kV_+-\omega)^2[(kV_- -\omega)^2-\omega_{p-}^2]=0$$

Low-frequency limit ($V_-=0$)

$$\omega \sim \frac{(\gamma_{jt}\omega_{p,am}/\omega_{p,jt})}{(1+\gamma_{jt}\omega_{p,am}/\omega_{p,jt})}kV_{jt} \pm i\frac{(\gamma_{jt}\omega_{p,am}/\omega_{p,jt})^{1/2}}{(1+\gamma_{jt}\omega_{p,am}/\omega_{p,jt})}kV_{jt}.$$

(Nishikawa et al. 2014, arXiv:1405.5247)

Evolution of current filaments (J_x) and electric field (E_z)

$\gamma_j = 15, \quad m_i/m_e = 1836$

$t\omega_{pe} = 30$ $t\omega_{pe} = 40$ $t\omega_{pe} = 50$

J_x

E_z

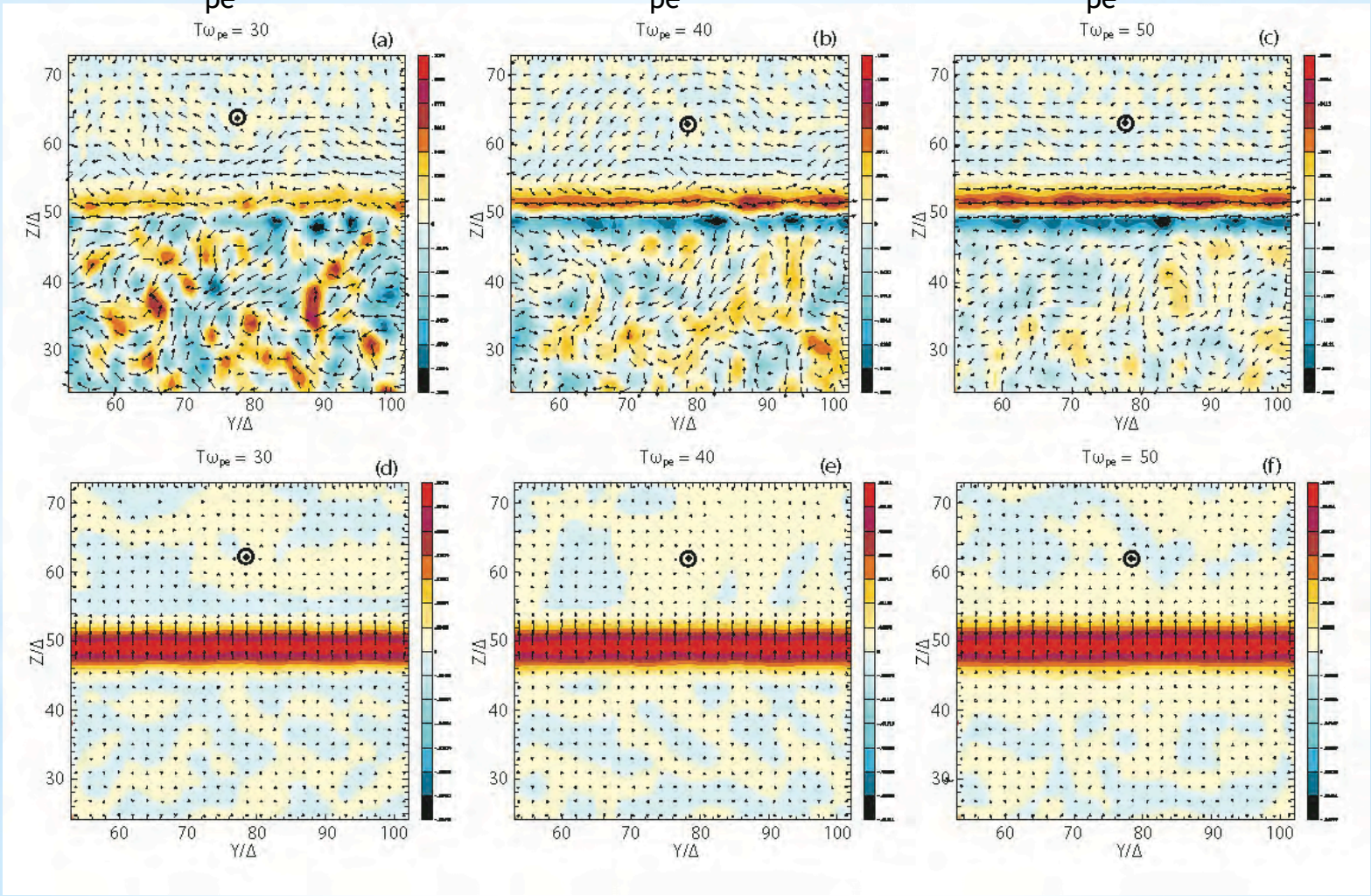

KKHI simulation of core jet-stationary sheath plasma

$\gamma_j = 1.5, \quad m_i/m_e = 20, \quad t = 50/\omega_{pe}$

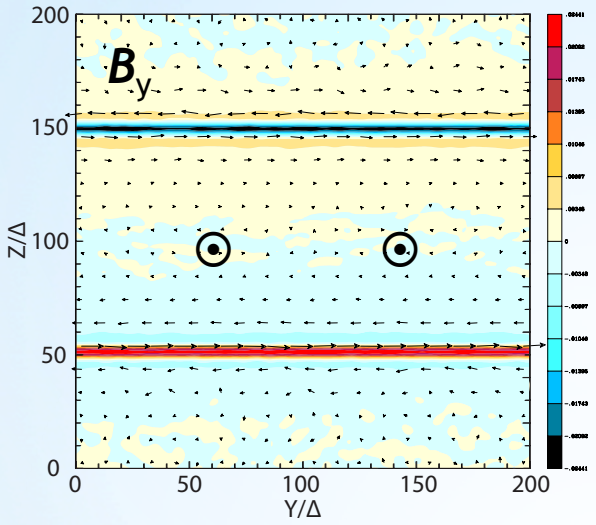

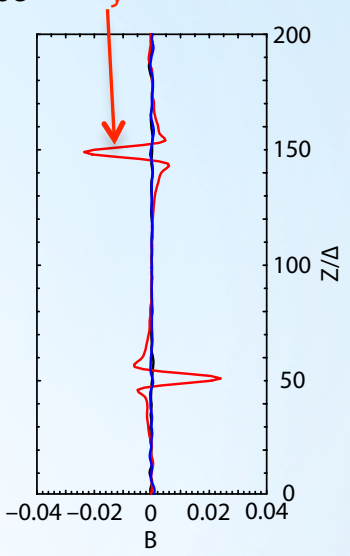

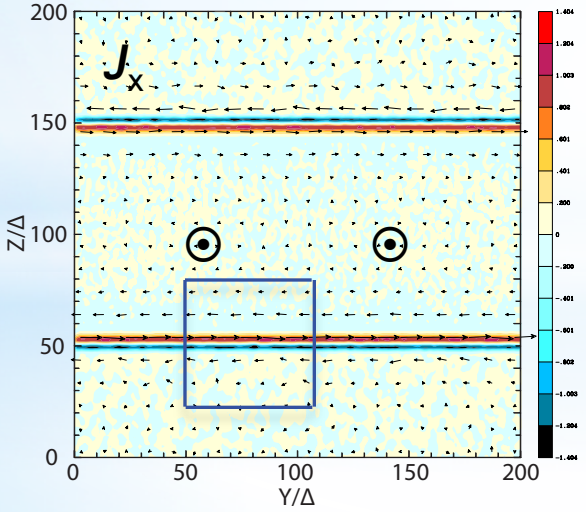

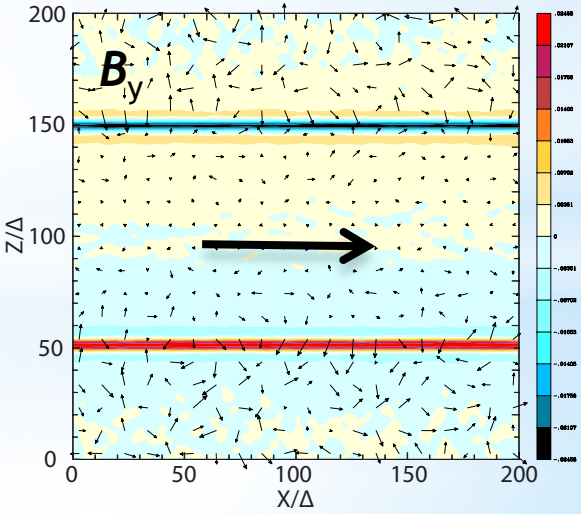

Time evolution of current filaments (J_x) generated by KKHI in the small box in y - z plane

$\gamma_j = 1.5, \quad m_i/m_e = 20$

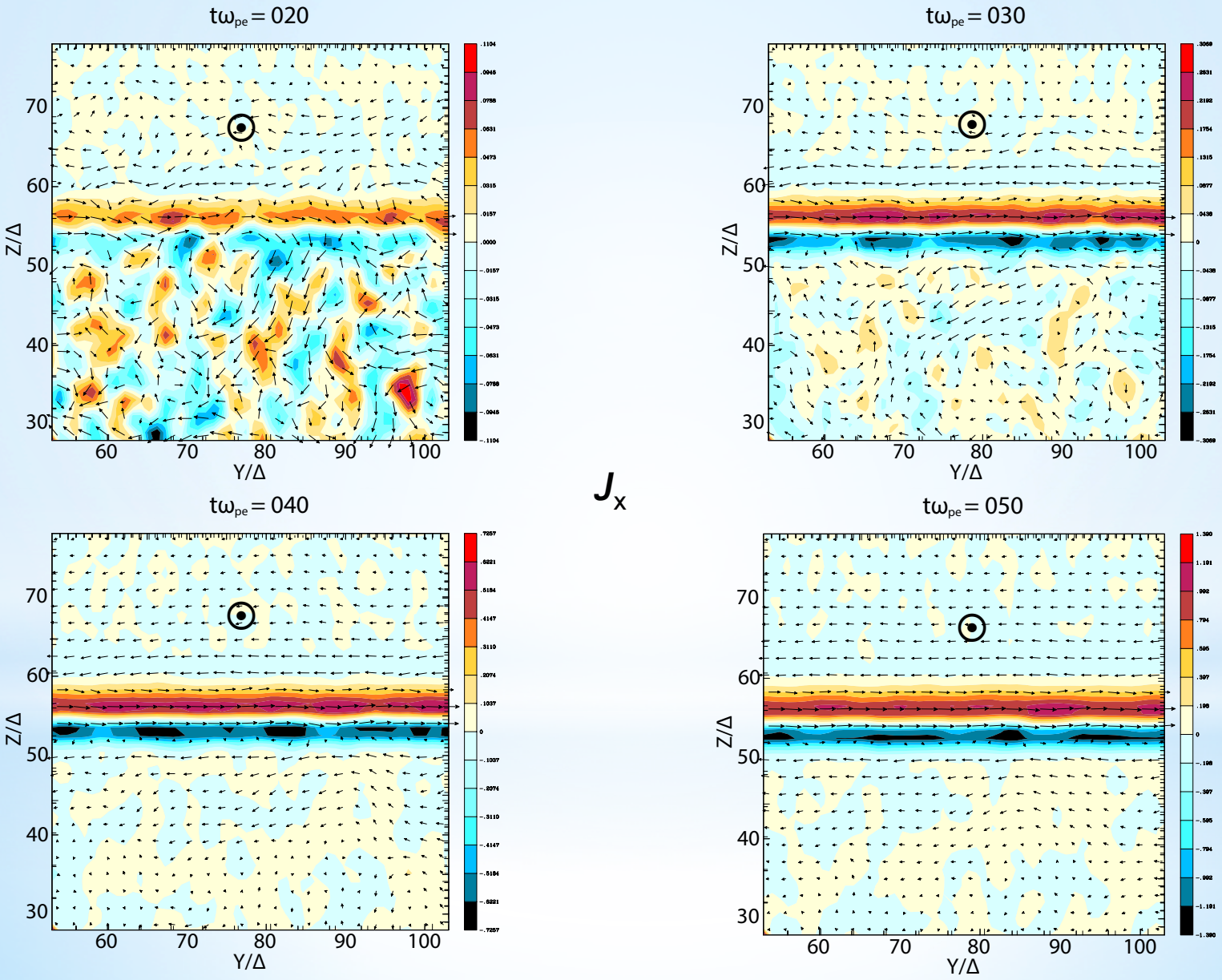

J_x

Motion of the electrons across the shear surface produce electric currents which generate magnetic field

$t = 30/\omega_{pe}$ $\gamma_j = 1.5$, $m_i/m_e = 20$

J_x

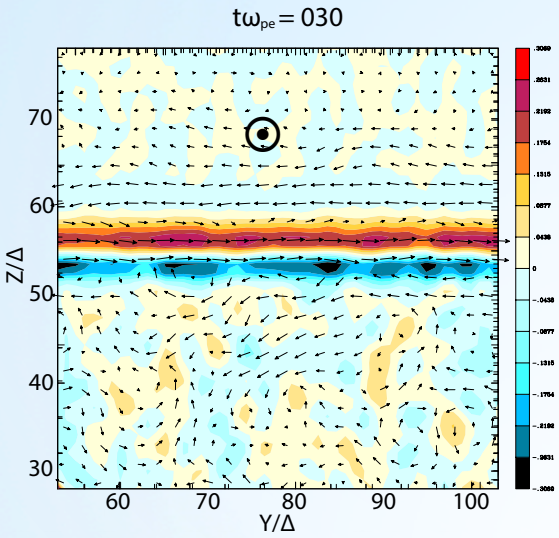

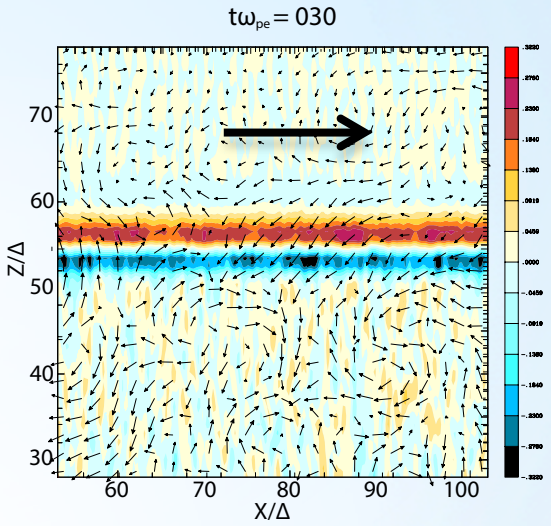

B_y

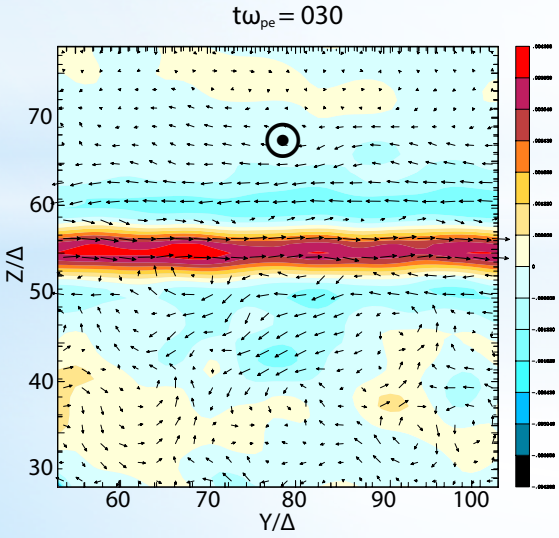

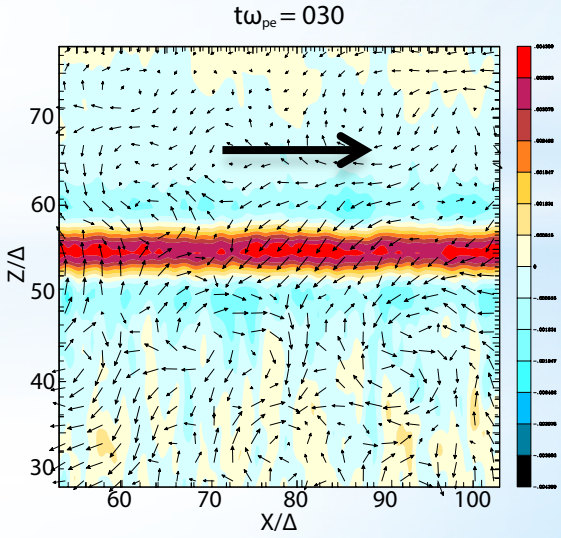

J_x Current structures $\gamma_{jt} = 15$ $t = 300\omega_{pe}^{-1}$

e - p

$e^{\pm}$

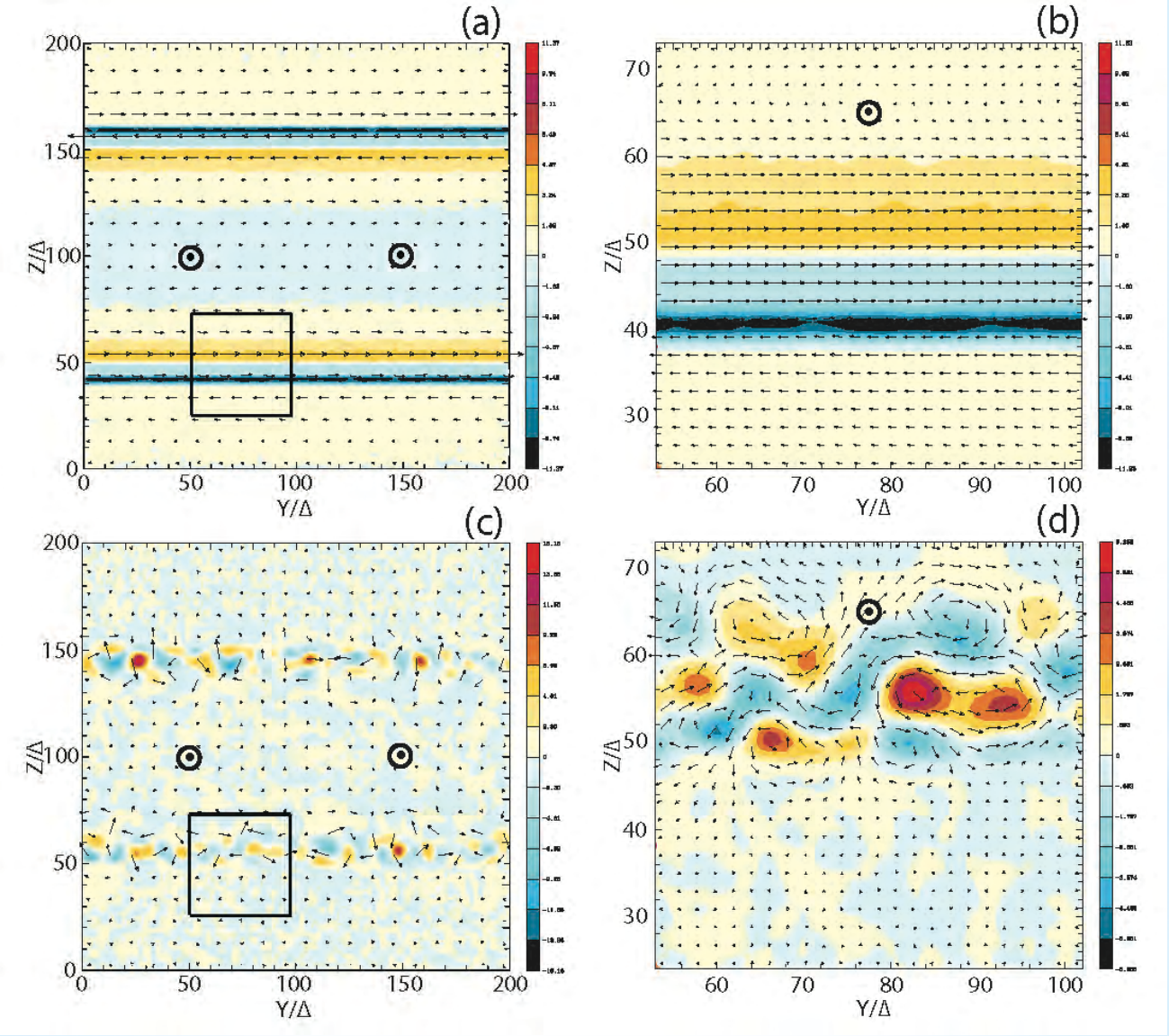

(Nishikawa et al. 2014, arXiv:1405.5247)

3D structure of current filaments and magnetic field

$e_{\pm}$ $\gamma_{jt} = 5$ $t = 250\omega_{pe}^{-1}$

J_x with magnetic field lines

B^2 with current streaming lines

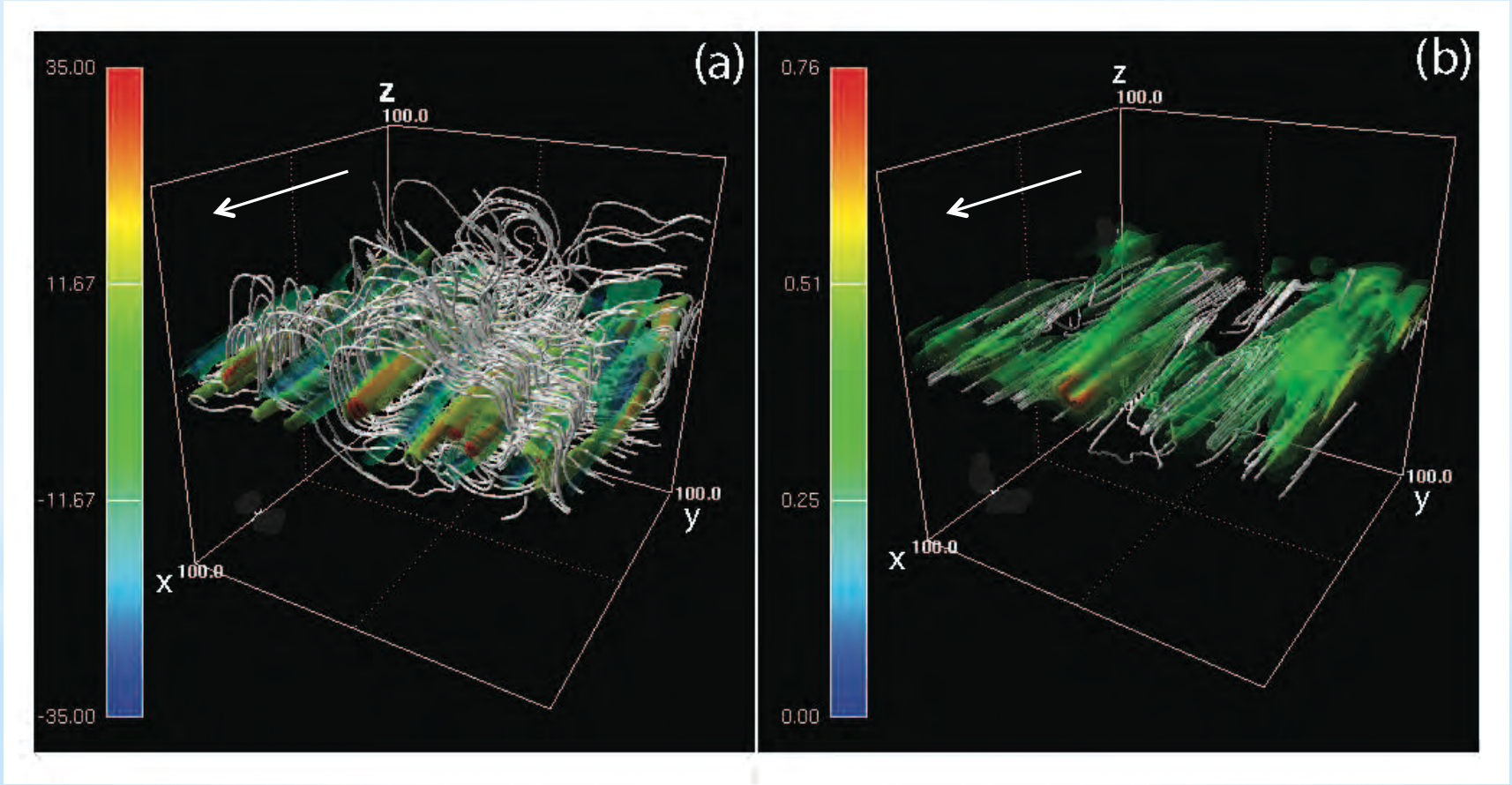

(Nishikawa et al. 2014, arXiv:1405.5247)

Snap shot of electron density of global jet simulations

$\gamma_{jt} = 5$ $\quad t = 500\omega_{pe}^{-1}$

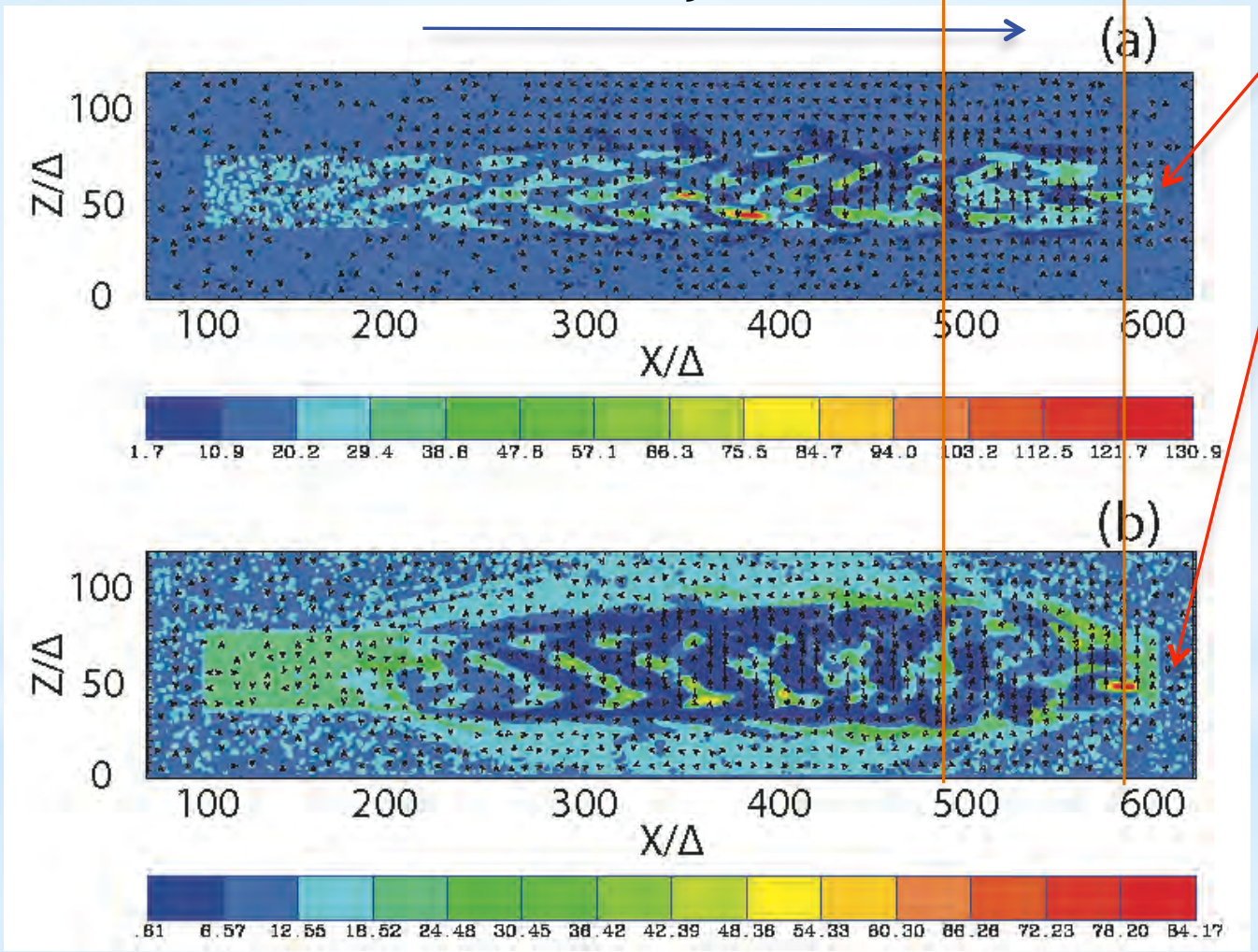

e - p

$e^{\pm}$

(Nishikawa et al. in progress, 2014)

Snap shots of current structures with transverse magnetic fields

$\gamma_{jt} = 5$ $\quad t = 500\omega_{pe}^{-1}$

X/Δ = 480 X/Δ = 580

e - p

$e^{\pm}$

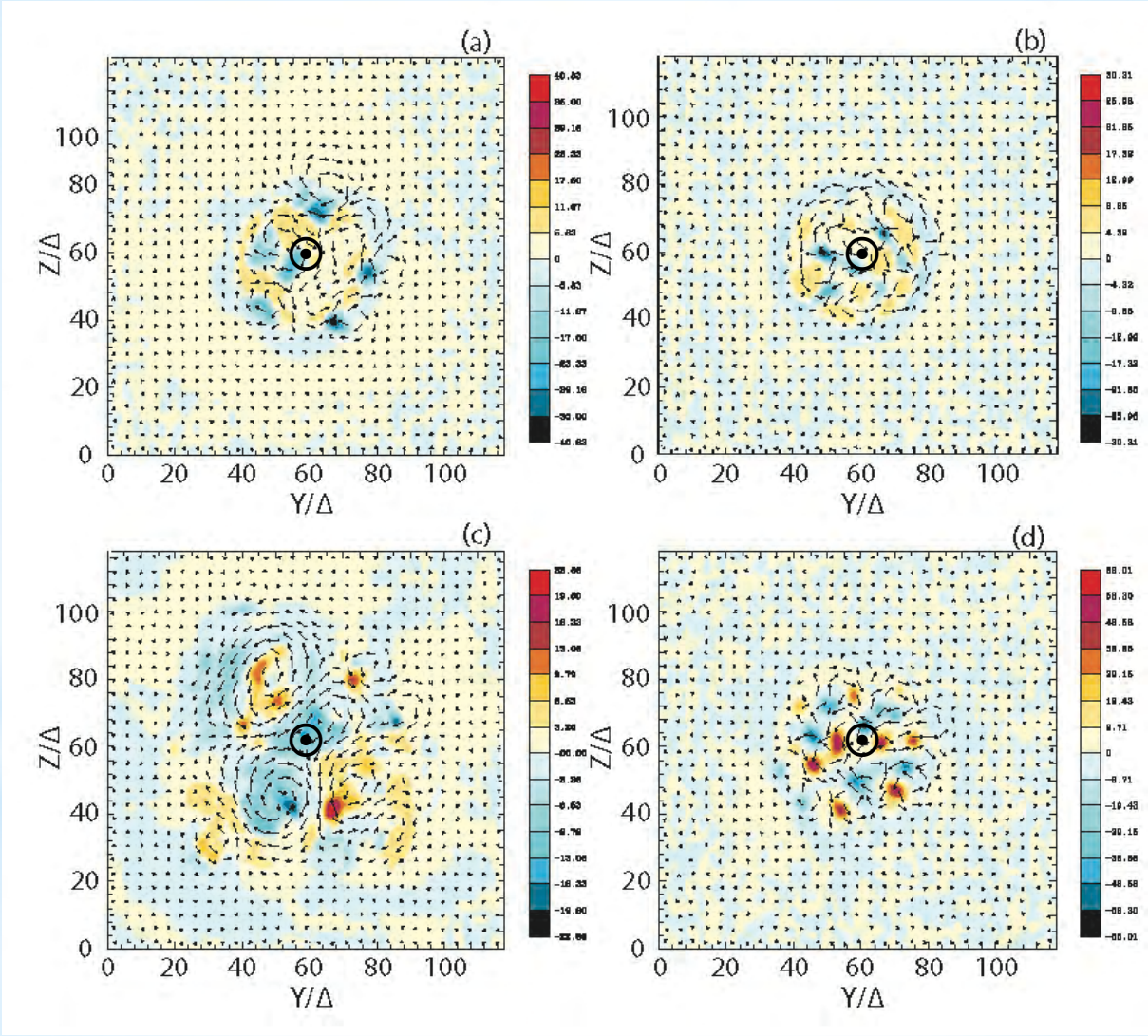

⊙ Jet center

(Nishikawa et al. in progress, 2014)

3D snapshots of current isosurfaces with magnetic field lines

$\gamma_{jt} = 5$ $\quad t = 500\omega_{pe}^{-1}$

Evolution of shock and instability is different for electron-proton and electron-positron

e - p $\quad$ $e^{\pm}$

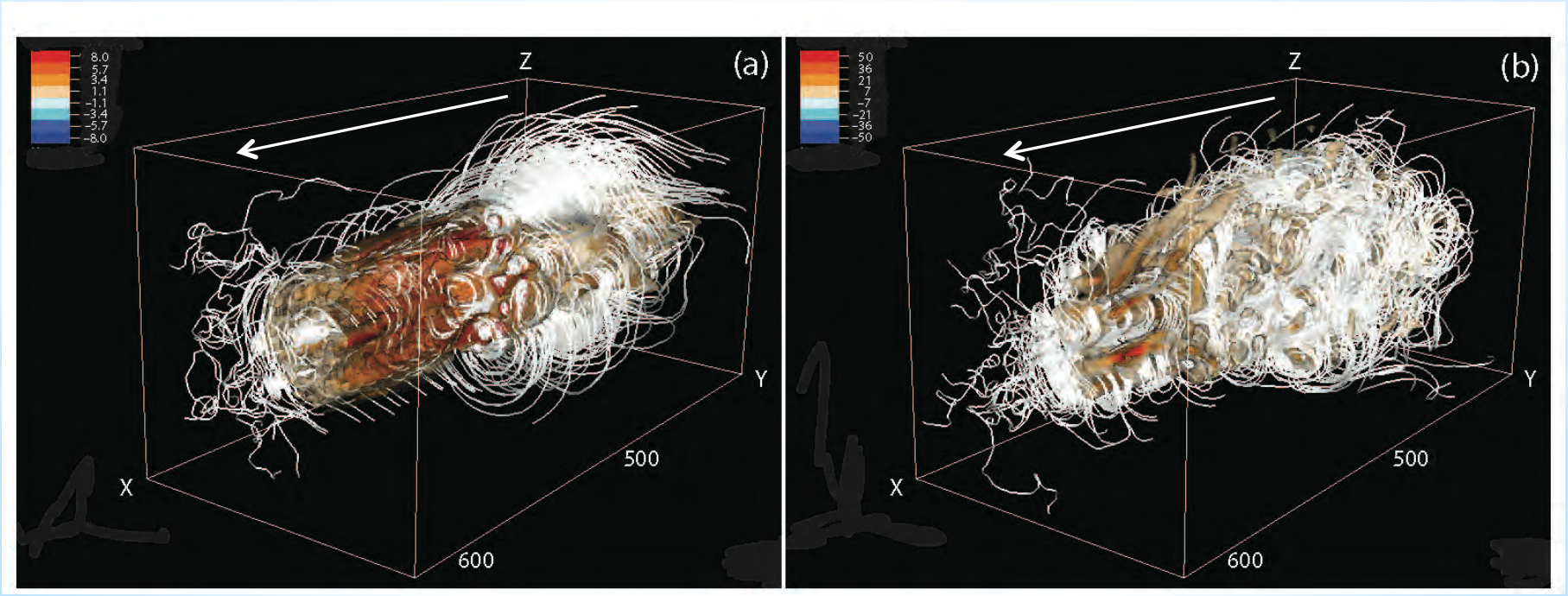

(Nishikawa et al. in progress, 2014)

Summary of Kinetic Kelvin-Helmholtz Instability

1. Static electric field grows due to the charge separation by the negative and positive current filaments
2. Current filaments at the velocity shear generate magnetic field transverse to the jet along the velocity shear
3. Jet with high Lorentz factor with core-sheath case generate higher magnetic field even after saturated in the case counter-streaming case with moderately relativistic jet
4. Non-relativistic jet generate KKHI quickly and magnetic field grows faster than the jet with higher Lorentz factor
5. For the jet-sheath case with Lorentz factor 15 the evolution of KKHI does not change with the mass ratio between 20 and 1836
6. Strong magnetic field will affect electron trajectories and create synchrotron-like (jitter) radiation which will be investigated
7. KKHI need to be investigated with shocks

(for detail please see (Nishikawa et al. 2014, arXiv:1405.5247)

Present theory of Synchrotron radiation

- Fermi acceleration (Monte Carlo simulations are not self-consistent; particles are crossing the shock surface many times and remain accelerated, the strengths of turbulent magnetic fields are assumed), Some simulations exhibit Fermi acceleration (Spitkovsky 2008)
- The strength of magnetic fields is estimated based on equipartition - magnetic field energy is comparable to the thermal energy): $\varepsilon_B \sim u(T)$
- The distribution of accelerated electrons is approximated by the power law ($F(\gamma) = \gamma^{-p}$; $p = 2.2$?) (ε_e)
- Synchrotron emission is calculated based on p and ε_B
- There are many assumptions in this calculation!

Synchrotron Emission: radiation from accelerated

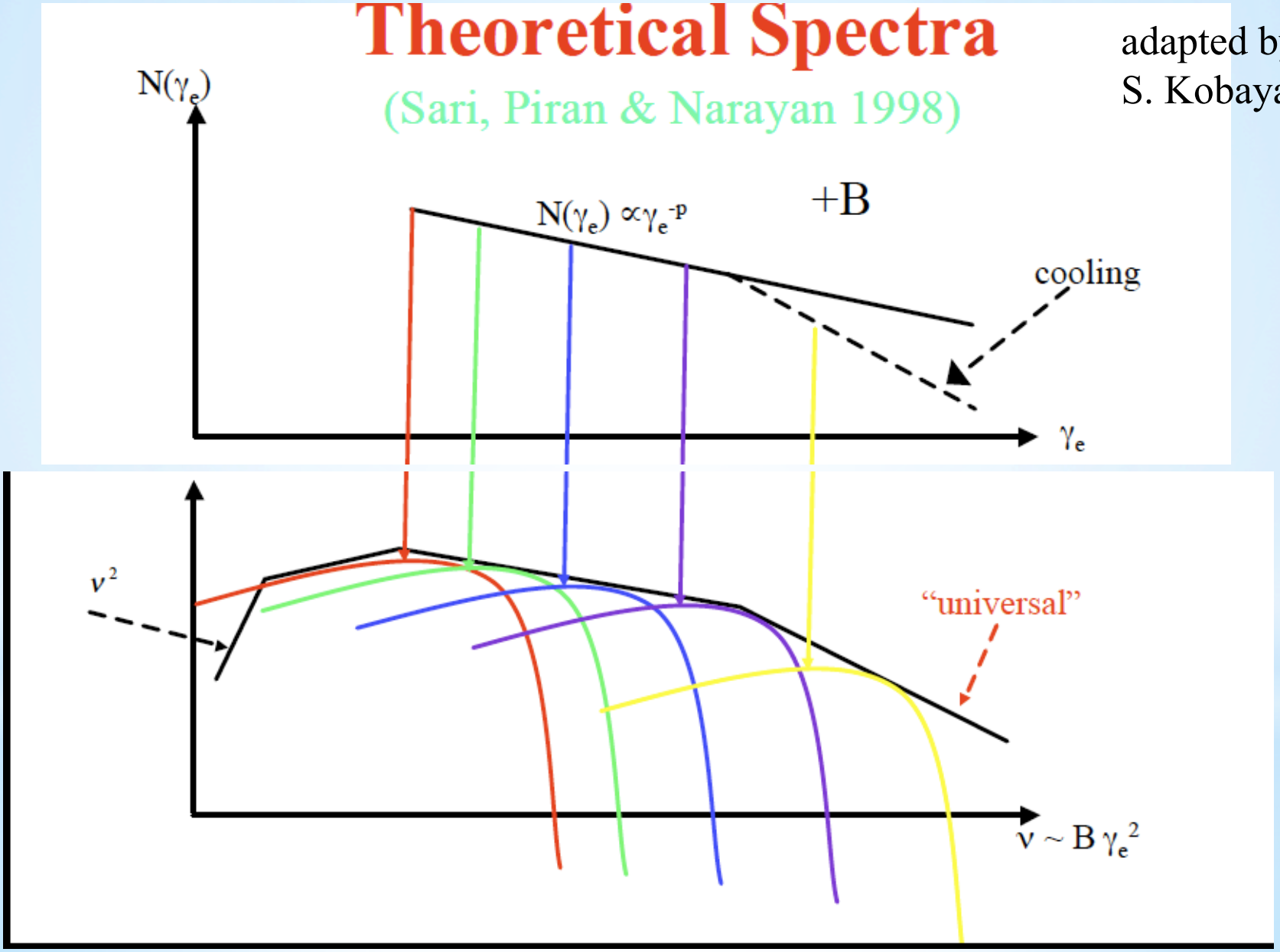

Self-consistent calculation of radiation

- Electrons are accelerated by the electromagnetic field generated by the Weibel instability and KKHI (without the assumption used in test-particle simulations for Fermi acceleration)
- Radiation is calculated using the particle trajectory in the self-consistent turbulent magnetic field
- This calculation includes Jitter radiation (Medvedev 2000, 2006) which is different from standard synchrotron emission
- Radiation from electrons in our simulation is reported in Nishikawa et al. Adv. Sci. Rev, 47, 1434, 2011.

Radiation from particles in collisionless shock

To obtain a spectrum, "just" integrate:

$$\frac{d^2W}{d\Omega d\omega} = \frac{\mu_0 c q^2}{16\pi^3}\left|\int_{-\infty}^{\infty}\frac{\mathbf{n}\times[(\mathbf{n}-\boldsymbol{\beta})\times\dot{\boldsymbol{\beta}}]}{(1-\boldsymbol{\beta}\cdot\mathbf{n})^2}\, e^{i\omega(t'-\mathbf{n}\cdot\mathbf{r}_0(t')/c)}dt'\right|^2$$

where $\mathbf{r}_0$ is the position, $\boldsymbol{\beta}$ the velocity and $\dot{\boldsymbol{\beta}}$ the acceleration

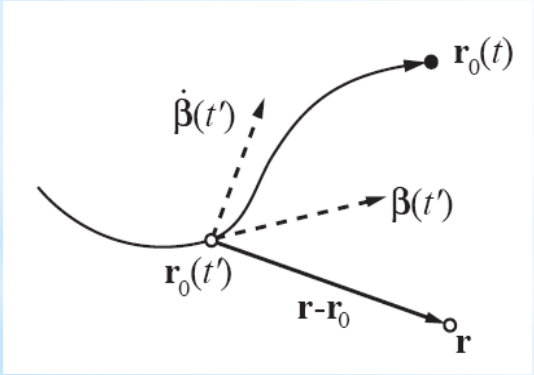

New approach: Calculate radiation from integrating position, velocity, and acceleration of ensemble of particles (electrons and positrons)

Hededal, Thesis 2005 (astro-ph/0506559)
Nishikawa et al. 2008 (astro-ph/0802.2558), 2011
Sironi & Spitkovsky, 2009, ApJ
Martins et al. 2009, Proc. of SPIE Vol. 7359
Frederiksen et al. 2010, ApJL

*Radiation from collisionless shock with **static** electromagnetic fields*

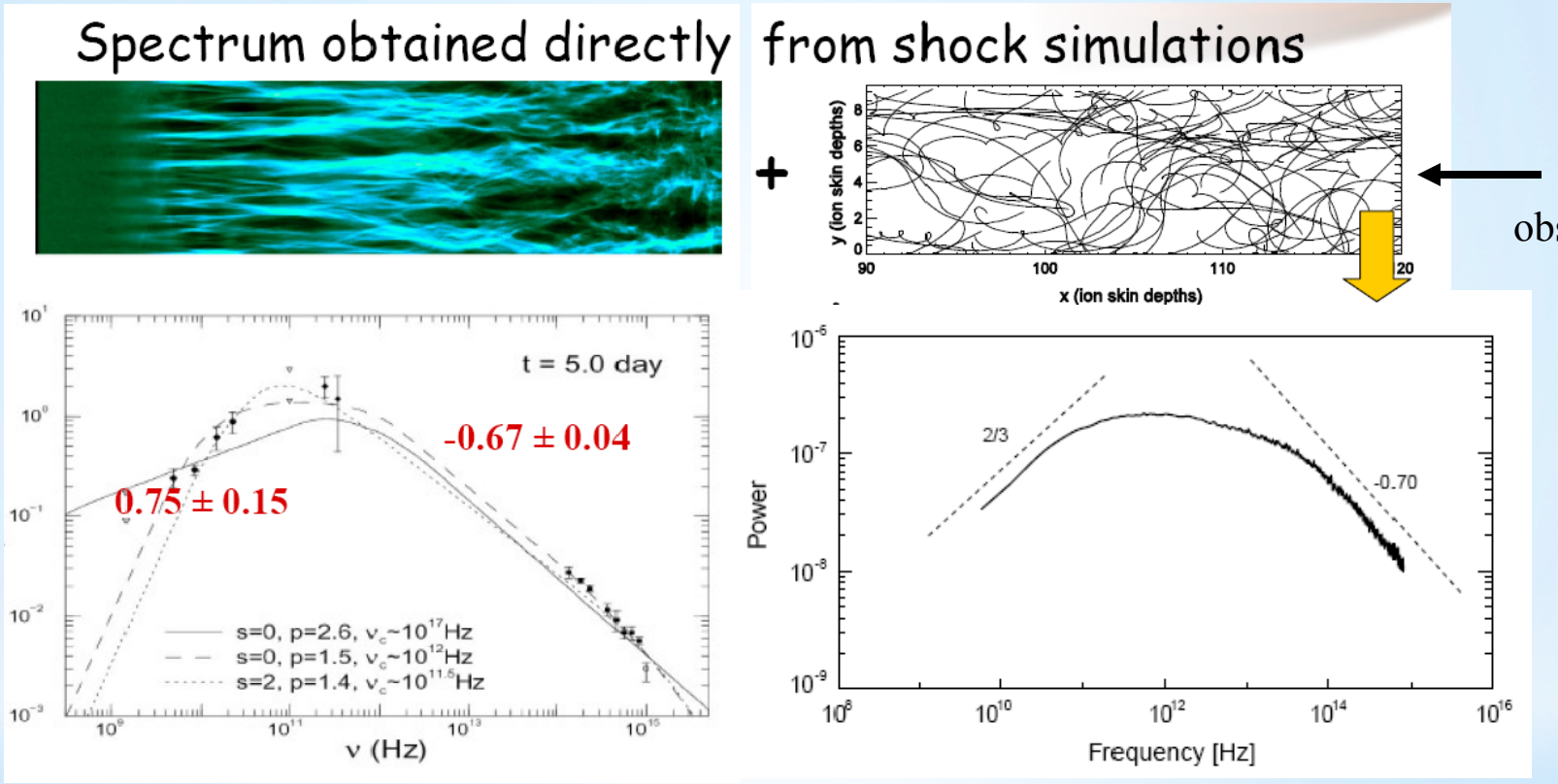

GRB 000301c (Panaitescu 2001)

Shock simulations

Hededal Thesis: http://www.astro.ku.dk/~hededal

Synchrotron radiation from gyrating electrons in a uniform magnetic field

electron trajectories

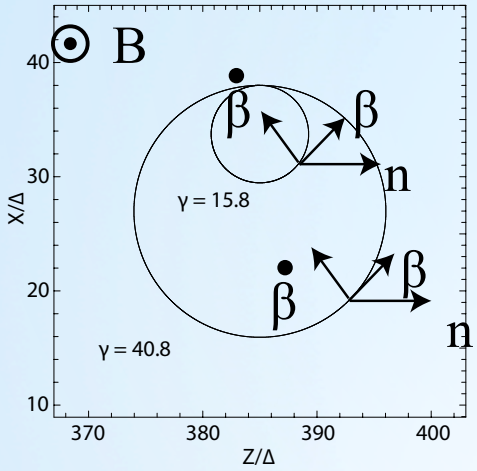

radiation electric field observed at long distance

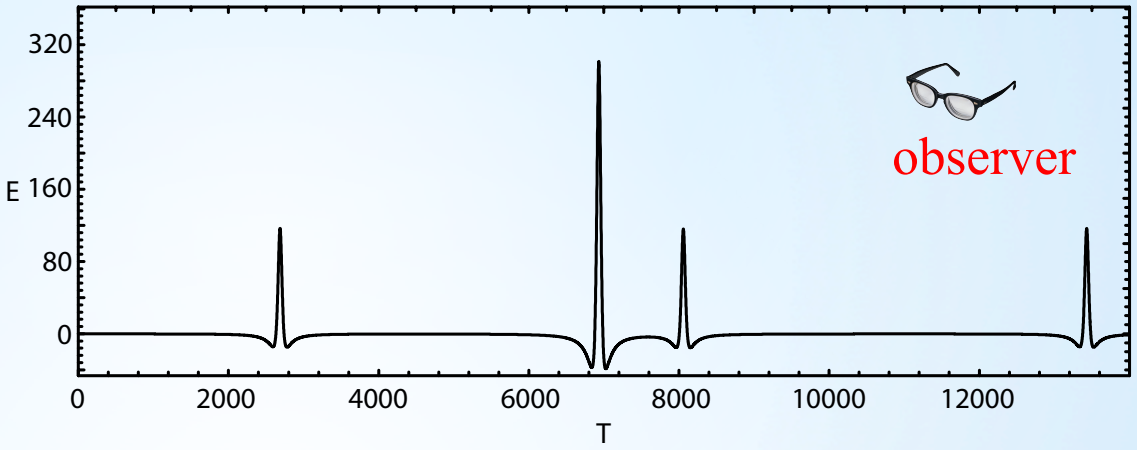

spectra with different viewing angles

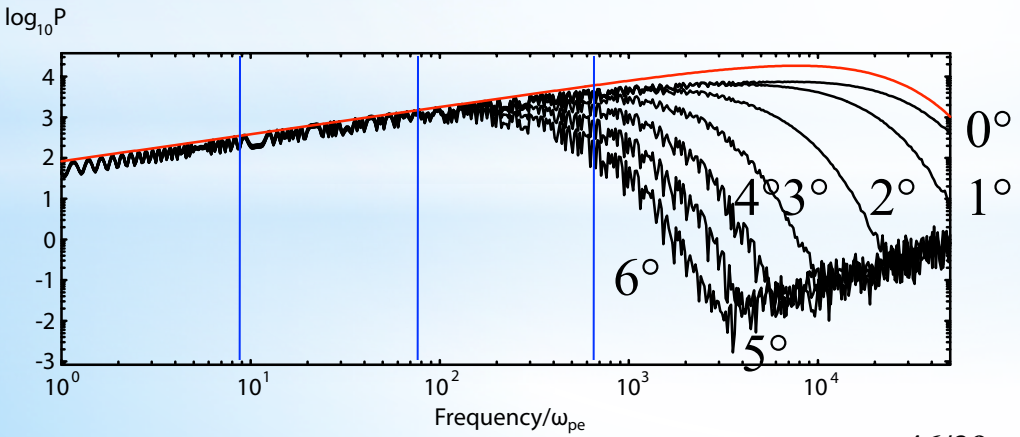

time evolution of three frequencies

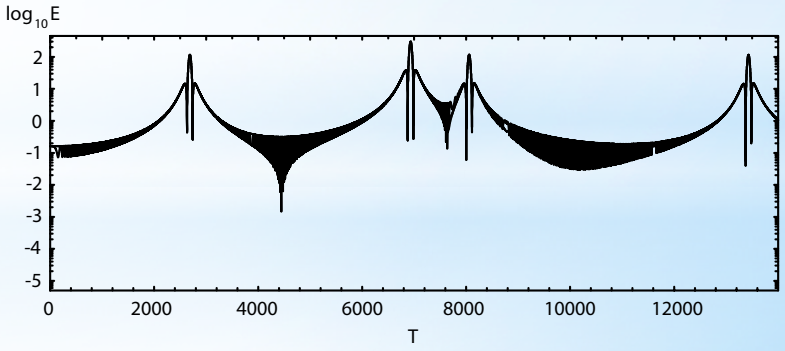

theoretical synchrotron spectrum

$f/\omega_{pe} = 8.5,\ 74.8,\ 654.$

Synchrotron radiation from propagating electrons in a uniform magnetic field

electron trajectories

radiation electric field observed at long distance

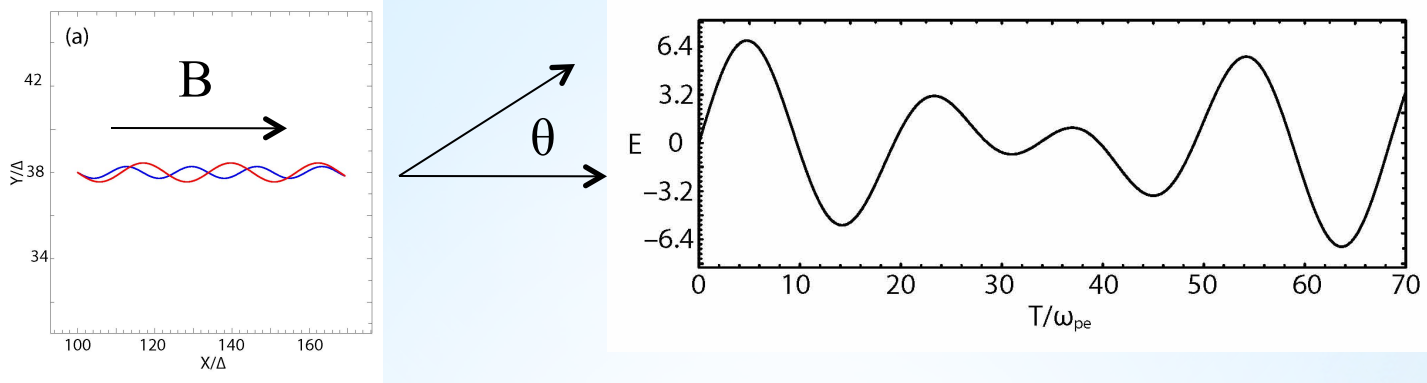

spectra with different viewing angles (helical)

$\theta_\gamma = 4.25°$

gyrating

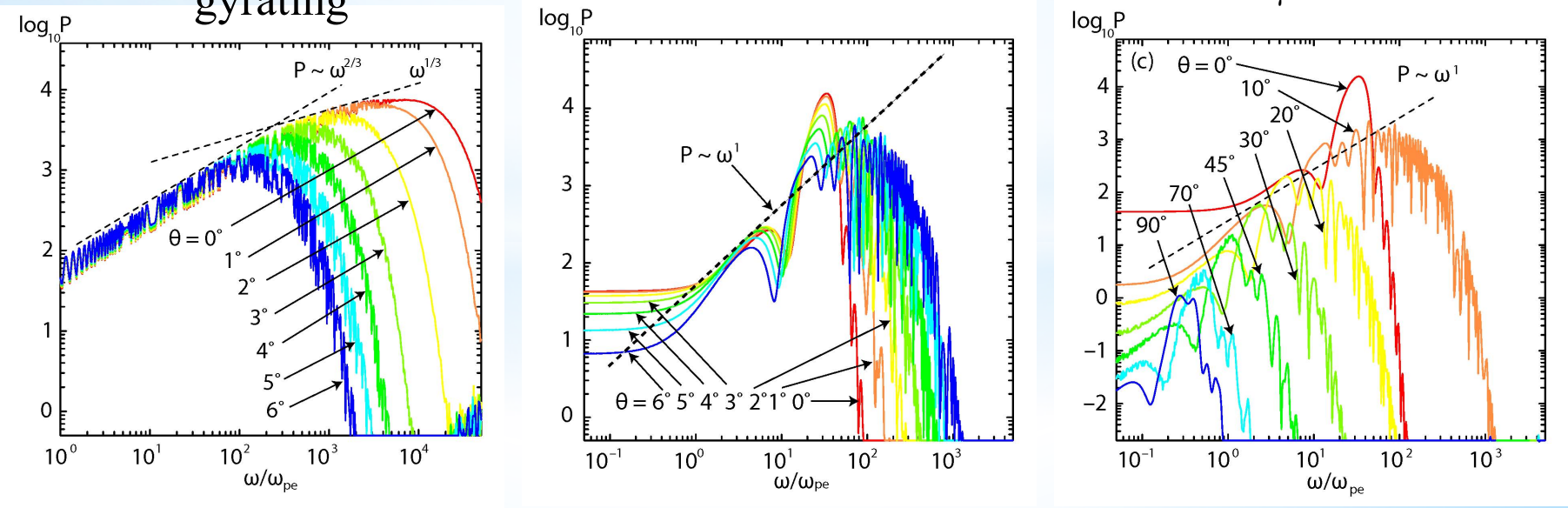

(Nishikawa et al. Advances in Space Research, 2011)

Synchrotron vs. `Jitter'

- (a) Synchrotron emission assumes large-scale homogeneous magnetic fields
- (b) `Jitter' radiation (Medvedev 2000) occurs where the gyro-radius is larger than the randomness of turbulent magnetic fields

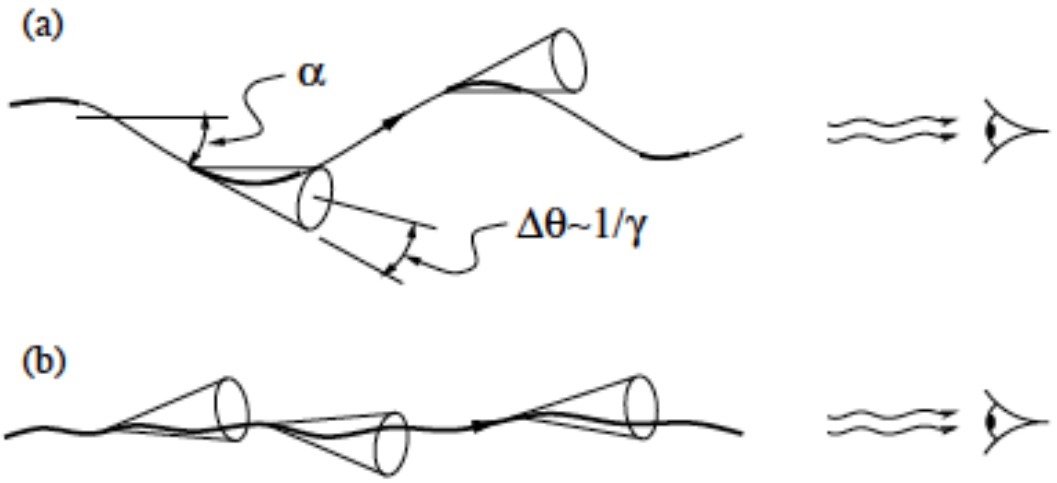

FIG. 1.—Emission from various points along the particle's trajectory. (*a*) $\alpha \gg \Delta\theta$; emission from selected parts (*bold portions*) of the trajectory is seen by an observer. (*b*) $\alpha \ll \Delta\theta$; emission from the entire trajectory is observed.

TABLE 1. Seven cases of radiation

	B_x	$V_{j1,2}$	$V_{\perp,1}$	$V_{\perp,2}$	γ_{max}	θ_Γ	**Remarks**
P	3.70 (B_z)	0.0c	0.998c	0.9997c	40.08	4.491	gyrating
A	3.70	0.99c	0.1c	0.12c	13.48	13.35	jet
B	3.70	0.9924c	0.1c	0.12c	36.70	4.905	jet
C	3.70	0.99c	0.01c	0.012c	7.114	25.30	jet
D	0.370	0.99c	0.01c	0.012c	7.114	25.30	jet
E	0.370	0.99c	0.1c	0.12c	13.48	13.35	$\Delta t = 0.005$
F	0.370	0.99c	0.1c	0.12c	13.48	13.35	$\Delta t = 0.025$

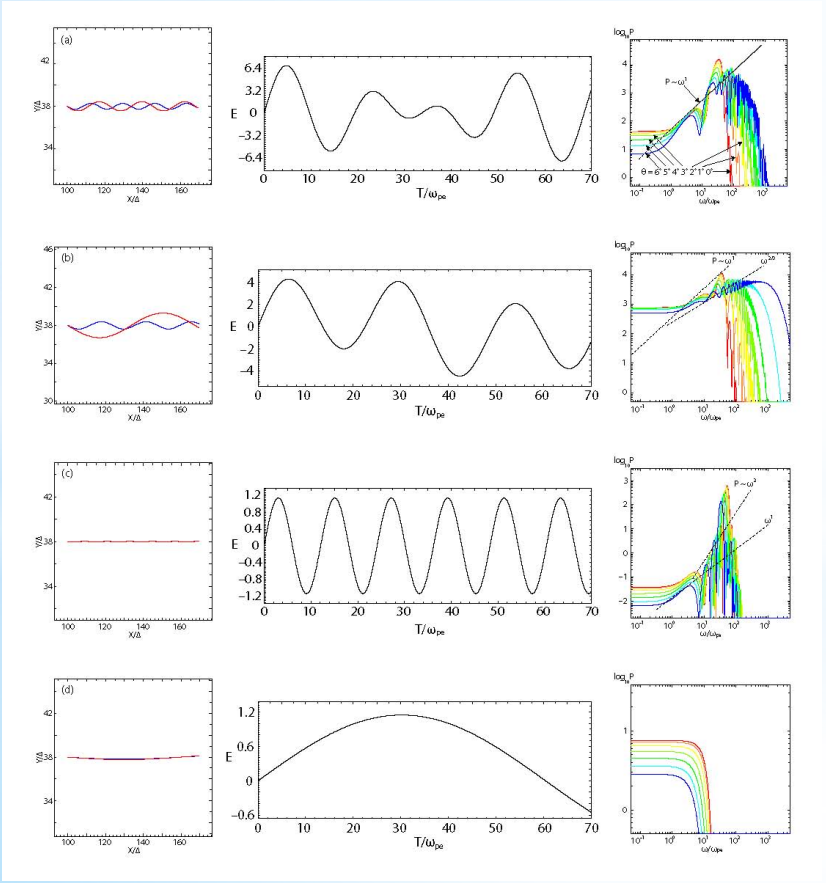

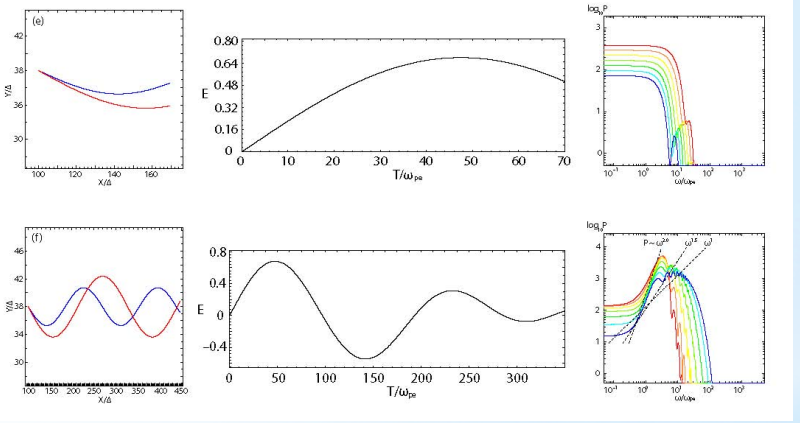

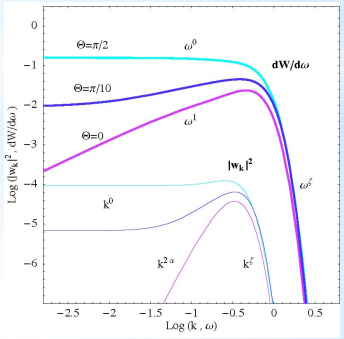

(Nishikawa et al. astro-ph/0809.5067)

TABLE 1. Seven cases of radiation

	B_x	$V_{j1,2}$	$V_{\perp,1}$	$V_{\perp,2}$	γ_{max}	θ_Γ	**Remarks**
P	3.70 (B_z)	0.0c	0.998c	0.9997c	40.08	4.491	gyrating
A	3.70	0.99c	0.1c	0.12c	13.48	13.35	jet
B	3.70	0.9924c	0.1c	0.12c	36.70	4.905	jet
C	3.70	0.99c	0.01c	0.012c	7.114	25.30	jet
D	0.370	0.99c	0.01c	0.012c	7.114	25.30	jet
E	0.370	0.99c	0.1c	0.12c	13.48	13.35	$\Delta t = 0.005$
F	0.370	0.99c	0.1c	0.12c	13.48	13.35	$\Delta t = 0.025$

Case A

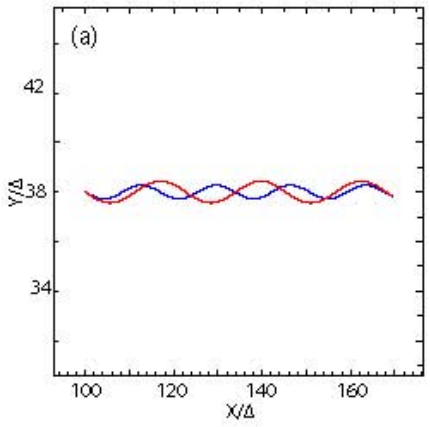

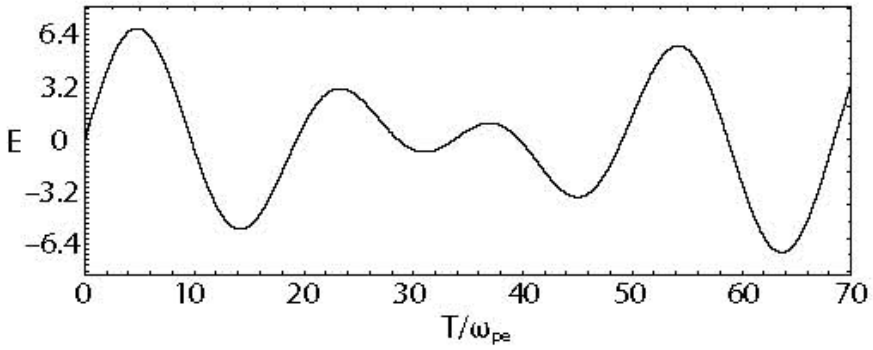

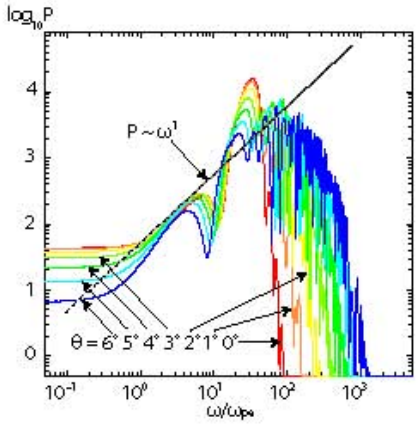

 (Nishikawa et al. astro-ph/0809.5067)

TABLE 1. Seven cases of radiation

	B_x	$V_{j1,2}$	$V_{\perp,1}$	$V_{\perp,2}$	γ_{max}	θ_Γ	**Remarks**
P	3.70 (B_z)	0.0c	0.998c	0.9997c	40.08	4.491	gyrating
A	3.70	0.99c	0.1c	0.12c	13.48	13.35	jet
B	3.70	0.9924c	0.1c	0.12c	36.70	4.905	jet
C	3.70	0.99c	0.01c	0.012c	7.114	25.30	jet
D	0.370	0.99c	0.01c	0.012c	7.114	25.30	jet
E	0.370	0.99c	0.1c	0.12c	13.48	13.35	$\Delta t = 0.005$
F	0.370	0.99c	0.1c	0.12c	13.48	13.35	$\Delta t = 0.025$

Case B

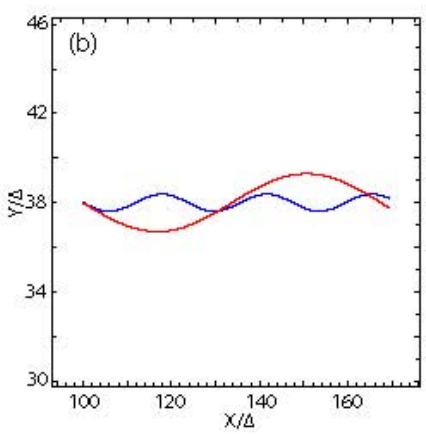

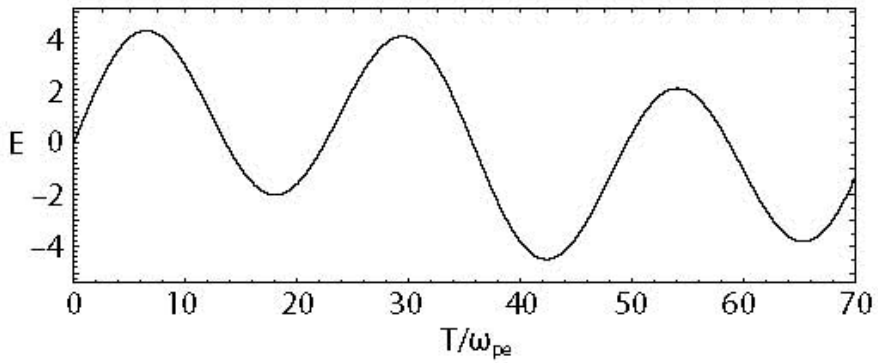

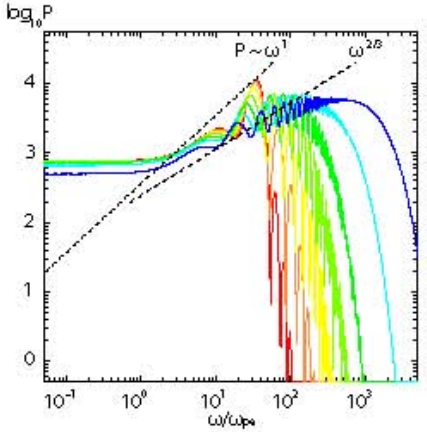

 (Nishikawa et al. astro-ph/0809.5067)

TABLE 1. Seven cases of radiation

	B_x	$V_{j1,2}$	$V_{\perp,1}$	$V_{\perp,2}$	γ_{max}	θ_Γ	**Remarks**
P	3.70 (B_z)	0.0c	0.998c	0.9997c	40.08	4.491	gyrating
A	3.70	0.99c	0.1c	0.12c	13.48	13.35	jet
B	3.70	0.9924c	0.1c	0.12c	36.70	4.905	jet
C	3.70	0.99c	0.01c	0.012c	7.114	25.30	jet
D	0.370	0.99c	0.01c	0.012c	7.114	25.30	jet
E	0.370	0.99c	0.1c	0.12c	13.48	13.35	$\Delta t = 0.005$
F	0.370	0.99c	0.1c	0.12c	13.48	13.35	$\Delta t = 0.025$

Case C

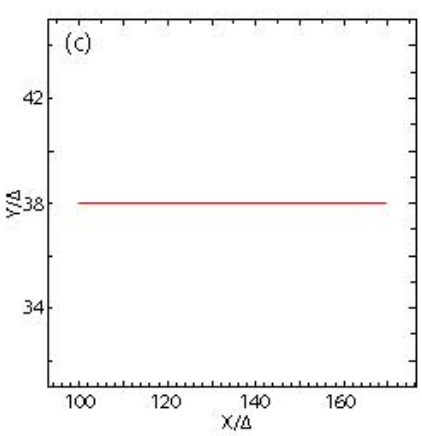

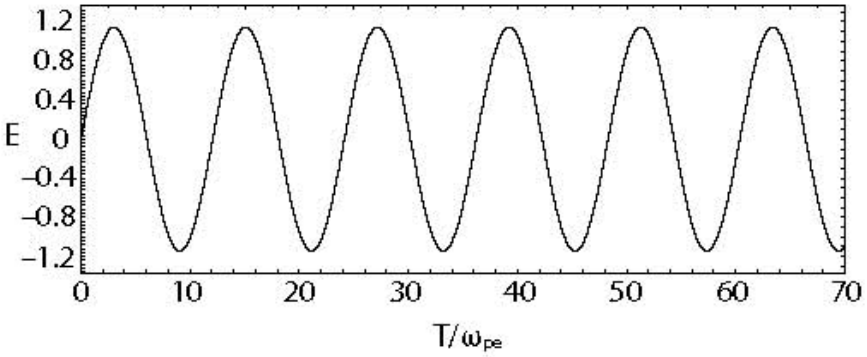

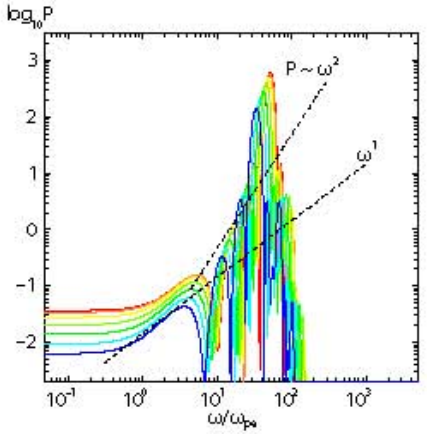

 (Nishikawa et al. astro-ph/0809.5067)

TABLE 1. Seven cases of radiation

	B_x	$V_{j1,2}$	$V_{\perp,1}$	$V_{\perp,2}$	γ_{max}	θ_Γ	**Remarks**
P	3.70 (B_z)	0.0c	0.998c	0.9997c	40.08	4.491	gyrating
A	3.70	0.99c	0.1c	0.12c	13.48	13.35	jet
B	3.70	0.9924c	0.1c	0.12c	36.70	4.905	jet
C	3.70	0.99c	0.01c	0.012c	7.114	25.30	jet
D	0.370	0.99c	0.01c	0.012c	7.114	25.30	jet
E	0.370	0.99c	0.1c	0.12c	13.48	13.35	$\Delta t = 0.005$
F	0.370	0.99c	0.1c	0.12c	13.48	13.35	$\Delta t = 0.025$

Case D

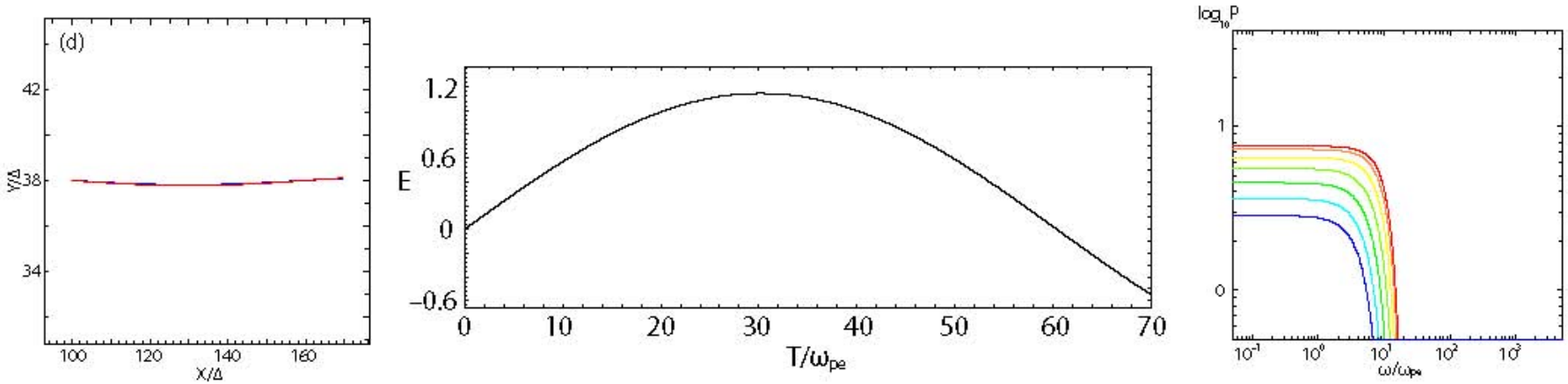

 (Nishikawa et al. astro-ph/0809.5067)

TABLE 1. Seven cases of radiation

	B_x	$V_{j1,2}$	$V_{\perp,1}$	$V_{\perp,2}$	γ_{max}	θ_Γ	**Remarks**
P	3.70 (B_z)	0.0c	0.998c	0.9997c	40.08	4.491	gyrating
A	3.70	0.99c	0.1c	0.12c	13.48	13.35	jet
B	3.70	0.9924c	0.1c	0.12c	36.70	4.905	jet
C	3.70	0.99c	0.01c	0.012c	7.114	25.30	jet
D	0.370	0.99c	0.01c	0.012c	7.114	25.30	jet
E	0.370	0.99c	0.1c	0.12c	13.48	13.35	$\Delta t = 0.005$
F	0.370	0.99c	0.1c	0.12c	13.48	13.35	$\Delta t = 0.025$

Case E

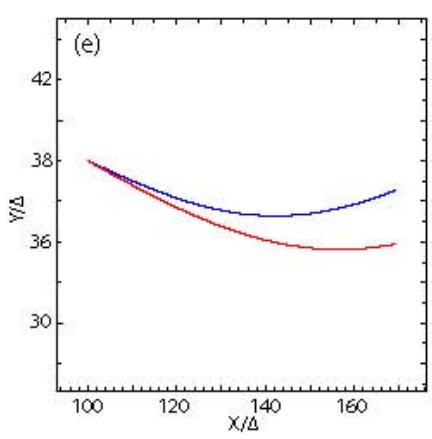

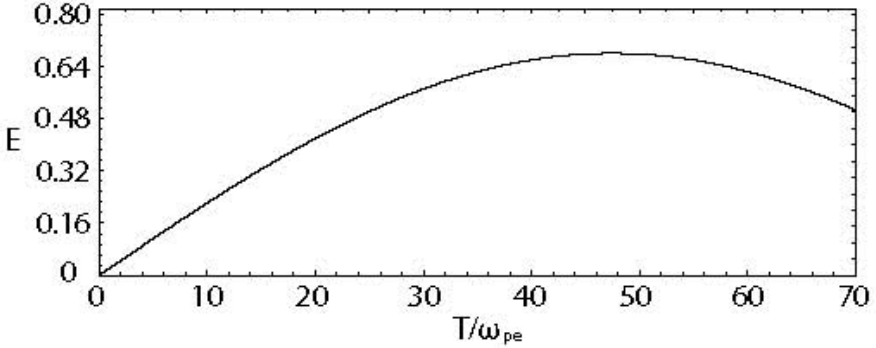

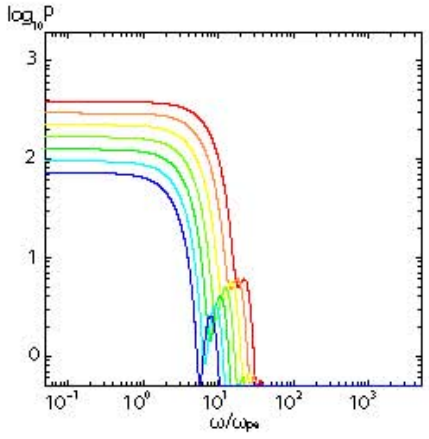

 (Nishikawa et al. astro-ph/0809.5067)

TABLE 1. Seven cases of radiation

	B_x	$V_{j1,2}$	$V_{\perp,1}$	$V_{\perp,2}$	γ_{max}	θ_Γ	**Remarks**
P	3.70 (B_z)	0.0c	0.998c	0.9997c	40.08	4.491	gyrating
A	3.70	0.99c	0.1c	0.12c	13.48	13.35	jet
B	3.70	0.9924c	0.1c	0.12c	36.70	4.905	jet
C	3.70	0.99c	0.01c	0.012c	7.114	25.30	jet
D	0.370	0.99c	0.01c	0.012c	7.114	25.30	jet
E	0.370	0.99c	0.1c	0.12c	13.48	13.35	$\Delta t = 0.005$
F	0.370	0.99c	0.1c	0.12c	13.48	13.35	$\Delta t = 0.025$

Case F

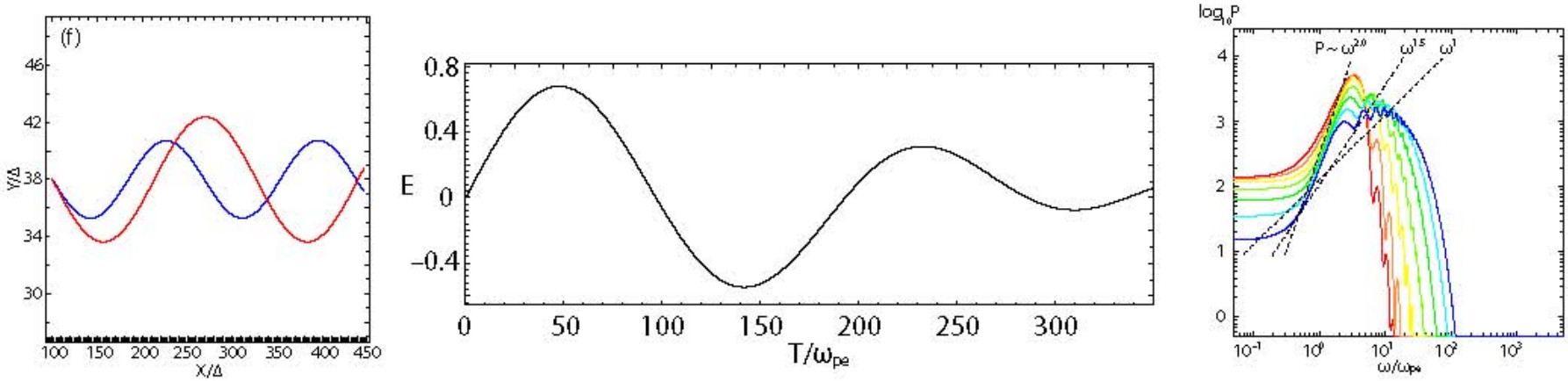

 (Nishikawa et al. astro-ph/0809.5067)

Synchrotron vs. `Jitter'

- (a) Synchrotron emission assumes large-scale homogeneous magnetic fields
- (b) `Jitter' radiation (Medvedev 2000) occurs where the gyro-radius is larger than the randomness of turbulent magnetic fields

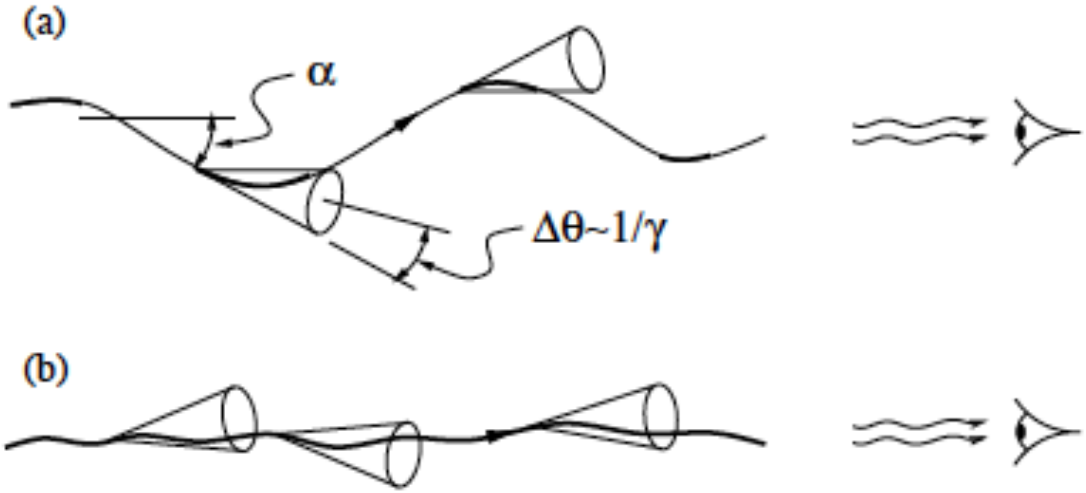

FIG. 1.—Emission from various points along the particle's trajectory. (*a*) $\alpha \gg \Delta\theta$; emission from selected parts (*bold portions*) of the trajectory is seen by an observer. (*b*) $\alpha \ll \Delta\theta$; emission from the entire trajectory is observed.

Radiation from test (accelerated) particles in static turbulent magnetic fields generated by the Weibel instability in 2D PIC simulation

$t = 2250\omega_{pe}^{-1}$

number density

$t_s = 3000\Delta t = 135\omega_p^{-1}$ $\Delta t = 0.045\omega_p^{-1}$

$N_s \sim 10{,}000$

test particle simulation in a fixed snapshot of electromagnetic filed

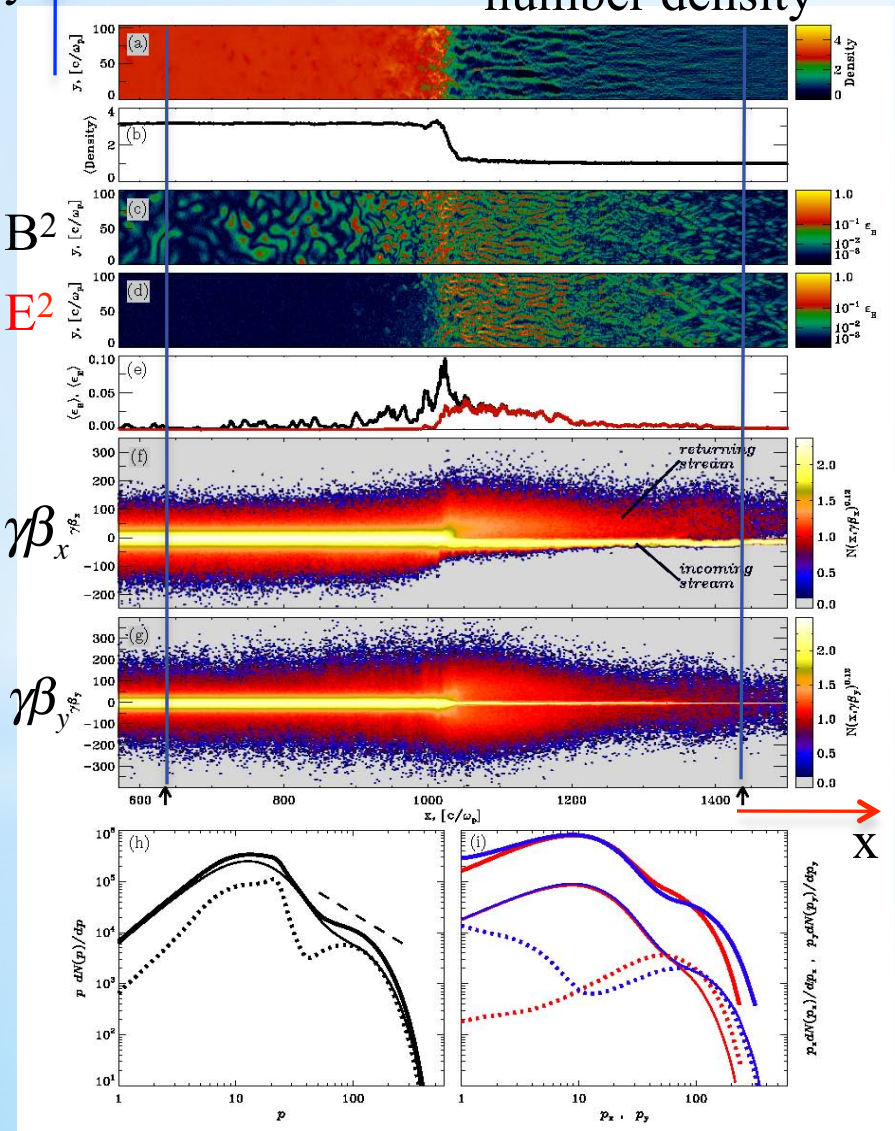

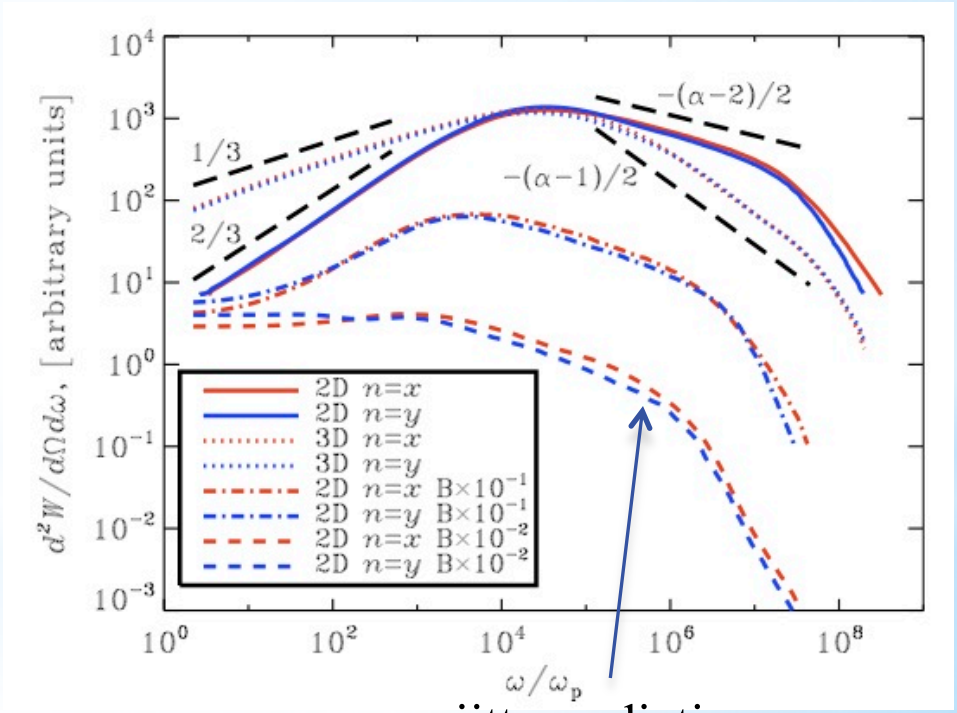

jitter radiation

(Sironi & Spitkovsky 2009)

Radiation from electrons in self-consistent electromagnetic field from a 2D PIC simulation

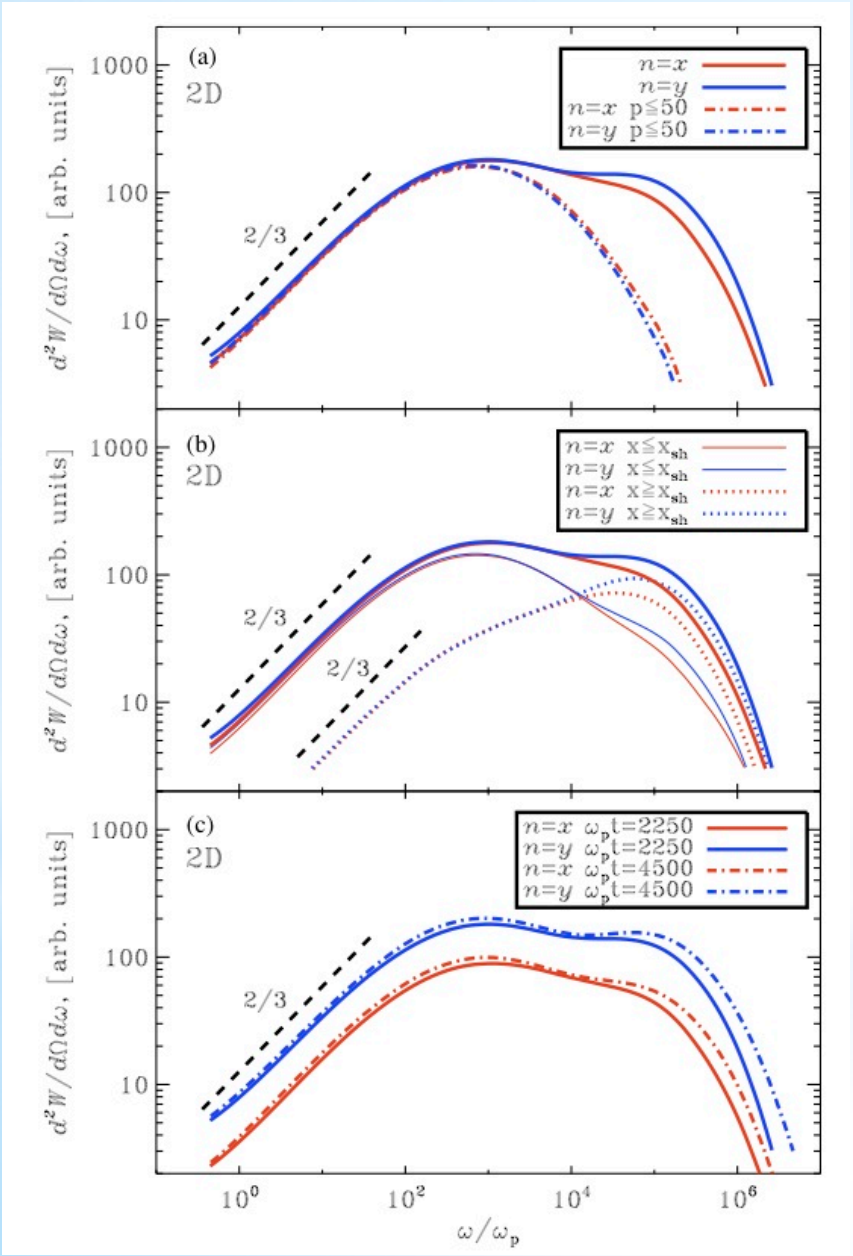

Due to the radiation is calculated in downstream frame the radiation is isotropic. An additional Lorentz transformation is required, if the down-stream medium is moving with respect to the observer (no beaming effect is taken account and they are different from the observed radiation).

They conclude that jitter regime is obtained only if with artificially reduced the strength of the electromagnetic filed?
($K \equiv qB\lambda / mc^2$)

This conclusion is due to that radiation is calculated in downstream frame?

(Sironi & Spitkovsky 2009)

Importance of Synchrotron radiation calculated in 3-D system

$\gamma = 6$, P^+ e^- counter-streaming jet, no shock generated

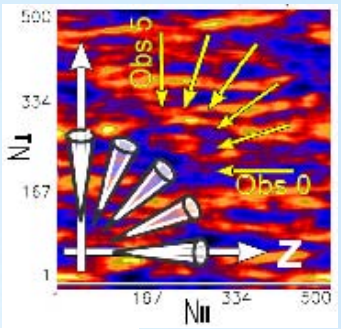

3D

2D

6<t<16

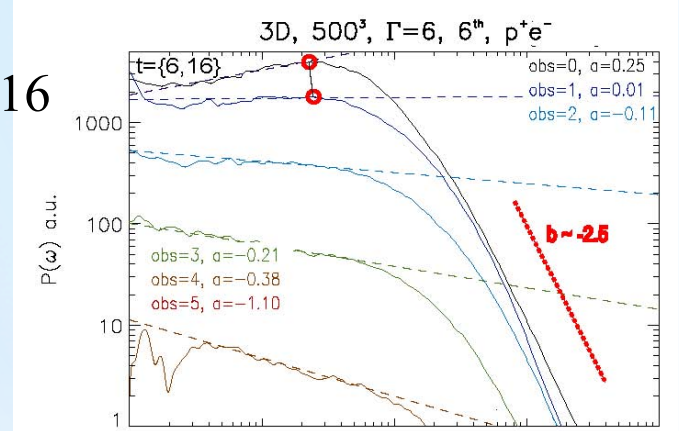

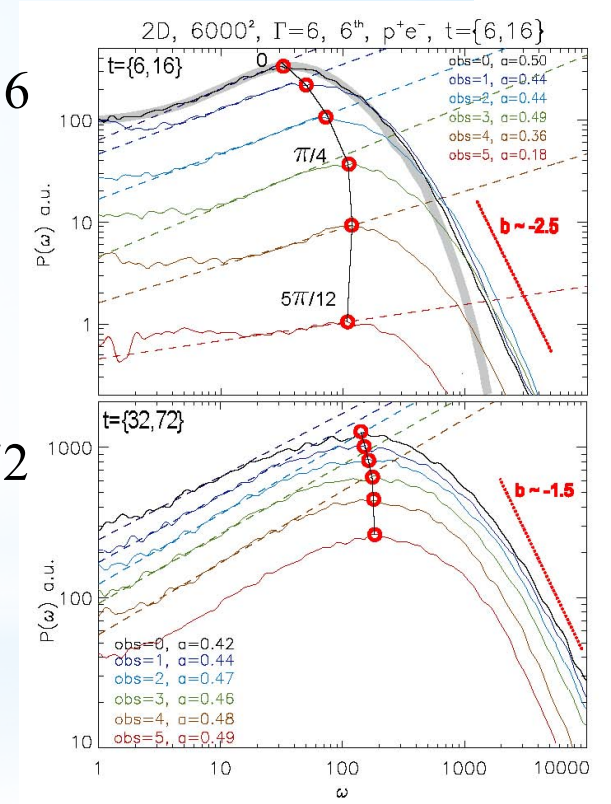

32<t<72

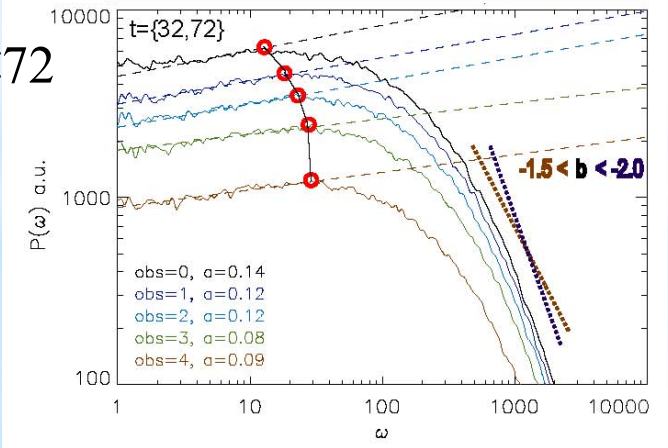

32<t<72

Frederiksen et al. ApJL 2010

Radiation from electrons by tracing trajectories self-consistently

using a small simulation system

initial setup for jitter radiation

select electrons
randomly (12,150)
in jet and ambient

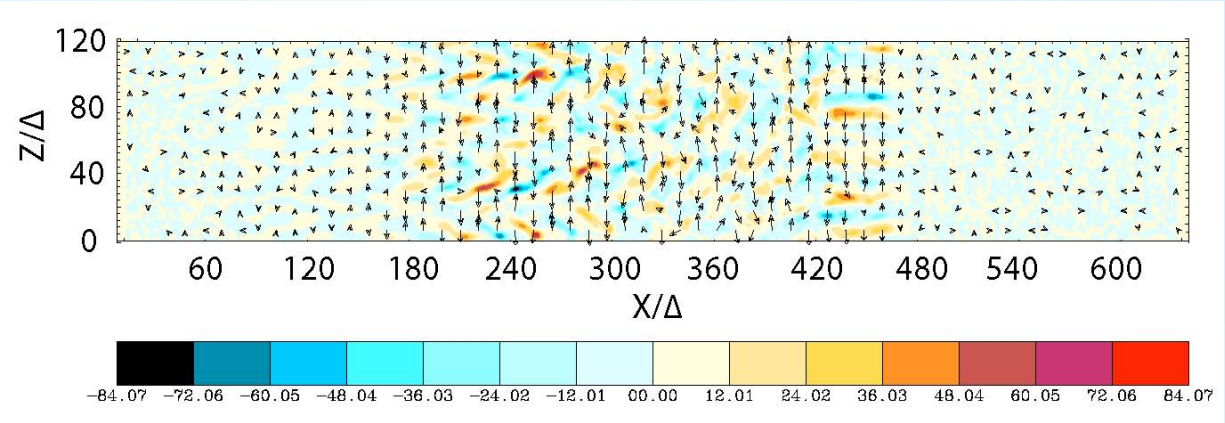

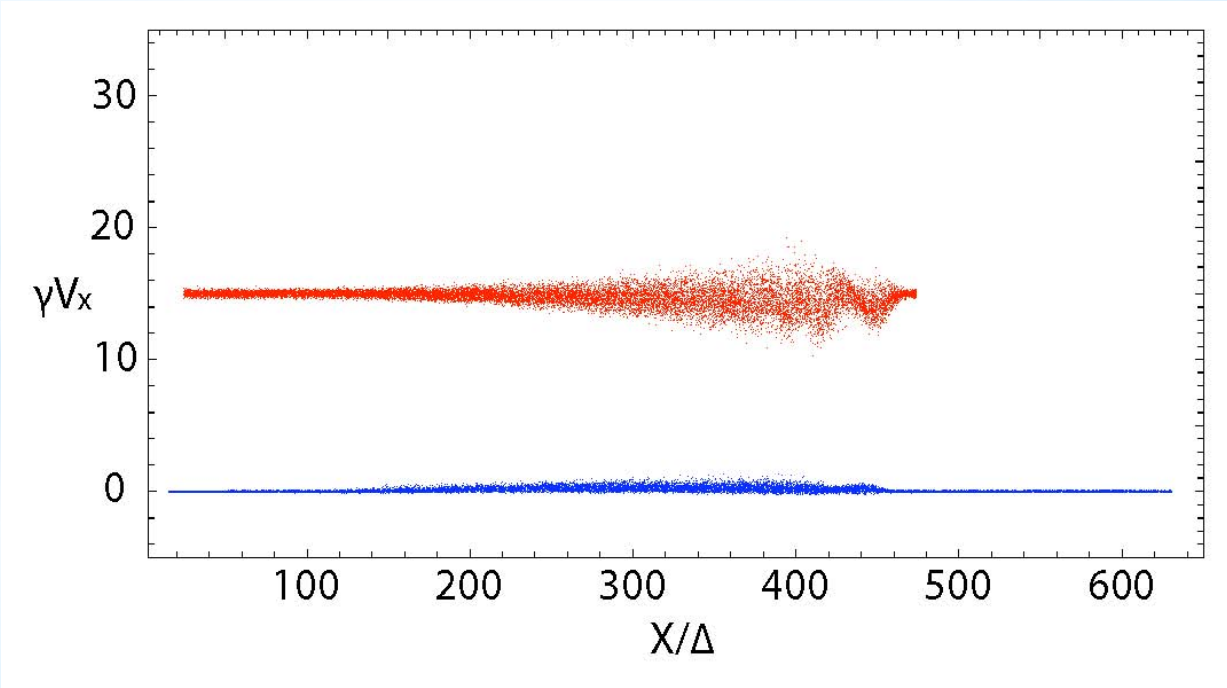

final condition for radiation

15,000 steps

dt = 0.005 ω_{pe}^{-1}

$n_\omega = 100$

$n_\theta = 2$

$\Delta x_{jet} = 75\Delta$

$t_r = 75\ \omega_{pe}^{-1}$

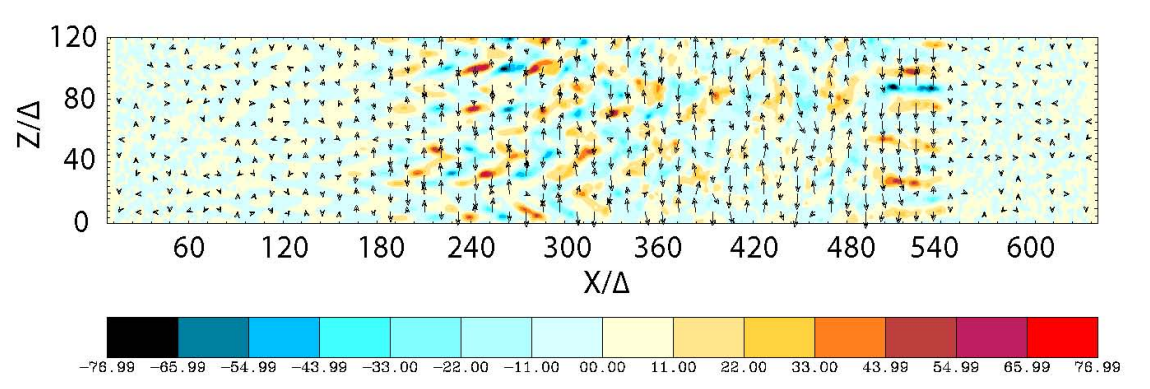

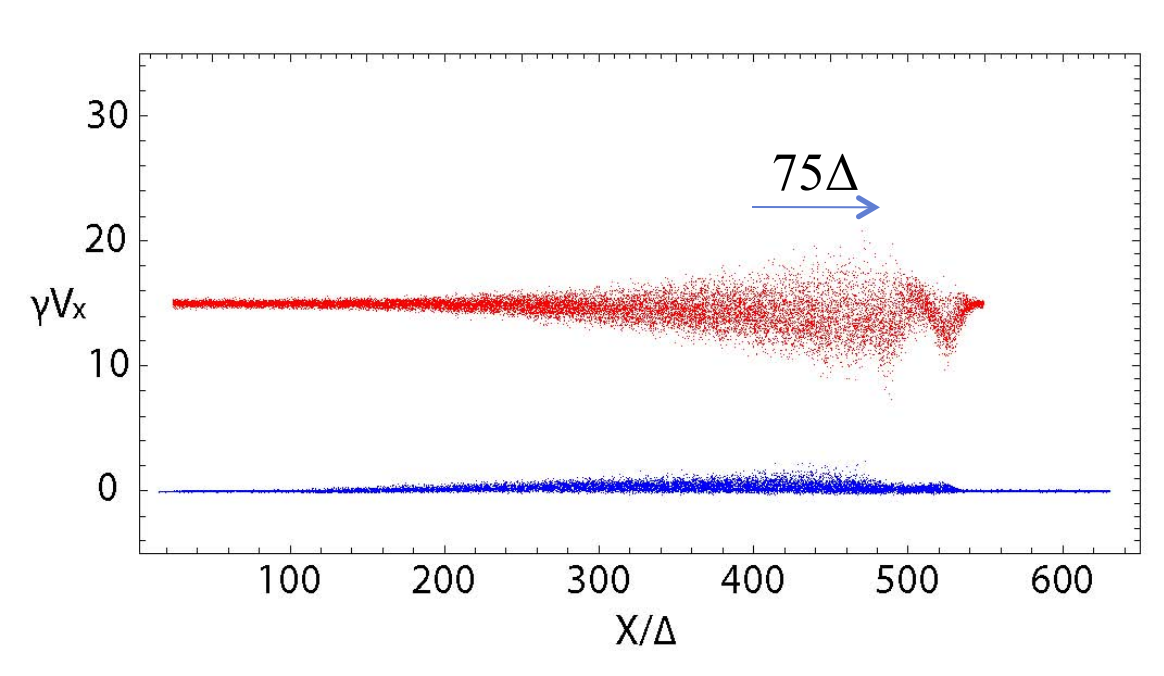

Calculated spectra for jet electrons and ambient electrons

$a = \lambda e|\delta B|/mc^2 < 1$ (λ: the length scale and $|\delta B|$ is the magnitude of the fluctuations)

$\gamma = 15$

$\theta = 0°$ and $5°$ $\theta_\gamma = 3.81^\circ$

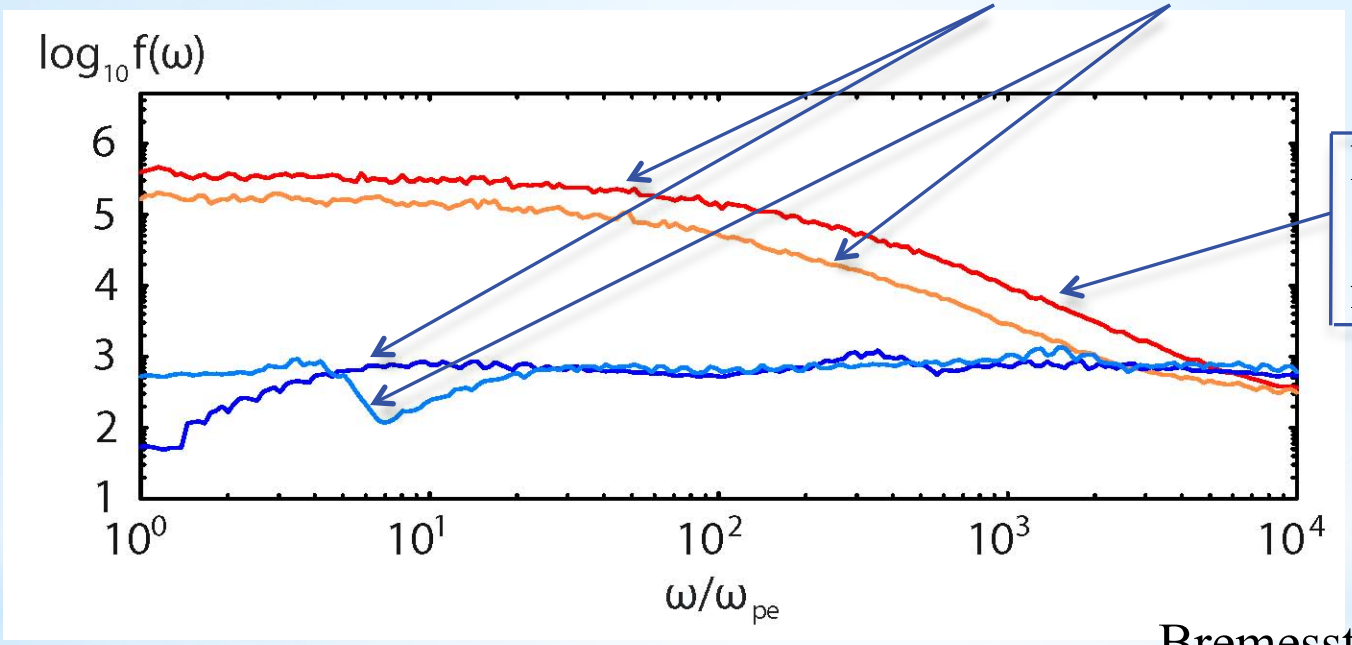

high frequency due to turbulent magnetic field

Bremesstrahlung (ballistic)

Case D

$\gamma = 7.11$

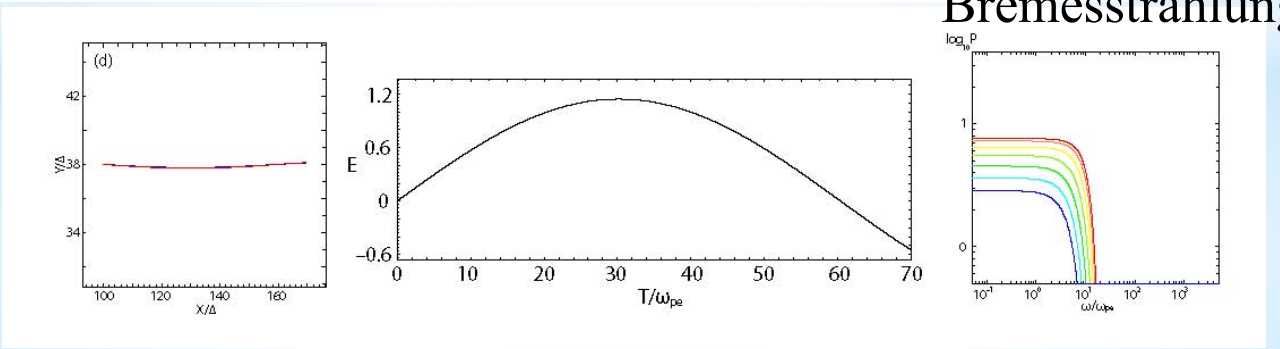

Nishikawa et al. 2009 (arXiv:0906.5018)

3D jitter radiation (diffusive synchrotron radiation) with a ensemble of mono-energetic electrons (γ = 3) in turbulent magnetic fields (Medvedev 2000; 2006, Fleishman 2006) (ballistic)

$P_B(k) \propto k^{\mu}$

2d slice of magnetic field

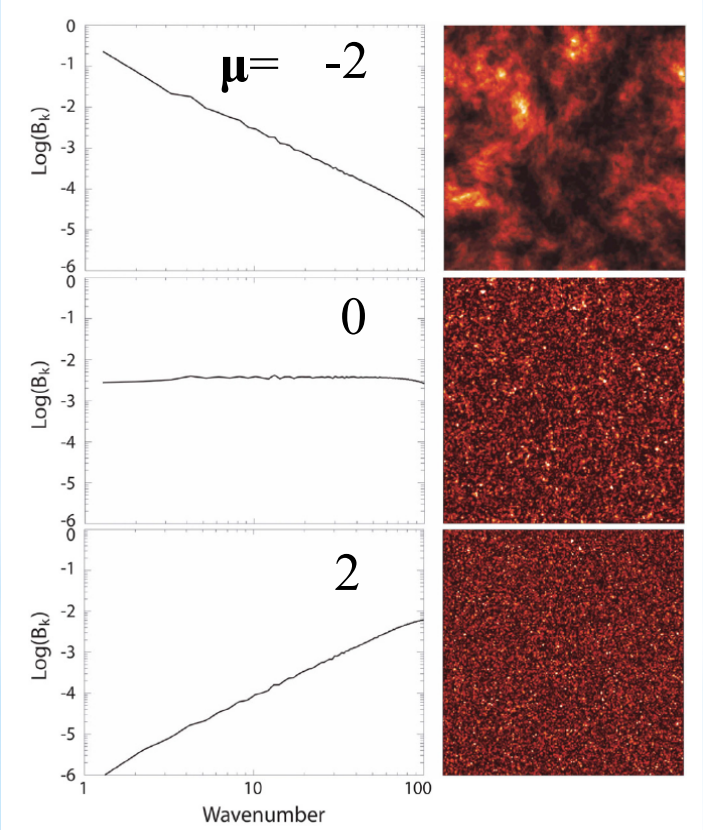

3D jitter radiation with γ = 3 electrons

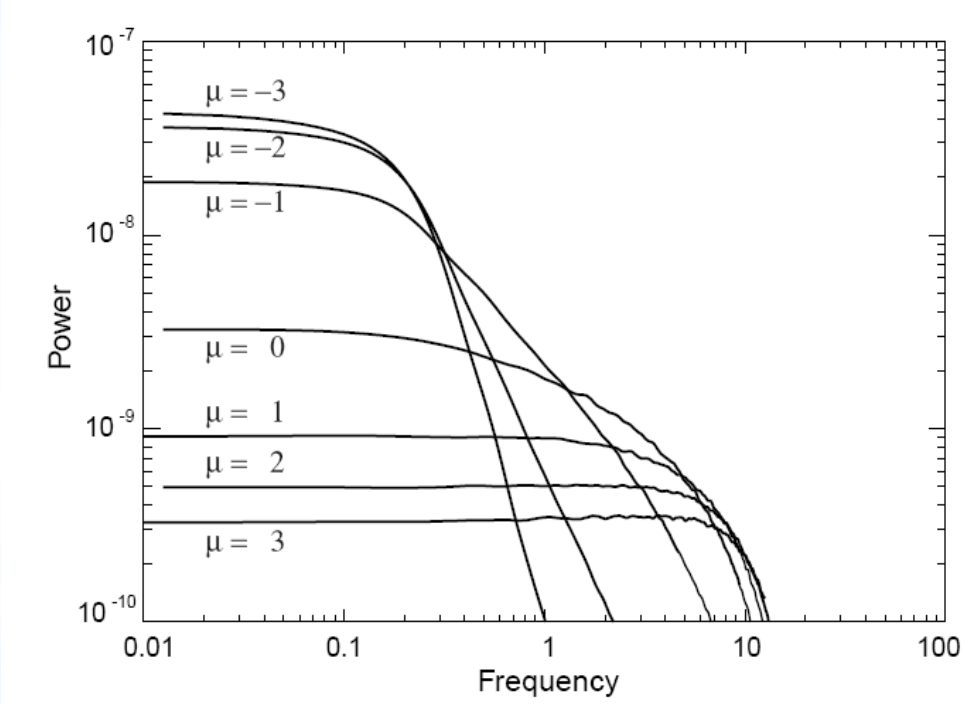

Hededal & Nordlund (astro-ph/0511662)

Dependence on Lorentz factors of jets

γ = 15

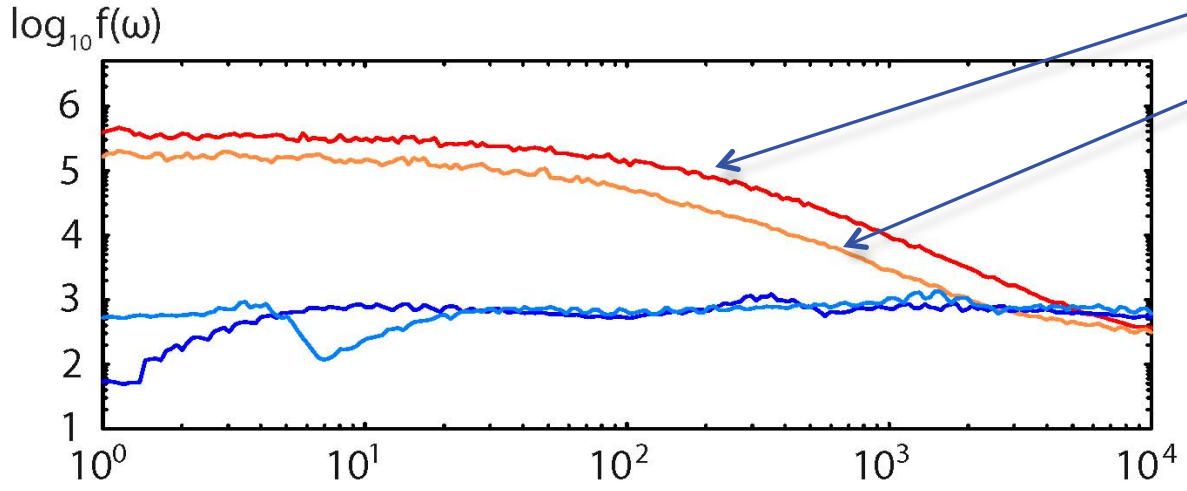

θ = 0°

5° $\theta_\gamma = 3.81^\circ$

γ = 100

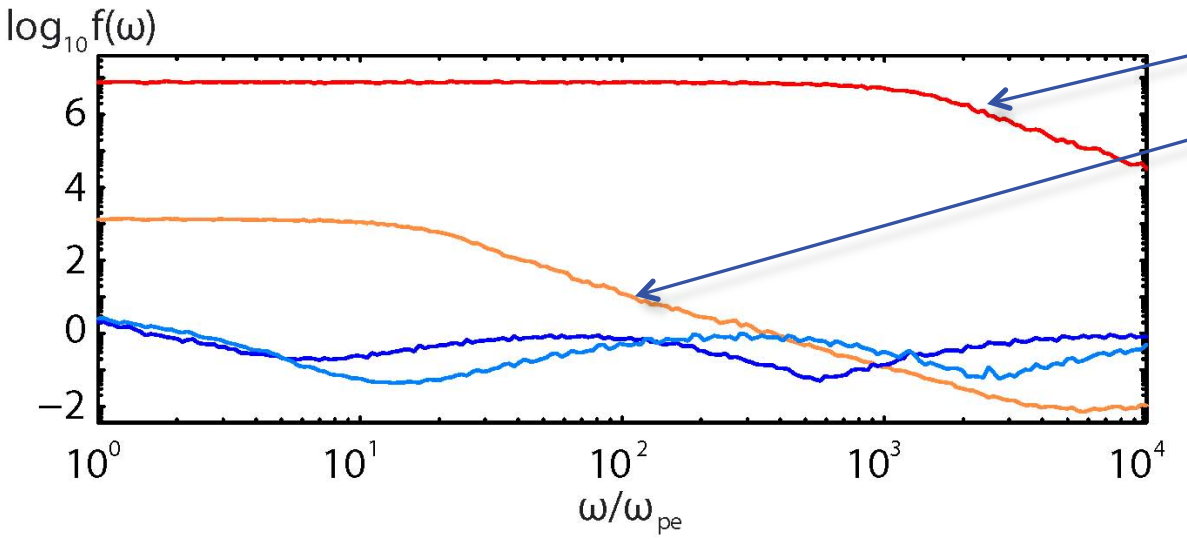

θ = 0°

5° $\theta_\gamma = 0.57^\circ$

Narrow beaming angle

Observations and numerical spectrum

GRB 080916C

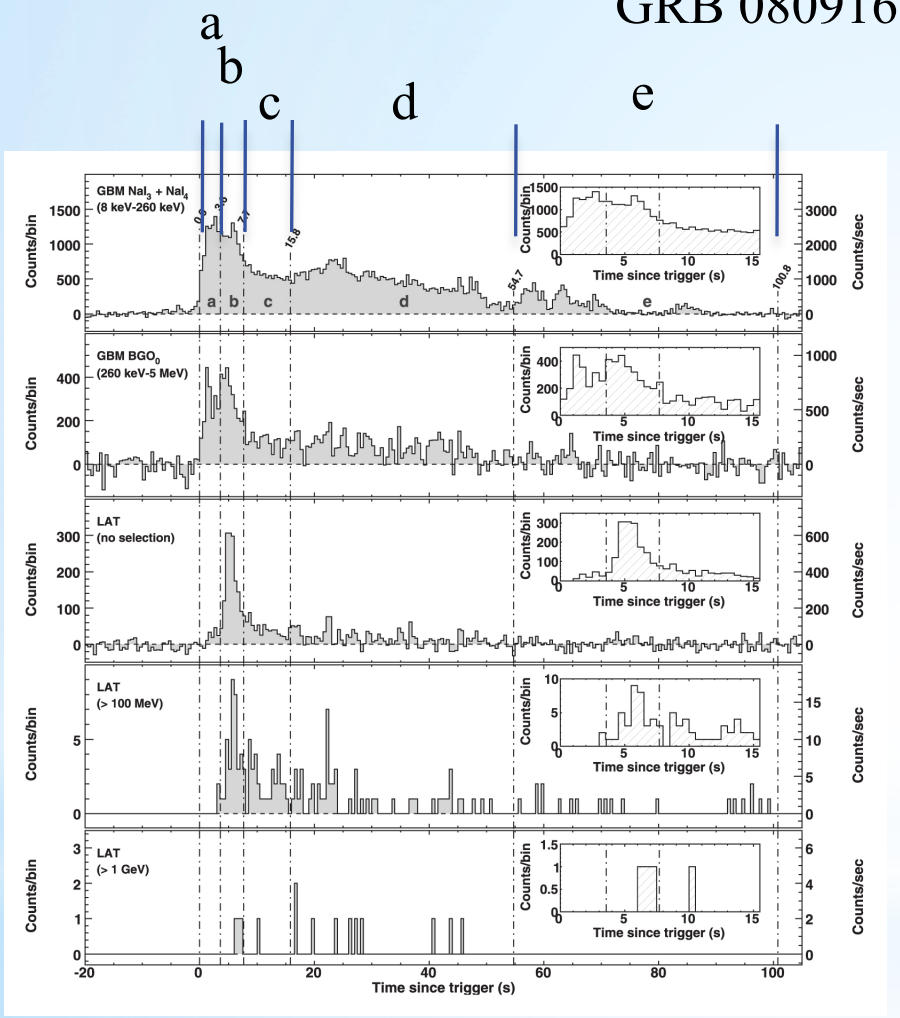

Abdo et al. 2009, Science

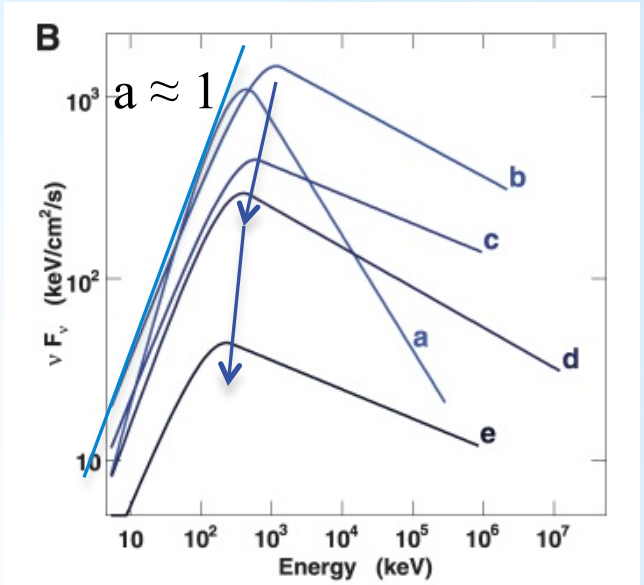

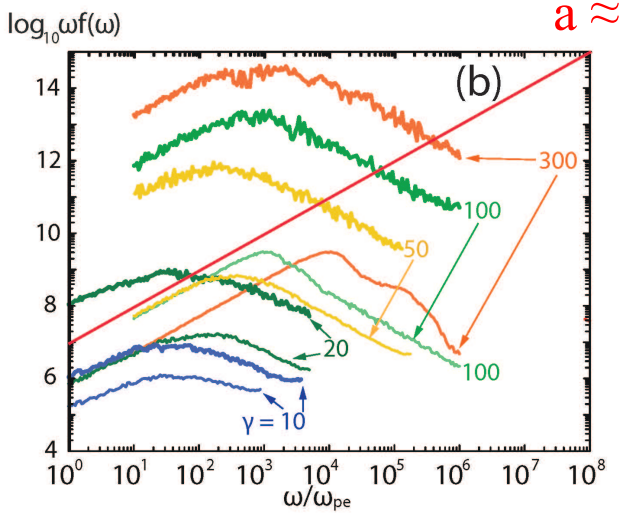

(Nishikawa et al. 2012)

Radiation in a small system

without iteration

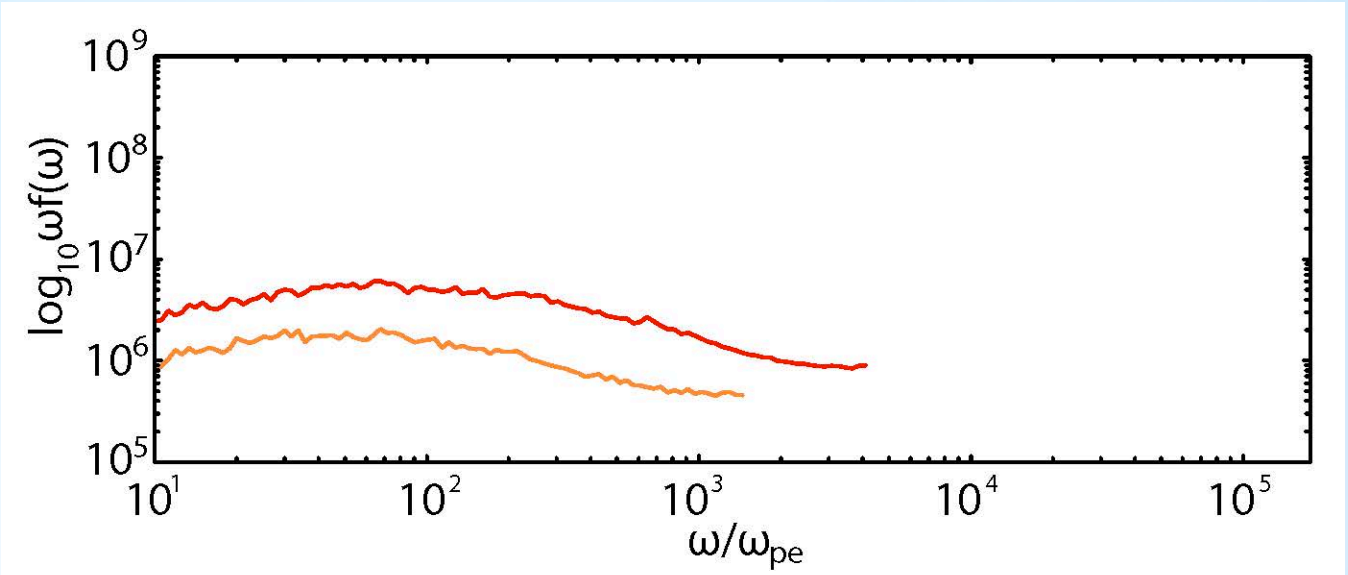

with iteration

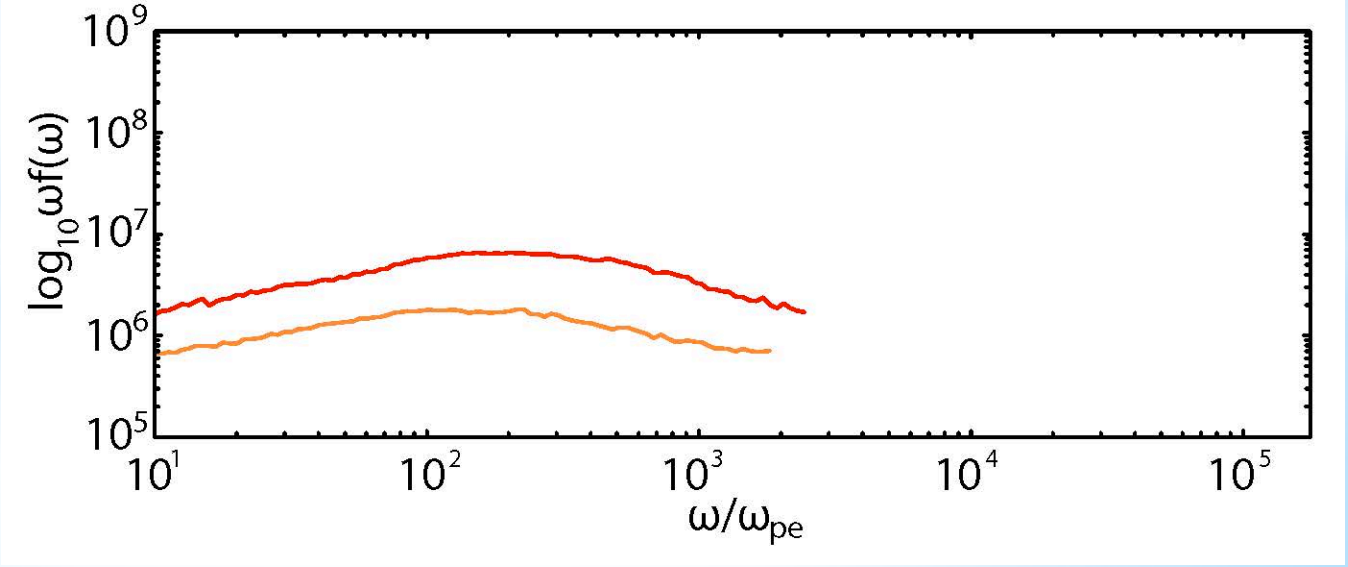

Radiation in a larger system at early time

System size: 8000 × 240 × 240
Electron-positron: $\gamma = 15$

Sampled particles 115,200

(a) $150\,\omega_{pe}^{-1} \le t \le 225\,\omega_{pe}^{-1}$

(b) $200\,\omega_{pe}^{-1} \le t \le 275\,\omega_{pe}^{-1}$

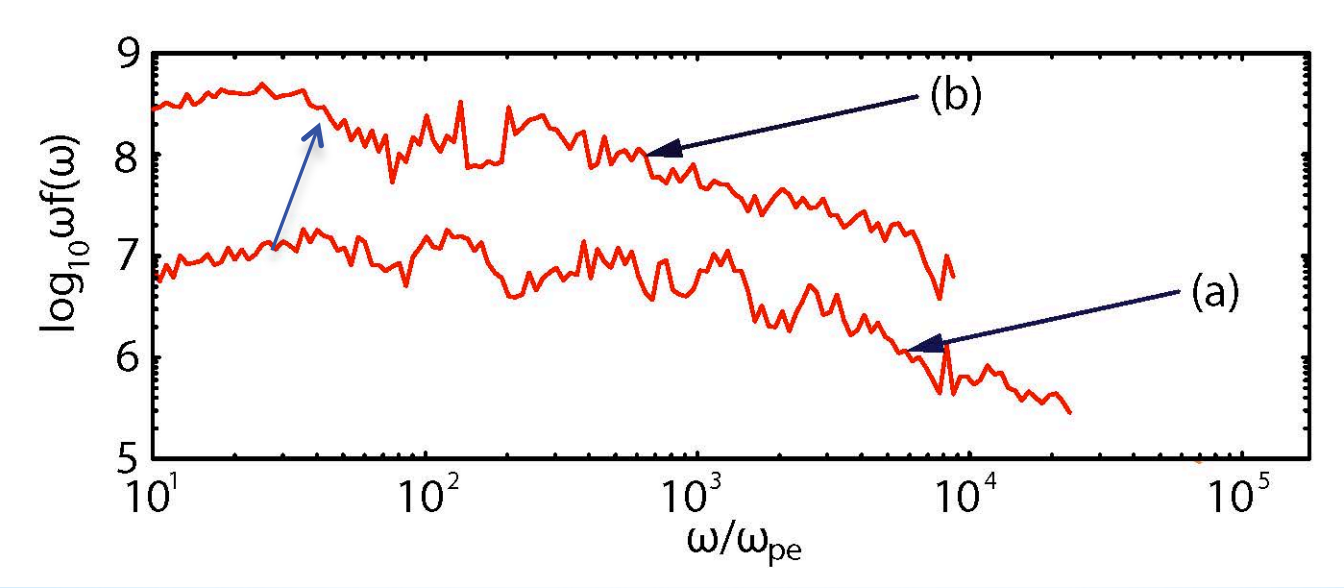

Nishikawa et al. in progress

Electron shock surfing acceleration

θ = 90

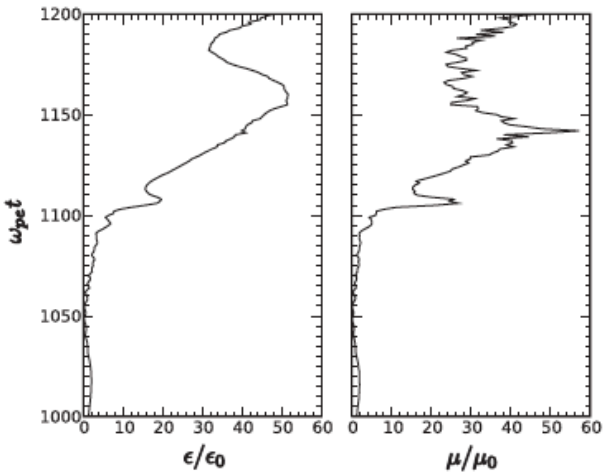

Figure 5. Time history of an accelerated electron: energy (left) and the first adiabatic invariant (right).

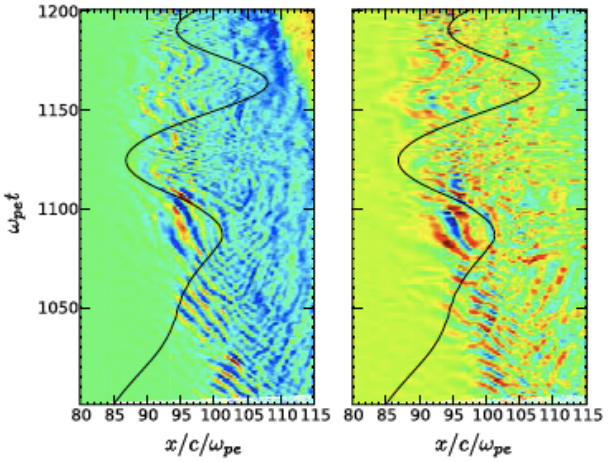

Figure 6. Electron trajectory and electric fields E_x (left) and E_y (right), respectively.

(Sironi & Spitkovsky, 2009, 2011,ApJ)

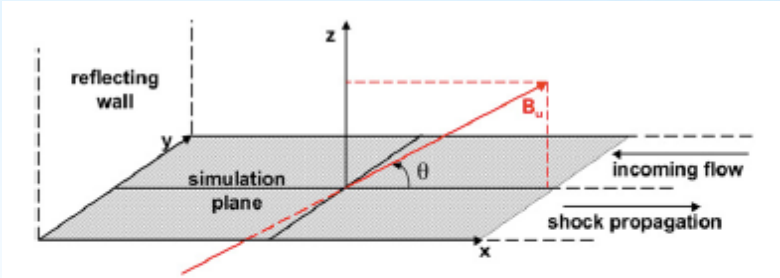

Figure 1. Simulation geometry and configuration of the upstream magnetic field.

(A color version of this figure is available in the online journal.)

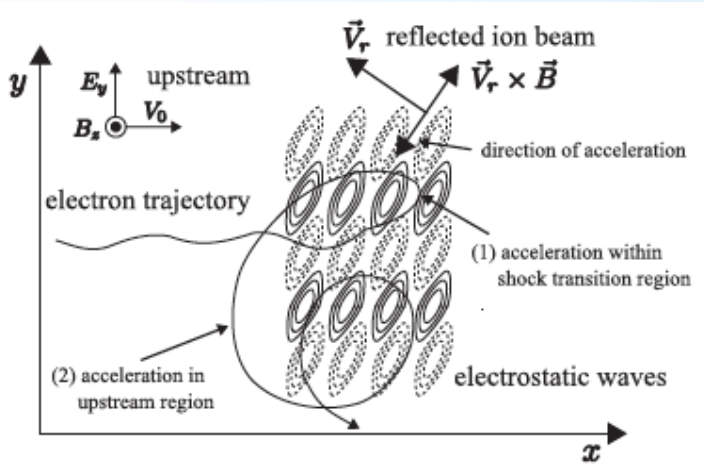

Figure 8. Schematic illustration of acceleration mechanism. Electrons are accelerated in two steps: (1) they are accelerated by the stochastic electron shock surfing in the shock transition region and preferentially transported to the upstream region. (2) The accelerated electrons escaping into the upstream suffer further acceleration by the constant motional electric field.

(Amano & Hoshino, 2009, ApJ)

The importance of the magnetic-field angle

* A SNR blast waves moves into a ***B*** with a preferred direction
  * The angle between B and shock normal varies from 90 deg to 0 deg.

* The physics of acceleration at parallel and perpendicular shocks is different

$$\tau_{acc} \propto \frac{\kappa_{nn}}{V_{shock}^2}$$

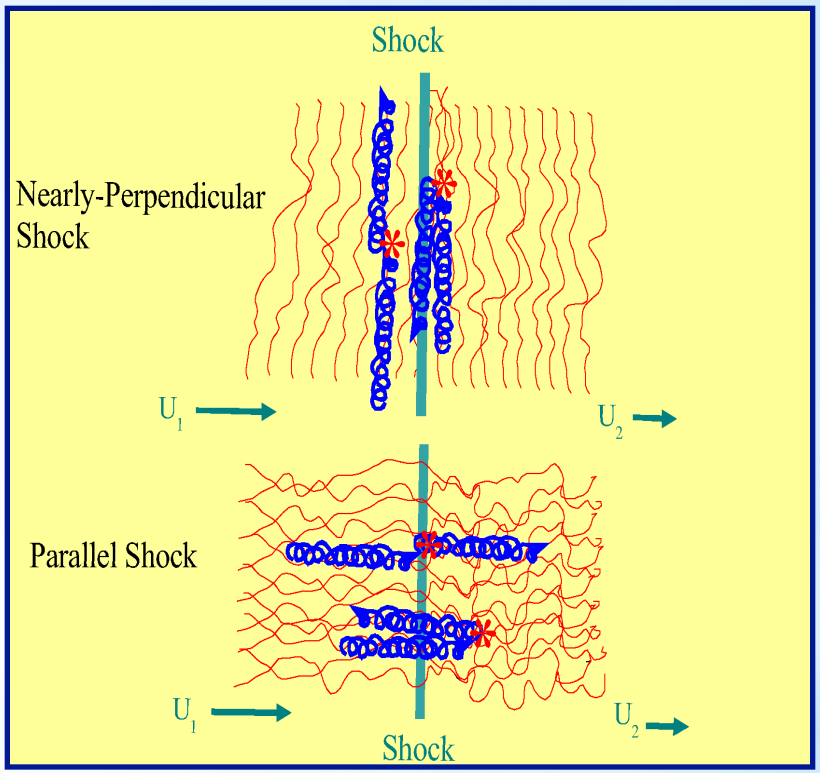

Parallel shocks → slow

Perpendicular shocks → fast

($K_\perp < K_\parallel$)

- for a given time interval or size of shock, a perpendicular shock will yield a larger maximum energy than a parallel shock.

Jokippi and Giacalone, Isradynamic 2008

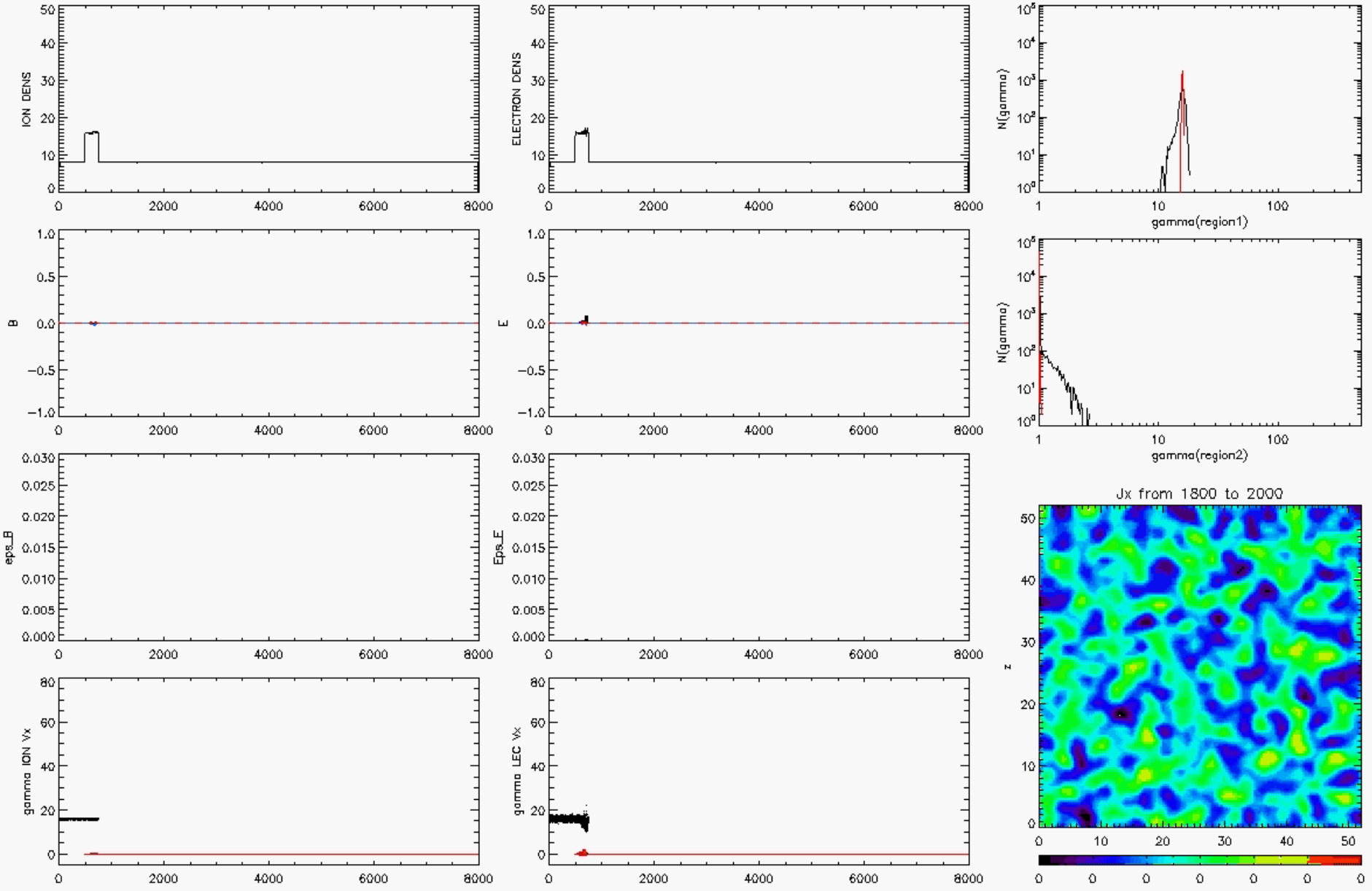
ION DENS
ELECTRON DENS
N(gamma)
gamma(region1)
gamma(region2)
B
E
eps_B
Eps_E
Jx from 1800 to 2000
gamma ION Vx
gamma LEC Vx
z

Perpendicular magnetic field

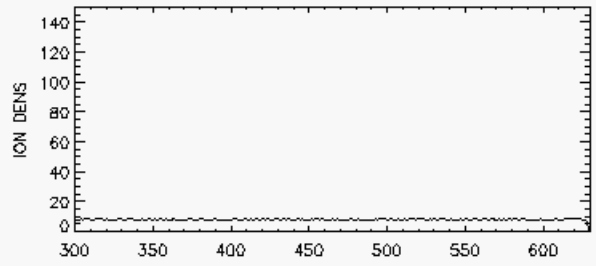

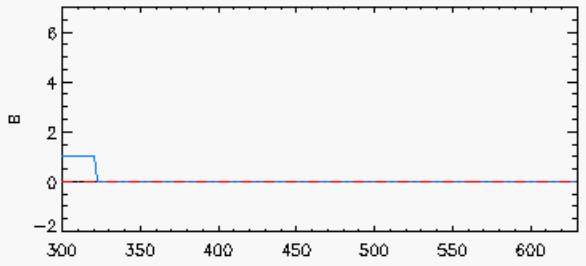

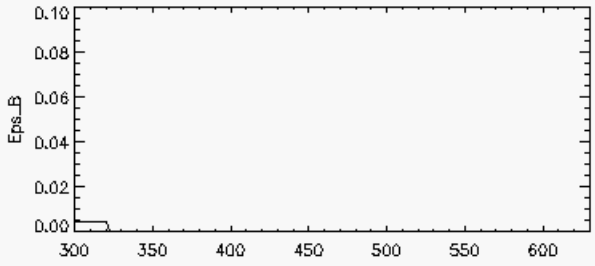

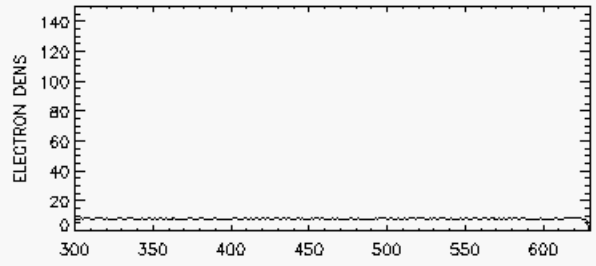

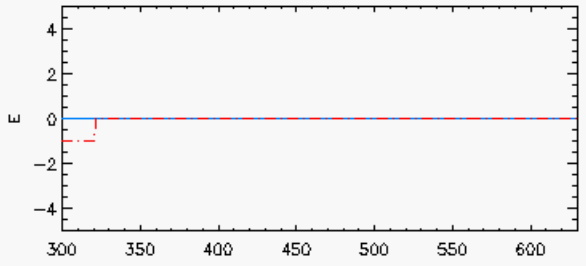

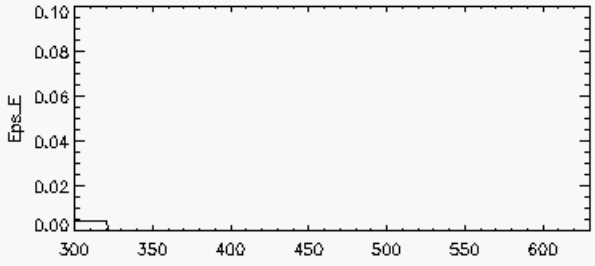

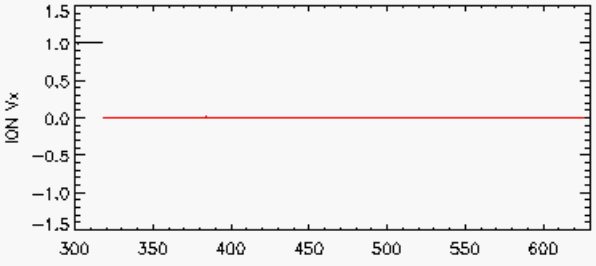

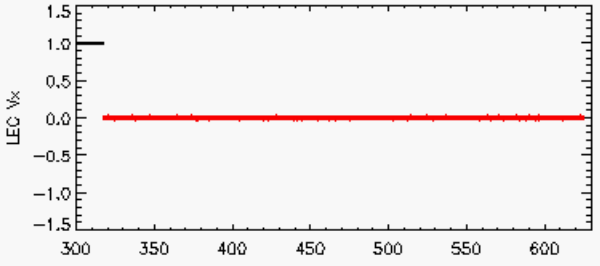

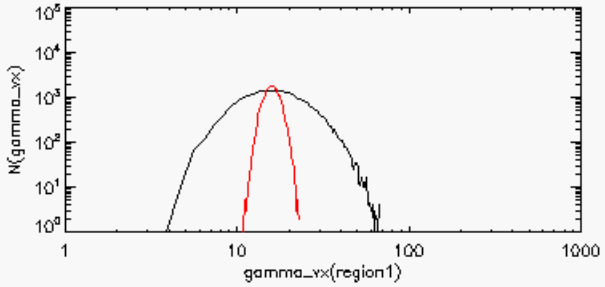

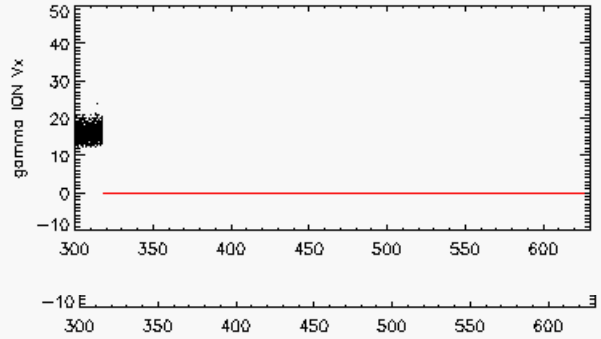

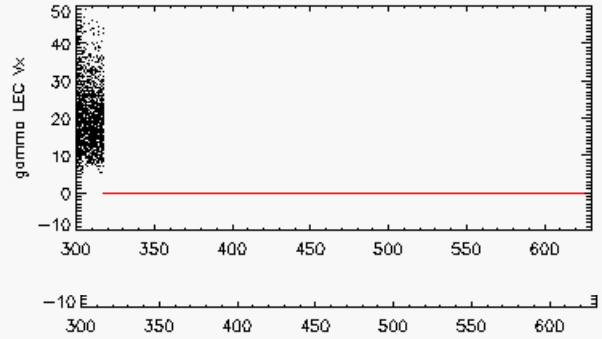

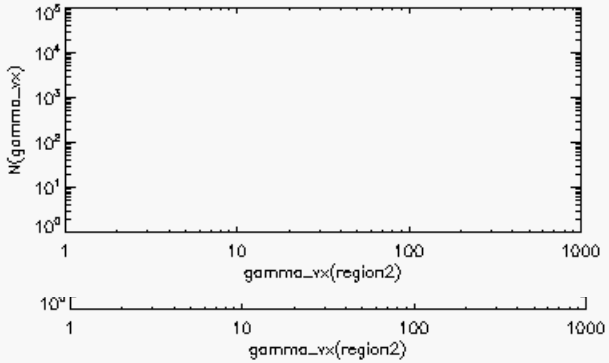

Reconnection in jet

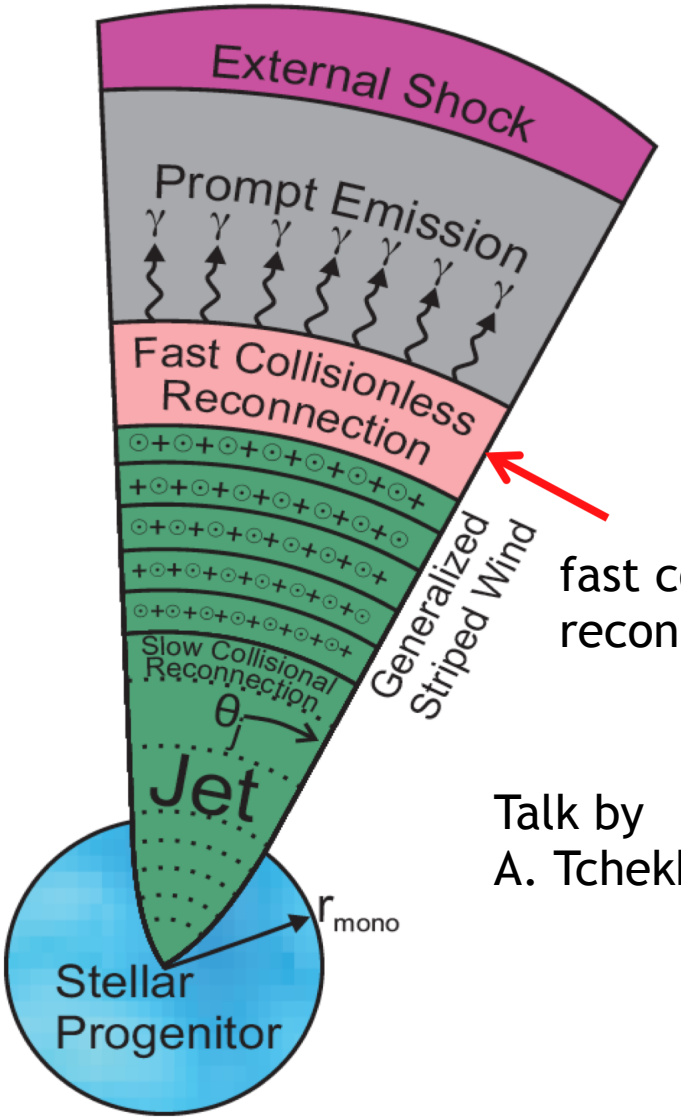

fast collisionless reconnection

Talk by
A. Tchekhovskov

Reconnection switch concept: Collapsar model or some other system produces a jet (with opening half-angle θ_j) corresponding to a generalized stripped wind containing many field reversals that develop into dissipative current sheets (McKinney and Uzdensky, 2012, MNRAS, 419, 573). This reconnection needs to be investigated by resistive RMHD, which is in progress within our research effort.

(see also Bing's talk)

Simulations with magnetic field in jets

no magnetic field anti-parallel magnetic field

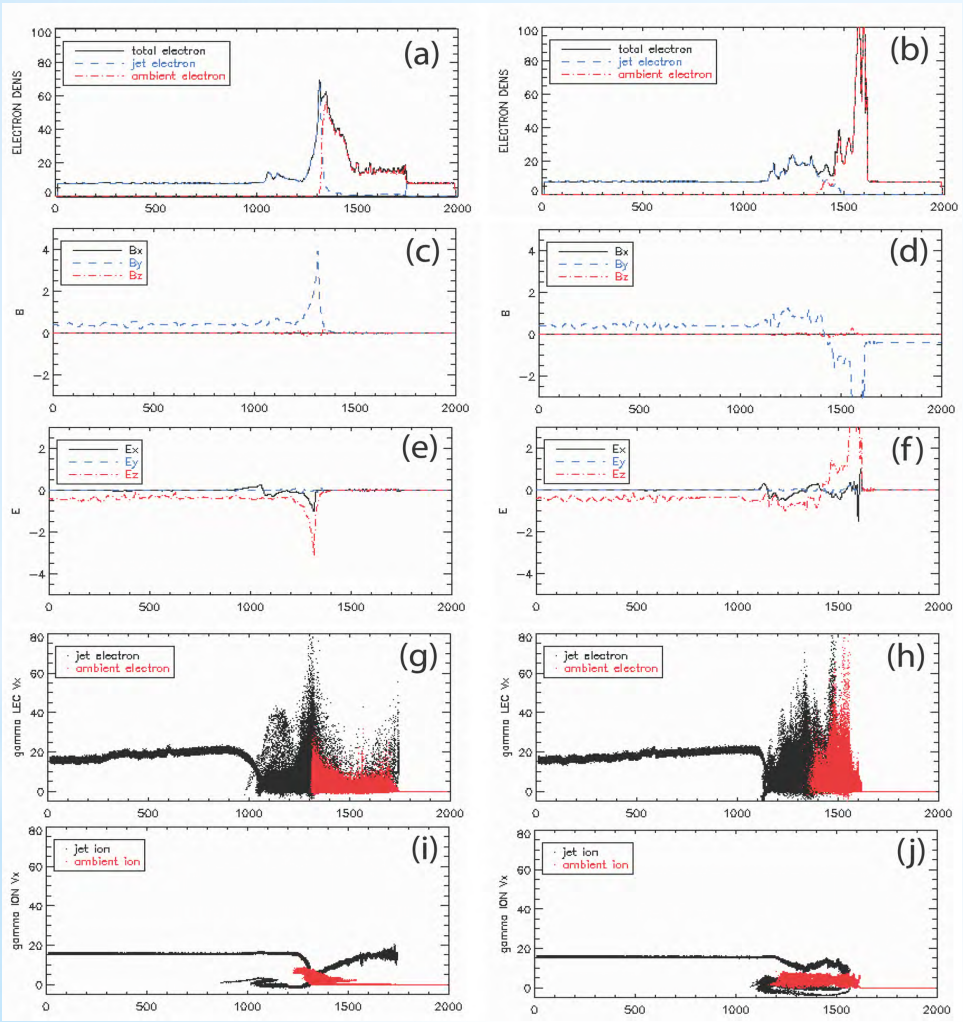

Snapshots for unmagnetized ambient plasma (left column) and anti-parallel magnetic field in the ambient plasma (right column) at t = 1450 ω_{pe}^{-1} (Choi, Min, and Nishikawa, 2012). The averaged values of electron density (a) and (b), magnetic field (c) and (d), electric field (e) and (f), phase space of electrons (g) and (h), and phase space of ions (i) and (j). Reconnection occurs for the case of anti- parallel magnetic fields and is indicated by the positive E_y component in (f).

Choi, Min, KN, 2013 (in progress)

(Nishikawa et al. 2012)

lical magnetic field

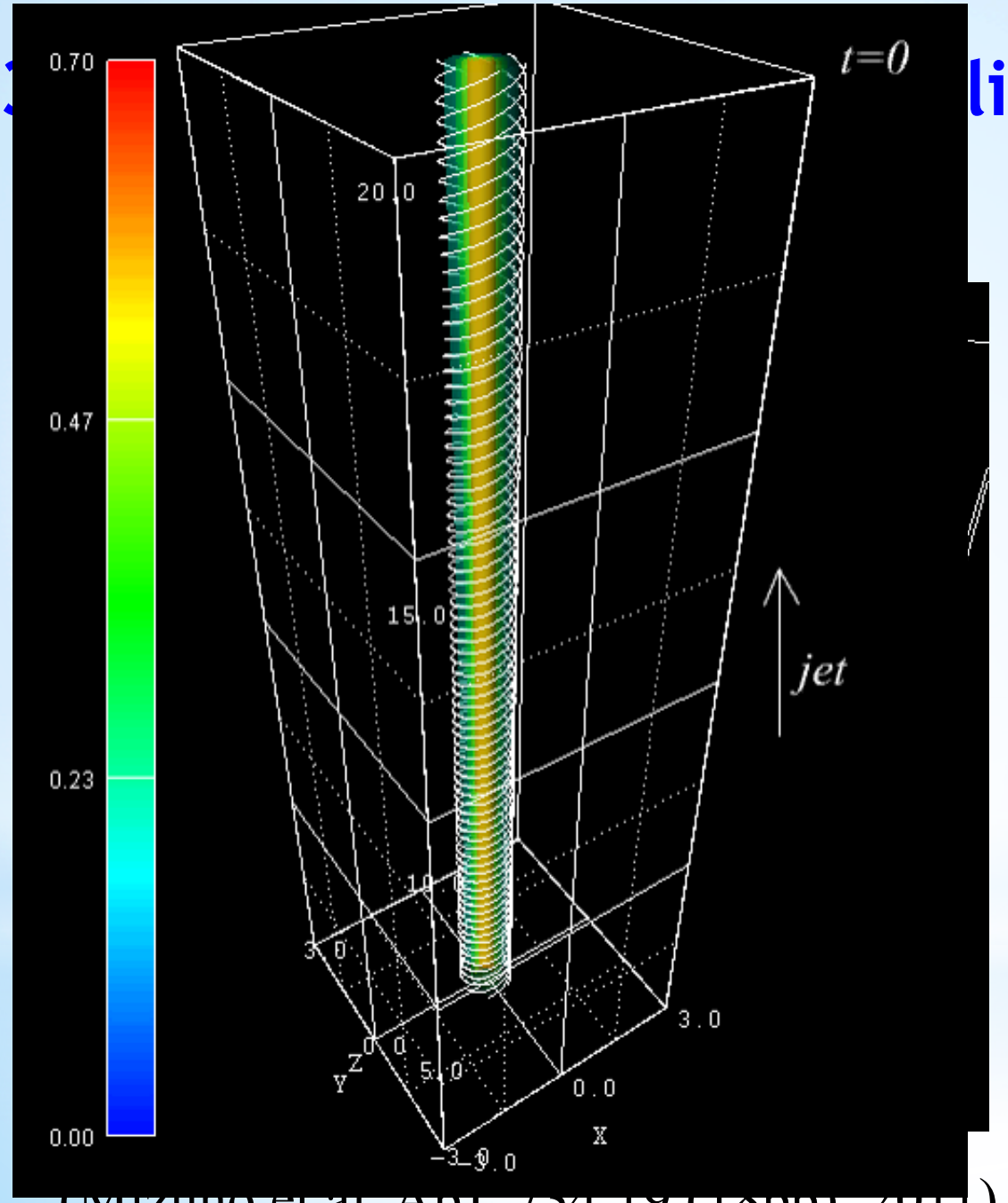

(Mizuno et al. ApJ, 734:19 (18pp), 2011)

Relativistic jet with helical magnetic field, which leads to the kink instability and subsequent reconnection, can be simulated using resistive relativistic MHD (this simulation was performed with ideal RMHD code).

3D RHD simulation of recollimation shock similar parameters of Gómez et al. (1997)

t = 100 R_{jet}/c

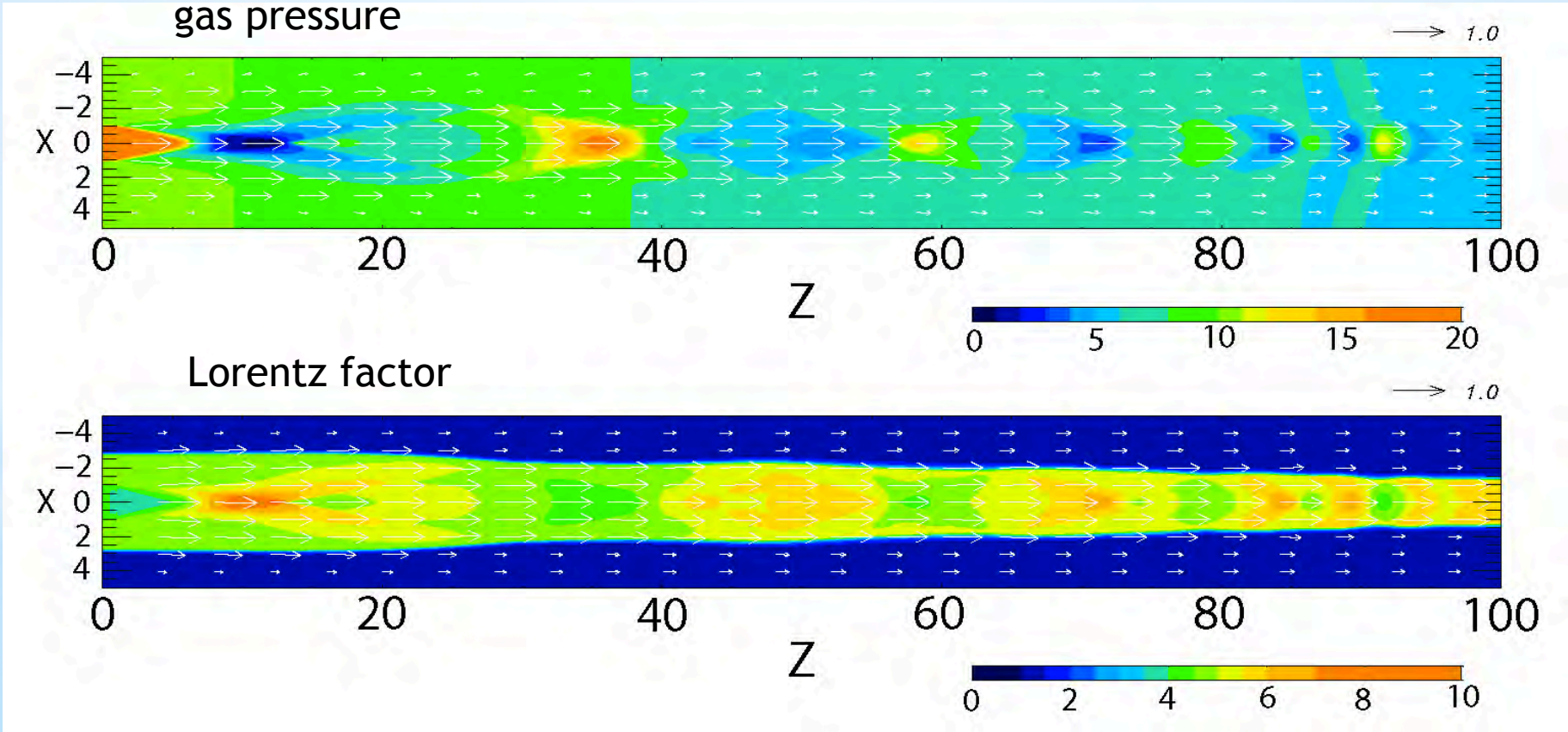

(Mizuno et al. in progress, 2014)

The gas pressure of a jet obtained by RMHD simulation with an initial over-pressure

Series of recolimation shocks

Propagation of perturbed shock

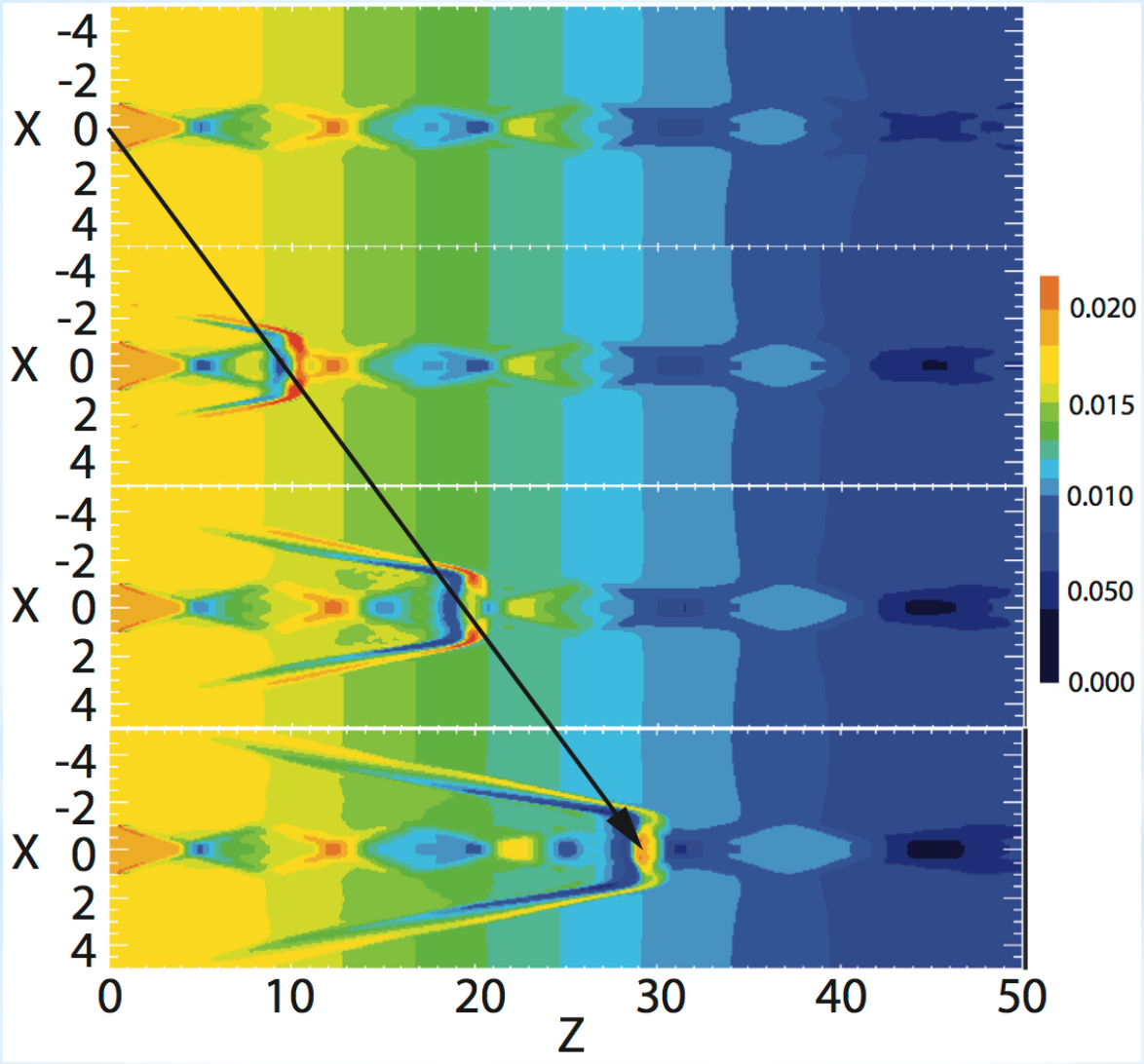

(Mizuno et al. in progress, 2014)

Summary

- Spectra from two electrons were calculated for different conditions.
- The magnetic fields created by the Weibel instability generate highly inhomogeneous magnetic fields, which are responsible for itter radiation (Medvedev, 2000, 2006; Fleishman 2006; Frederiksen et al. 2010, Medvedev et al 2011, Nishikawa et al. 2011)
- Our new numerical approach of calculating radiation from electrons based on self-consistent simulations provides more realistic spectra including jitter radiation
- Need further calculation of synthetic spectra with spectral evolution
- Reconnection is very important to release magnetic field energy to kinetic energy
- Recollimation shock may create gamma-ray flash by moving perturbation

Future plans

- Further simulations with a systematic parameter survey will be performed in order to understand shock dynamics including KKHI and reconnection
- Further simulations will be performed to calculate self-consistent radiation including time evolution of spectrum and time variability using larger systems
- Investigate radiation processes from the accelerated electrons in turbulent magnetic fields and compare with observations using global simulation of shock, KKHI and reconnection with helical magnetic field in jet (GRBs, SNRs, AGNs, etc)
- Particle acceleration and radiation in recollimation shocks

GRB progenitor (collapsar, merger, magnetar)

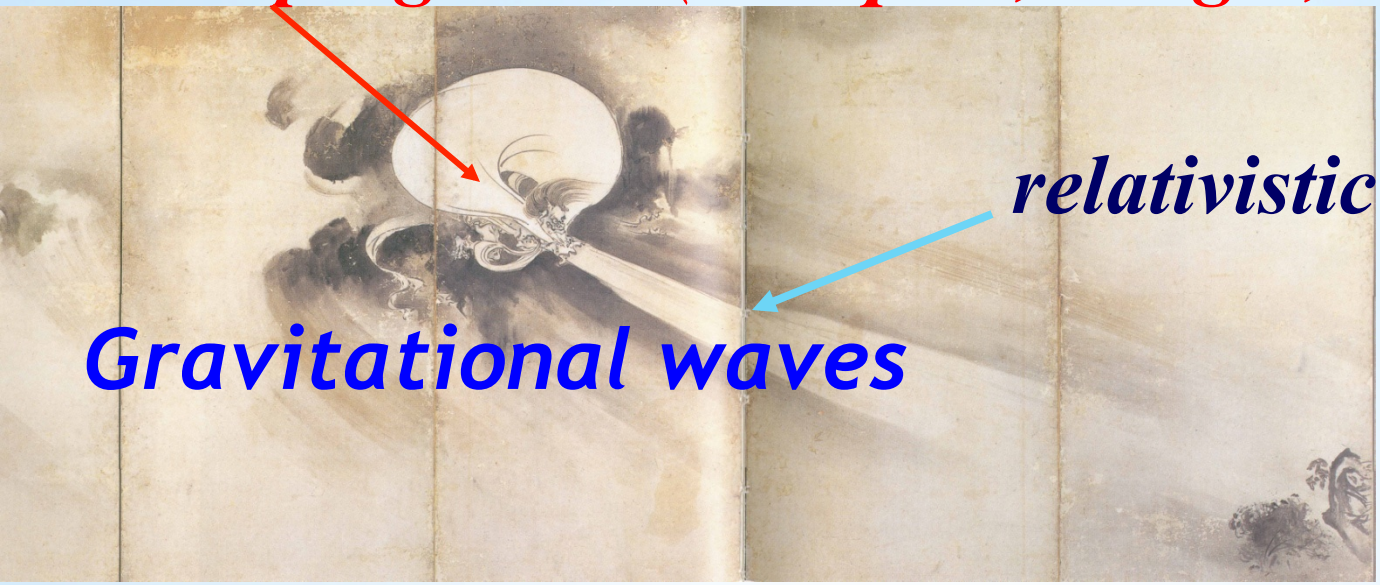

relativistic jet

Gravitational waves

Fushin

(god of wind)

EM emission

(shocks, acceleration)

Raishin

(god of lightning)

(Tanyu Kano 1657)

Emission Lines from Tori

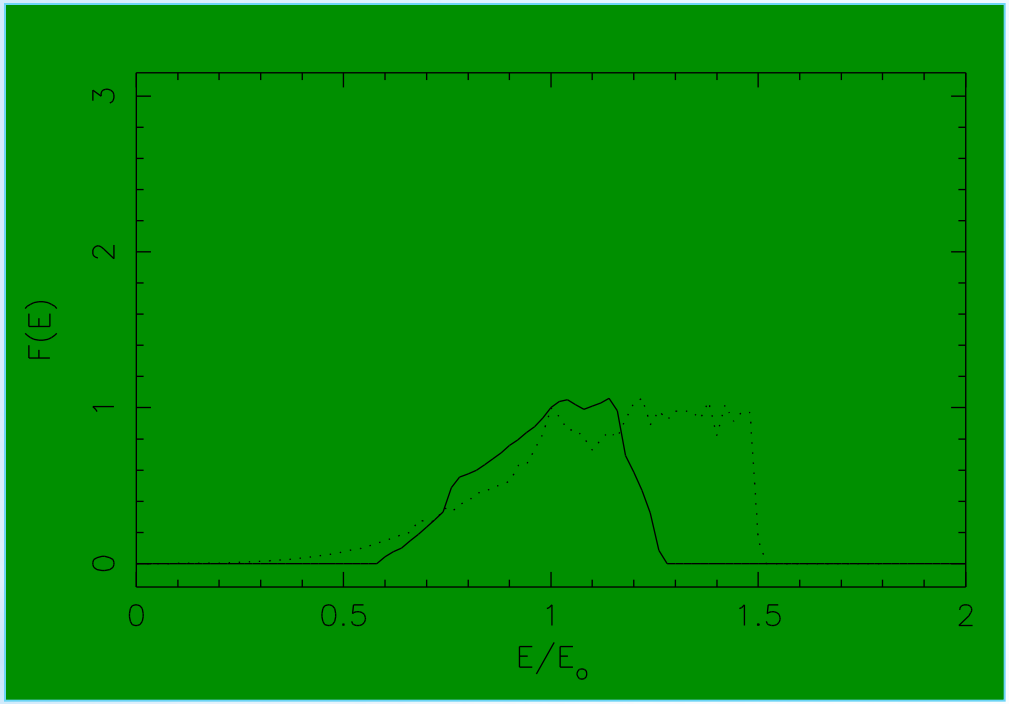

Comparison of emission line between accretion torus (solid) and disk (dotted) inclined at 85°.

- Inner most region is obscured – weakening the red and blue wings.
- A broad emission line centered at 6.4keV results.
- This may explain why not many sources with asymmetric lines like MCG-6-30-15 are observed.

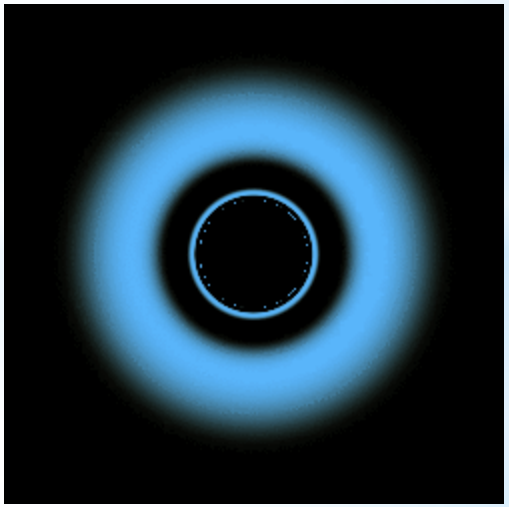

Partially transparent torus around a Kerr Black Hole.

(Fuerst & Wu 2004, A&A, 424, 733)

*Relativistic Radiation Transfer

Fuerst, Mizuno, Nishikawa, & Wu, 2007, ApJL, submitted

- We have calculated the thermal free-free emission and thermal synchrotron emission from a relativistic flows in black hole systems based on the results of our 2D GRMHD simulations (rotating BH cases).
- We consider a general relativistic radiation transfer formulation (Fuerst & Wu 2004, A&A, 424, 733) and solve the transfer equation using a ray-tracing algorithm.
- In this algorithm, we treat general relativistic effect (light bending, gravitational lensing, gravitational redshift, frame-dragging effect etc.).

Image of Emission, absorption & scattering

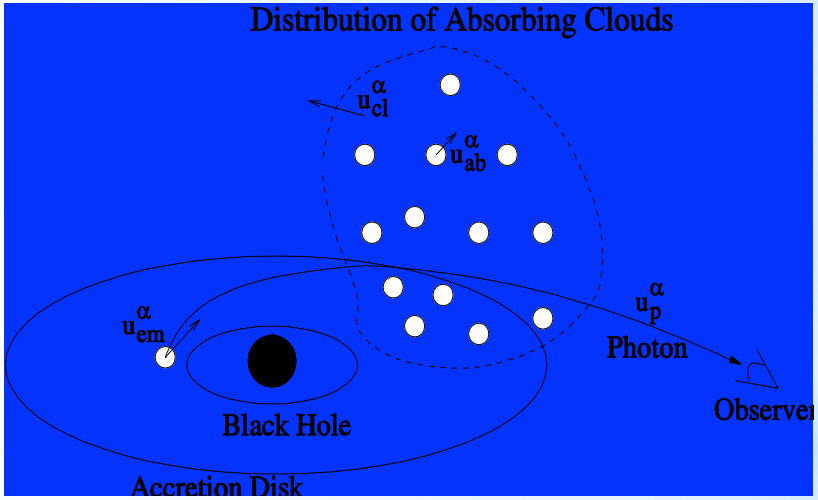

*Relativistic Radiation Transfer

Project image of thermal emission (<20 rs)

2D GRMHD simulations (*old version)* (a = 0.95, B = 0.1 $(\rho c^2)^{-2}$)

- **The radiation image shows the front side of the accretion disk and the other side of the disk at the top and bottom regions.**
- **It is because the general relativistic effects.**

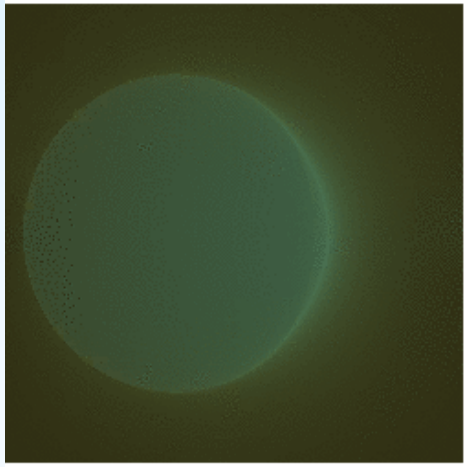

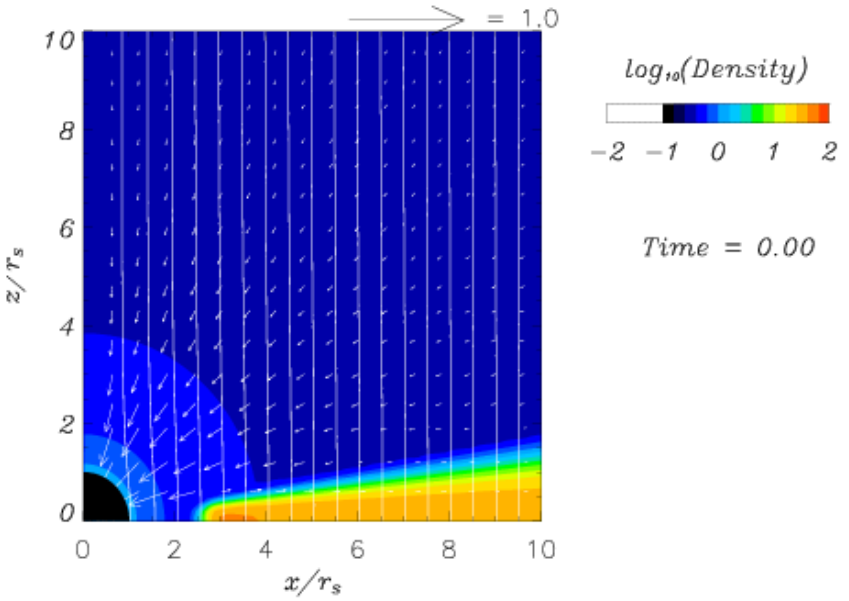

- **We can see the propagation of waves and the strong radiation from geometrically thick disk near the BHs.**
- **The jet generated in GRMHD simulation is not visible in the radiation image.**
- **This is because we assume the thermal free-free emission. It has a strong density dependence and the jet is less dense than the disk.**
- **If we calculate the emission with weaker dependence on the density, such as non-thermal process or Compton scattering, the jet would be visible.**

(Wu et al. 2008)

* *Radiation images of black hole-disk system*

- **The radiation image shows the front side of the accretion disk and the other side of the disk at the top and bottom regions because the general relativistic effects.**
- **We can see the formation of two-component jet based on synchrotron emission and the strong thermal radiation from hot dense gas near the BHs.**
- **A beaming synchrotron emission (green-spark) is seen the surface of the disk (time-dependent). It would be a origin of QPOs?**

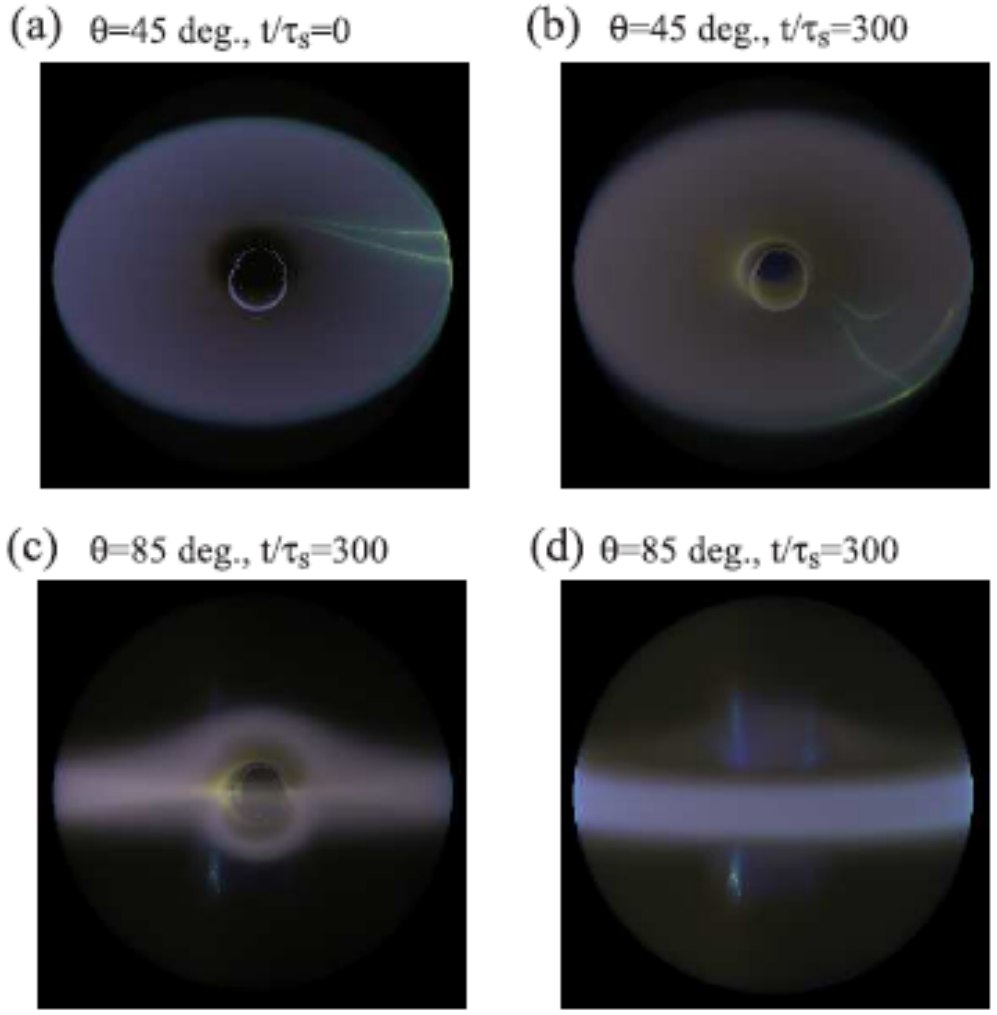

Fuerst, Mizuno, Nishikawa, & Wu, 2007, ApJL, submitted

* Summary

* **Simulation results show electromagnetic stream instability driven by streaming $e^{\pm}$ pairs are responsible for the excitation of near-equipartition, turbulent magnetic fields and a structure with leading and trailing shocks.**
* **Shock is similar to the shock in simulations with the constant contact discontinuity.**
* **The spectrum from jet electrons in a weak magnetic field in a small system shows a Bremsstrahlung like spectrum with higher frequency enhancement with turbulent magnetic field.**
* **The magnetic fields created by Weibel instability generate highly inhomogeneous magnetic fields, which is responsible for jitter radiation (Medvedev, 2000, 2006; Fleishman 2006).**

Future plans of our simulations of relativistic jets

- **Calculate radiation with larger 3-D systems for different parameters including magnetic fields in order to compare with observational data**

- **Include inverse Compton emission beside synchrotron radiation to obtain high frequency radiation**

- **Simulations with magnetic fields including turbulent magnetic fields with pair plasma and electron-ion plasma**

- **Reconnection simulations for additional acceleration mechanism including magnetic reconnection**

- **Non-relativistic jet simulations for understanding SNRs**

* Gamma-Ray Large Area Space Telescope (FERMI)

(launched on June 11, 2008) http://www-glast.stanford.edu/

Compton Gamma-Ray Observatory (CGRO)

Burst And Transient Source Experiment

(BATSE) (1991-2000)

PI: Jerry Fishman

Fermi (GLAST)

All sky monitor

* **Large Area Telescope (LAT) PI: Peter Michaelson: gamma-ray energies between 20 MeV to about 300 GeV**
* **Fermi Gamma-ray Burst Monitor (GBM) PI: Bill Paciaas (UAH) (Chip Meegan (Retired;USRA)): X-rays and gamma rays with energies between 8 keV and 25 MeV**

(http://gammaray.nsstc.nasa.gov/gbm/)

The combination of the GBM and the LAT provides a powerful tool for studying radiation from relativistic jets and gamma-ray bursts, particularly for time-resolved spectral studies over very large energy band.

* Jet formation in general relativistic PIC simulation

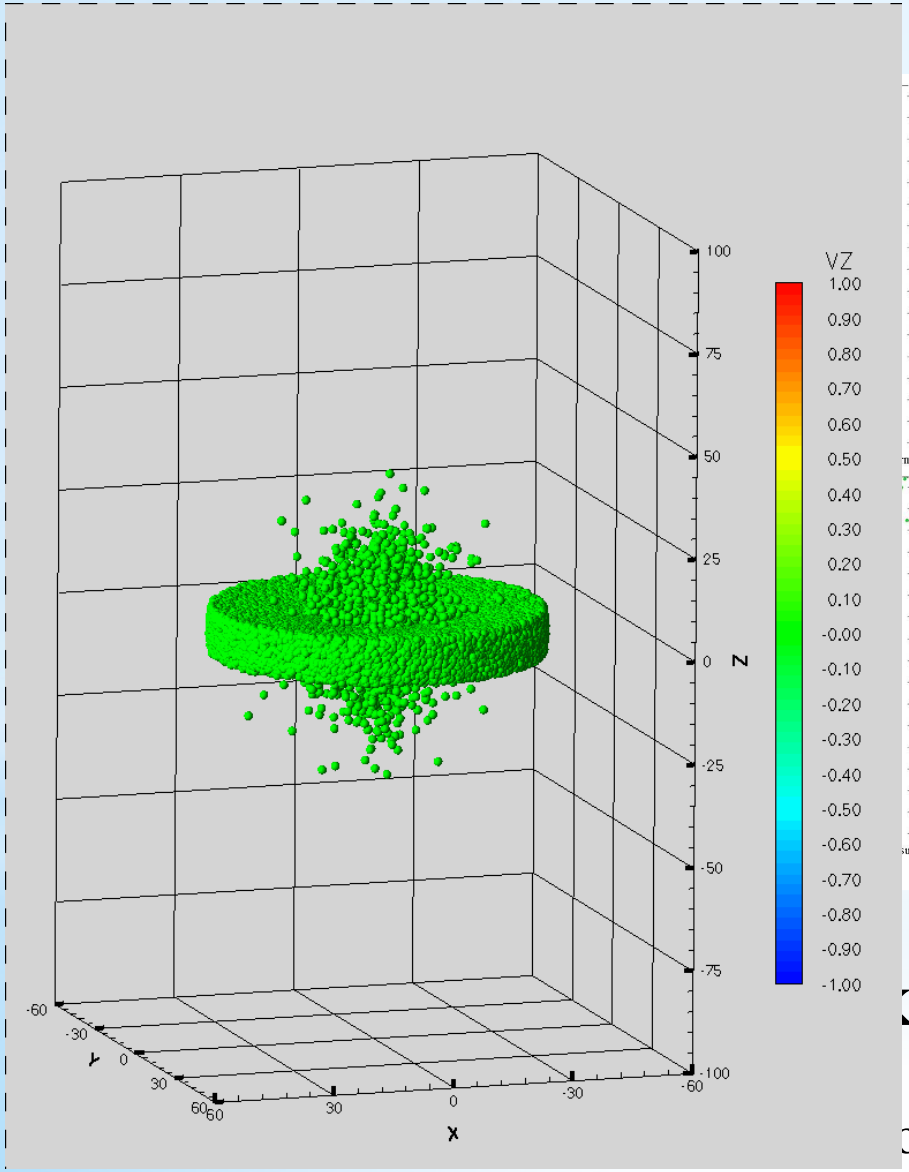

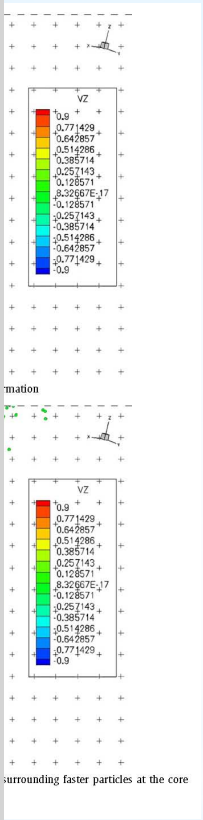

Keplerian motion of electrons and positrons may excite charge separation instability, then generate jet

Kerr–Schild metric in electromagnetic
& K.-I. Nishikawa,
ons 181 (2010) 1750–1757

Summary

- **We have developed a new three-dimensional general relativistic magnetohydrodynamic (GRMHD) code ``RAISHIN" (RelAtivIStic magnetoHydrodynamic sImulatioN, RAISHIN is the Japanese ancient god of lightning) by using a conservative, high-resolution shock-capturing scheme.**
- **The flux-interpolated, constrained transport scheme is used to maintain a divergence-free magnetic field.**
- **We have performed simulations of jet formation from a geometrically thin accretion disk near both non-rotating and rotating black holes. Similar to previous results (Koide et al. 2000, Nishikawa et al. 2005a) we find magnetically driven jets.**
- **It appears that the rotating black hole creates a second, faster, and more collimated inner outflow. Kinematic jet structure could be a sensitive function of the black hole spin parameter and magnetic field strength.**
- **GRPIC simulations will be complementary to GRMHD simulations.**

* Standard radiation model by E. Waxman (2006)

- the luminosity and spectrum of synchrotron radiation, the strength of the magnetic field and the energy distribution of the electrons
- Due to the lack of a first principles theory of collisionless shocks, we present in this section a purely phenomenological approach to the model of afterglow radiation emission
- we simply assume that a fraction ε_B of the post-shock thermal energy density is carried by the magnetic field, that a fraction ε_e is carried by electrons, and that the energy distribution of the electrons is a power-law, $\mathbf{d}\log n_e/\mathbf{d}\log \boldsymbol{\varepsilon} = \mathbf{p}$ (above some minimum energy $\boldsymbol{\varepsilon}_0$ which is determined by ε_e and **p**)
- $\boldsymbol{\varepsilon}_B$, $\boldsymbol{\varepsilon}_e$ and **p** are treated as free parameters, to be determined by observations
- the constraints implied on these parameters by observations are independent of any assumptions regarding the nature of the afterglow shock and the processes responsible for particle acceleration or magnetic field generation
- The parameters ε_B, $\boldsymbol{\varepsilon}_e$ and **p**, together with the parameters **E** and **n** which determine the shock dynamics, completely determine the magnetic field strength and electron distribution (including their temporal and spatial dependence).

Fermi Observations of High-Energy Gamma-Ray Emission from GRB 080916C

*Light curves for GRB 080916C observed with the GBM and the LAT (*Abdo et al. 2009)

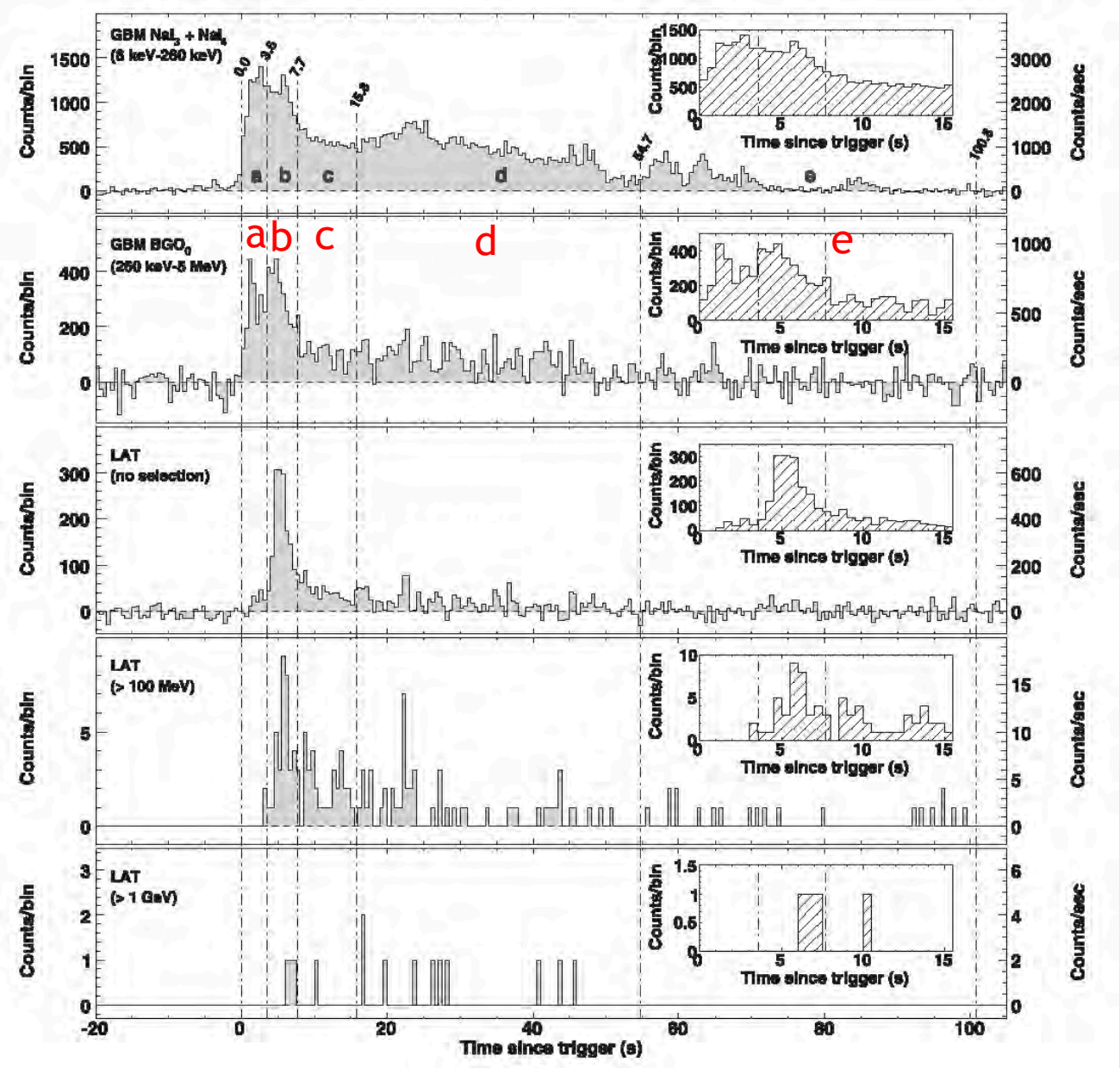

Synthetic spectra with different Lorentz factors with cold and warm thermal temperatures

synthetic spectra

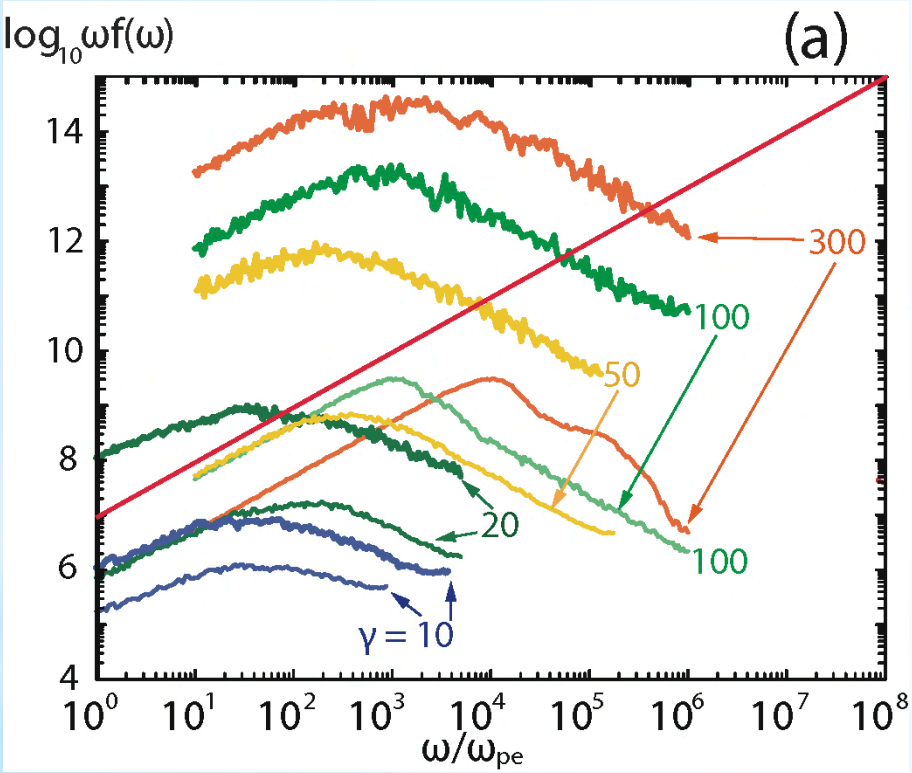

modeled Fermi spectra in vF units

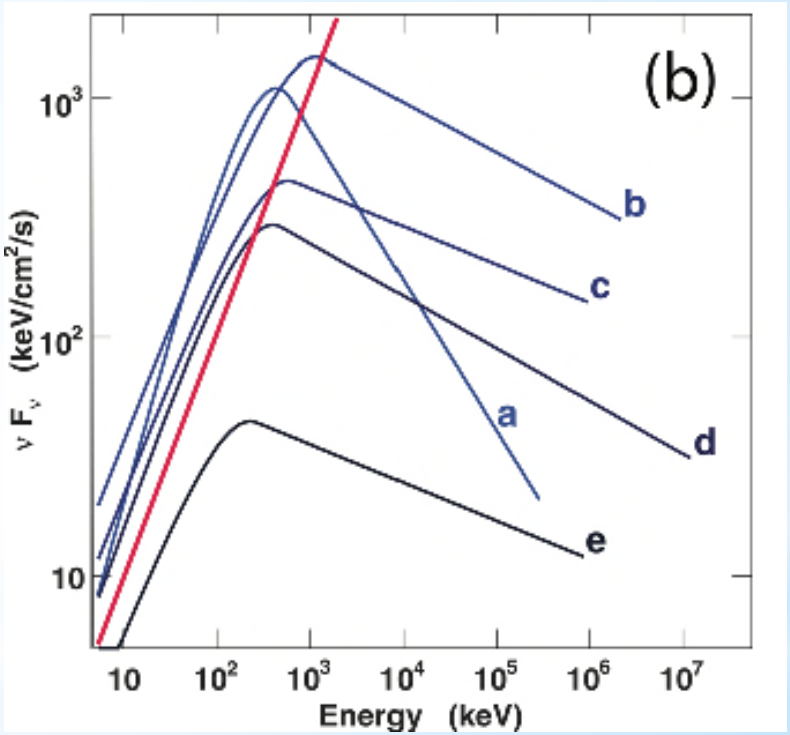

(thin lines) and warm (thick lines) electron jets.
The red lines indicate slope in vF ~ 1

(Abdo et al. 2009)

(Nishikawa et al. 2012)